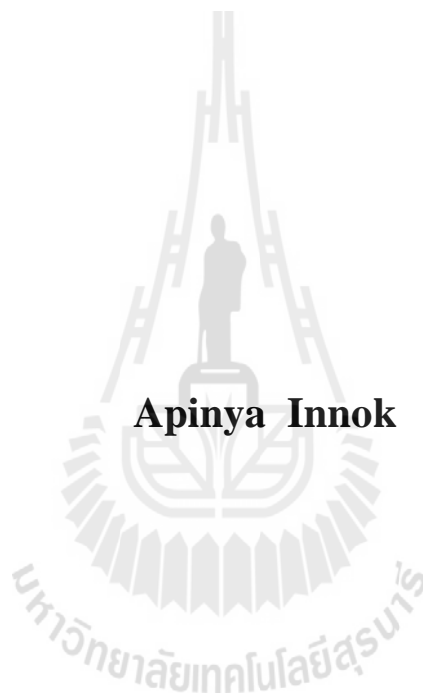


**ANGULAR BEAMFORMING TECHNIQUE
FOR MIMO SYSTEMS**



**A Thesis Submitted in Partial Fulfillment of the Requirements for the
Degree of Doctor of Philosophy in Telecommunication Engineering**

Suranaree University of Technology

Academic Year 2013

เทคนิคการก่อรูปด้าคตินเชิงมุมสำหรับระบบไมโม่

นางสาวอภิญญา อินทร์นอก



วิทยานิพนธ์นี้เป็นส่วนหนึ่งของการศึกษาตามหลักสูตรปริญญาวิศวกรรมศาสตรดุษฎีบัณฑิต

สาขาวิชาวิศวกรรมโทรคมนาคม

มหาวิทยาลัยเทคโนโลยีสุรนารี

ปีการศึกษา 2556

ANGULAR BEAMFORMING TECHNIQUE FOR MIMO SYSTEMS

Suranaree University of Technology has approved this thesis submitted in partial fulfillment of the requirements for the Degree of Doctor of Philosophy.

Thesis Examining Committee

(Asst. Prof. Dr. Chutima Prommak)

Chairperson

(Assoc. Prof. Dr. Peerapong Uthansakul)

Member (Thesis Advisor)

(Asst. Prof. Dr. Monthippa Uthansakul)

Member

(Asst. Prof. Dr. Chanchai Thaijiam)

Member

(Dr. Dheerasak Anantakul)

Member

(Prof. Dr. Sukit Limpijumnong)

Vice Rector for Academic Affairs
and Innovation

(Assoc. Prof. Ft. Lt. Dr. Kontorn Chamniprasart)

Dean of Institute of Engineering

อภิญา อินทร์นอก : เทคนิคการก่อรูปลำคลื่นเชิงมุมสำหรับระบบไมโม (ANGULAR BEAMFORMING TECHNIQUE FOR MIMO SYSTEMS) อาจารย์ที่ปรึกษา : รองศาสตราจารย์ ดร.พีระพงษ์ อุซารสกุล, 117 หน้า.

การก่อรูปลำคลื่นของระบบไมโม มีหลายรูปแบบ จากการสำรวจปริทัศน์วรรณกรรม ระบบที่มีการก่อรูปลำคลื่นแบบไอเคน ให้คุณภาพการทำงานของระบบดีที่สุด เพราะมีการรับรู้ข้อมูลช่องสัญญาณทั้งหมด แต่ในสถานการณ์จริงต้องมีการขาดหายของข้อมูล ด้วยเหตุผลการส่งและรับที่มีสัญญาณตกกระทบและสะท้อนหลายเส้นทาง ทำให้สัญญาณที่รับได้ไม่ถึงผู้รับทั้งหมด ดังนั้นการก่อรูปลำคลื่นแบบไอเคนจึงมีไว้เพื่อเปรียบเทียบให้เห็นความแตกต่างเพราะเป็นรูปแบบอุดมคติ ส่วนรูปแบบที่มีการรับรู้ข้อมูลลดลง เช่น การก่อรูปลำคลื่นแบบควอนไทซ์ ใช้การย้อนกลับของบิตข้อมูลในการหาเวกเตอร์ก่อรูปลำคลื่นที่เหมาะสม เพื่อการรับรู้สถานะข้อมูลของภาครับและภาคส่ง แต่อย่างไรก็ตามการก่อรูปลำคลื่นแบบควอนไทซ์ มีข้อเสียในเรื่องสมการในการหาเวกเตอร์ก่อรูปลำคลื่นที่ซับซ้อน และยากมากขึ้นเมื่อพิจารณาบิตย้อนกลับจำนวนมาก ทำให้วิทยานิพนธ์นี้นำเสนอแนวคิดที่จะมาแก้ไขข้อเสียของระบบควอนไทซ์ นั่นคือ การก่อรูปลำคลื่นเชิงมุม เนื่องจากแนวคิดเชิงมุมนี้ มีการพิจารณามุมที่ส่งออกไปและมุมที่รับเข้ามา จากจำนวนบิตย้อนกลับ ทำให้ไม่มีความซับซ้อนในการหาเวกเตอร์การก่อรูปลำคลื่น เพราะคิดจากมุมได้โดยตรง ดังนั้นจึงลดความซับซ้อนของระบบ โดยทำการจำลองแบบในโปรแกรมแมทแลบ พิจารณาการส่งข้อมูลทั้งหนึ่งสตรีมและหลายสตรีม เนื่องจากการสำรวจปริทัศน์วรรณกรรม มีพิจารณาการส่งและรับแค่หนึ่งสตรีม วิทยานิพนธ์นี้จึงทำเพิ่มโดยประยุกต์หลายสตรีมด้วย รวมถึงทำการหาบิตย้อนกลับที่น้อยที่สุดที่ทำให้ระบบมีประสิทธิภาพมากที่สุด ซึ่งเป็นข้อดีในการทำงาน เพราะบิตย้อนกลับน้อยส่งผลให้ความซับซ้อนในการทำงานของระบบน้อยด้วย อีกทั้งยังเปรียบเทียบเวลาในการประมวลผล เพื่อชี้ให้เห็นว่าการก่อรูปลำคลื่นเชิงมุมใช้เวลาในการประมวลผลน้อยกว่าการก่อรูปลำคลื่นแบบควอนไทซ์ และทำการสร้างชุดทดสอบในทางปฏิบัติ สำหรับการก่อรูปลำคลื่นเชิงมุมและควอนไทซ์ การส่งข้อมูลในแต่ละบิตกำหนดให้ไมโครโปรเซสเซอร์ทำงานโดยใส่สวิตซ์สำหรับคัดเลือกมุมในแต่ละบิตได้ทันที เนื่องจากไมโครโปรเซสเซอร์สามารถส่งข้อมูลเป็นแอนาล็อกไปที่เฟลชไฟเตอร์ได้เลยโดยตรง แนวคิดนี้น่าสนใจเพราะมีวิธีการดำเนินงานง่าย ไม่ซับซ้อน และไม่เปลืองค่าใช้จ่ายในการหาตัวปรับเฟส เมื่อใช้การก่อรูปลำคลื่นเชิงมุมเปรียบเทียบกับ การก่อรูปลำคลื่นแบบควอนไทซ์ ผลที่ได้จากการวัดจริงพบว่าความจุช่องสัญญาณจากการก่อรูปลำคลื่นเชิงมุมดีกว่าระบบควอนไทซ์

สาขาวิชาวิศวกรรมโทรคมนาคม
ปีการศึกษา 2556

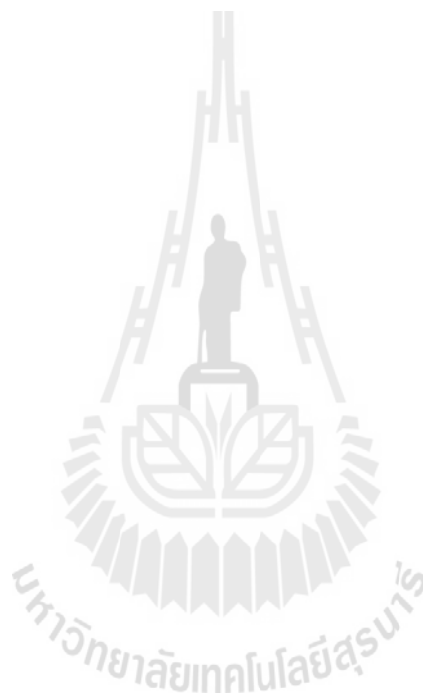
ลายมือชื่อนักศึกษา _____
ลายมือชื่ออาจารย์ที่ปรึกษา _____

APINYA INNOK : ANGULAR BEAMFORMING TECHNIQUE FOR
MIMO SYSTEMS. THESIS ADVISOR : ASSOC. PROF. PEERAPONG
UTHANSAKUL, Ph.D. 117 PP.

MIMO CAPACITY/EIGEN BEAMFORMING /QUANTIZED BEAMFORMING/
ANGULAR BEAMFORMING

Recently, the method of Multiple Input Multiple Output (MIMO) beamforming has gained a lot of attention. So far in literature, the Eigen Beamforming (EB) technique provides the best performance with the expense of knowing full channel information. However, it is impossible to fully know the channel in a real fading environment. Thus, EB has been studied as ideal technique and used as a reference to compare with other techniques. To fix the impairment of EB technique, the Quantized Beamforming (QB) technique has been presented by using only some feedback bits instead of all channel side information to calculate the suitable beamforming vectors. However, QB technique has a drawback in the complexity of finding the beamforming vectors. In this thesis, the new technique named as Angular Beamforming (AB) has been presented to overcome such a drawback of QB. This technique has a low complexity to find the suitable beamforming vector. The investigations are undertaken by sending multiple data streams into 4x4 MIMO systems. This thesis considered the effect of 1 data stream and multiple streams which have been originally studied. Also this thesis initially proposed the method to find the optimal feedback bits. From all simulation results, they indicate that AB technique spent a less simulation time than QB technique. This is attractive to be practically implemented. Finally, this thesis presents the feasibility of AB implementation.

The experiments are undertaken to verify the concept of AB and QB in practice by applying microprocessors and phase shifter. It is attractive because such a system is easy to implement, uncomplicated and low of cost. The measured results confirm that the AB technique outperforms the QB technique.



School of Telecommunication Engineering

Academic Year 2013

Student's Signature _____

Advisor's Signature _____

ACKNOWLEDGEMENTS

The author wishes to acknowledge the funding support from The Royal Golden Jubilee Ph.D. Program (RGJ).

The grateful thanks and appreciation are given to the thesis advisor, Assoc. Prof. Dr. Peerapong Uthansakul for his consistent supervision and thoughtfully comment on several drafts and advice towards the completion of this study.

My thanks go to Asst. Prof. Dr. Chutima Prommak, Asst. Prof. Dr. Monthippa Uthansakul, Asst. Prof. Dr. Chanchai Thaijiam and Dr. Dheerasak Anantakul for their valuable suggestion and guidance given as examination committees.

The author is also grateful to the financial support from Suranaree University of Technology (SUT).

Finally, I would also like to express my deep sense of gratitude to my parents for their support and encouragement me throughout the course of this study at the Suranaree University of Technology.

Apinya Innok

TABLE OF CONTENTS

	Page
ABSTRACT (THAI)	I
ABSTRACT (ENGLISH)	II
ACKNOWLEDGMENTS	IV
TABLE OF CONTENTS	V
LIST OF TABLES	IX
LIST OF FIGURES	X
LIST OF ABBREVIATIONS	XI
CHAPTER	
I INTRODUCTION	1
1.1 Background of problems	1
1.2 Thesis objectives	3
1.3 Scope of and limitation of the study	3
1.4 Contributions	4
1.5 Thesis organization	4
II LITERATURE REVIEW	6
2.1 Introduction	6
2.2 MIMO systems	6
2.2.1 Open loop systems	8

TABLE OF CONTENTS (Continued)

	Page
2.2.2 Closed loop systems.....	9
2.3 Literature Review.....	9
2.3.1 MIMO capacity.....	9
2.3.2 Angular beamforming technique	10
2.3.3 Quantized beamforming technique	11
2.3.4 Eigen beamforming technique	11
2.4 Chapter summary	12
III BACKGROUND THEORY.....	14
3.1 Introduction.....	14
3.2 Narrowband MIMO Model.....	15
3.3 Parallel Decomposition of the MIMO Channel.....	16
3.4 MIMO channel capacity	20
3.4.1 Static channels	20
3.4.2 Fading channels	24
3.4.3 Array domain processing	25
3.4.4 Angular domain processing	27
3.5 Chapter summary	30
IV MIMO Beamforming	31
4.1 Introduction.....	31
4.2 Angular beamforming technique	31
4.3 Quantized beamforming technique	35

TABLE OF CONTENTS (Continued)

	Page
4.4 Eigen beamforming technique.....	37
4.5 Simulation results	38
4.6 Chapter summary	44
V CHANNEL MEASUREMENT FOR MIMO	
BEAMFORMING	45
5.1 Introduction.....	45
5.2 Antennas	46
5.3 Weighting networks	47
5.3.1 Weighting systems	47
5.3.2 Control devices	61
5.4 Construction of channel measurement for MIMO beamforming.....	64
5.5 Chapter summary	65
VI EXPERIMENTAL RESULTS	66
6.1 Introduction.....	66
6.2 Experimental setup.....	66
6.3 Experimental result and discussion.....	67
6.4 Chapter summary	81
VII CONCLUSION	82
7.1 Conclusion	82
7.2 Future studies	83

TABLE OF CONTENTS (Continued)

	Page
REFERENCES	85
APPENDICES	
APPENDIX A PUBLICATIONS	88
BIOGRAPHY	117



LIST OF TABLES

Table	Page
4.1 Average capacity 4x4 MIMO beamforming for SNR=10 dB, 1 stream	40
4.2 Average capacity 4x4 MIMO beamforming for SNR=10 dB, 2 streams.....	40
4.3 Average capacity 4x4 MIMO beamforming for SNR=10 dB, 3 streams.....	40
4.4 Average capacity 4x4 MIMO beamforming for SNR=10 dB, 4 streams.....	40
4.5 The example of flop calculation for the QB technique	41
4.6 The example of flop calculation for the AB technique	43
5.1 Typical performance data for phase shifter	48
5.2 Verified angle for phase shifter at 2.4 GHz.....	50
5.3 Measurements parameter for 180 degree phase shifter at 2.4 GHz.....	58
5.4 Electrical specifications at 25°C.....	59
5.5 Summary of specification of microcontroller “ET-BASExMEGA128A1.....	63
6.1 Weighting coefficients (dB) for AB technique of 4 × 4 MIMO beamforming ...	68

LIST OF FIGURES

Figure	Page
2.1 Categories of MIMO systems	6
2.2 Illustrations of SISO, SIMO, MISO and MIMO	8
2.3 Schematic AB technique representation of MIMO channel	10
2.4 System overviews of QB technique	11
2.5 System overviews of EB technique	12
3.1 MIMO systems.....	15
3.2 Transmit precoding and receiving postcoding	18
3.3 Parallel decomposition of the MIMO channel.....	19
3.4 Array domain representations of 4×4 MIMO channel with four transmitting and receiving antenna	26
3.5 An example of \mathbf{H}^A with different angle spreads at the transmitter and receiver.....	29
4.1 4x4 MIMO Beamforming (a) 1 stream and (b) 4 streams	32
4.2 Capacity vs. SNR (a) 1 stream, (b) 2 streams, (c) 3 streams and (d) 4streams...	39
4.3 Complexity (Flop) vs. number of feedback bits for 1, 2, 3 and 4 streams.....	43
4.4 Simulation times vs. number of feedback bits for 1, 2, 3 and 4 streams.	44
5.1 The block diagram of channel measurement for MIMO beamforming.....	46
5.2 Monopole antenna structure.....	46
5.3 Photograph of phase shifter.	47

LIST OF FIGURES (Continued)

Figure	Page
5.4 Simplified schematic of phase shifter	48
5.5 Set up for phase shifter testing.....	49
5.6 Measured phase shifter	49
5.7 Diagram of phase shifter	55
5.8 Photograph of Phase Shifter.....	58
5.9 Photograph of measured return loss (S_{11}) of phase shifter.....	56
5.10 Measured return loss (S_{11}) of phase shifter Number 6 (Table 5.3)	56
5.11 Measured insertion loss (S_{21}) of phase shifter Number 6 (Table 5.3).....	57
5.12 Phase difference between input and output signal of phase shifter Number 6 (Table 5.3).....	57
5.13 Photograph of power splitter/combiner	58
5.14 Electrical schematic of the power splitter/combiner.....	59
5.15 Diagram of voltage multiplier.....	60
5.16 Photograph of voltage multiplier	60
5.17 Microcontroller “ET-BASE-xMEGA128A1	62
5.18 Measurement voltages from microcontroller.....	64
5.19 Photograph of full construction of channel measurement for MIMO beamforming	65

LIST OF FIGURES (Continued)

Figure	Page
6.1 Photograph of equipments of channel measurement For 4x4 MIMO beamforming	67
6.2 Assembly of MIMO beamforming tested in chamber room.....	72
6.3 (a) Simulated and (b) measured beam directions using AB technique for 1 bit feedback when the beam directions are 60° and 120°	72
6.4 (a) Simulated and (b) measured beam directions using AB technique for 2 bit feedback when the beam directions are 36°, 72°, 108° and 144°	73
6.5 (a) Simulated and (b) measured beam directions using AB technique for 3 bit feedback when the beam direction are 20°, 40°, 60°, 80°, 100°, 120°, 140° and 160°	73
6.6 Measurement scenarios	75
6.7 Block diagram of channel measurement for 4x4 MIMO beamforming	75
6.8 The photograph of measurement set up for location 1	76
6.9 The capacity versus SNR for AB at each locations	77
6.10 The capacity versus SNR for QB at each locations	78
6.11 The average capacity versus number of bit feedback for 4x4 MIMO beamforming using AB and QB techniques.....	79
6.12 The radiation patterns comparison between AB and QB techniques for 4 feedback bits.....	81

SYMBOLS AND ABBREVIATIONS

AB	=	Angular Beamforming
CSI	=	Channel Side Information
CSIR	=	Channel Side Information at the Receiver
CSIT	=	Channel Side Information at the Transmitter
DSP	=	Digital Signal Processing
EB	=	Eigen Beamforming
flop	=	floating point operation
MIMO	=	Multiple Input Multiple Output
MISO	=	Multiple Input Single Output
QB	=	Quantized Beamforming
SIMO	=	Single Input Multiple Output
SISO	=	Single Input Single Output
SM	=	Spatial Multipleing
SNR	=	Signal to Noise Ratios
SUT	=	Suranaree University of Technology
SVD	=	Singular Value Decomposition

CHAPTER I

INTRODUCTION

1.1 Background of problems

The Multiple Input Multiple Output (MIMO) systems provide a good quality of service such as channel capacity. Many works have proposed the method of Eigen Beamforming (EB) technique for MIMO systems (Sirikiat, L., A. et.al, (2006); Sun, L., et.al, (2009) and Shi, J., et.al, (2007)). This technique utilizes the properties of estimated channels by performing singular value decomposition (SVD) on channel matrix. Then, eigen-vectors compositing of channel matrix are considered as pre and post coding schemes for MIMO systems. This technique can improve the capacity performance but, both transmitter and receiver have to perfectly know the channel information. However, there are many unattractive issues of using EB technique in practice such as a requirement of high system complexity and many procedures for channel feedback transmission. In many real systems, the channel side information (CSI) is hardly possible to be known exactly at the transmitter and receiver. Most of real systems realize CSI by using feedback techniques such as Quantized Beamforming (QB) technique. The QB technique has been widely studied (Bishwaru, M., et.al, (2006) and Zheng, X., et.al, (2007)). QB technique uses only some feedback bits instead of all CSI to calculate the suitable beamforming vectors. However, QB technique has a drawback in the complexity of finding the beamforming vectors. Therefore, this thesis presents Angular Beamforming (AB) technique to overcome such a drawback of QB technique. AB technique is convenient for implementation because

the method of AB technique that finds beamforming vectors is easy. The details of QB and AB techniques are shown in the Chapter IV.

In the research areas of MIMO systems, many works (Vieira, R. D., et.al, (2006); Foschini, G. L., et.al, (1998); Telatar, I. E. (1995) and Foschini, G. J. (1996)) have been proposed to enhance the channel capacity. Some studies have been focused on theoretical works and performed by measurements. Moreover, most of them develop the technique to enhance the channel capacity through channel behaviour (Kermoal, J. P., et.al, (2000); Stridh, R., et.al, (2000) and Molisch, A. F., et.al, (2002)) such as adjusting transmitted powers according to eigen-value of channels so called as water filling method. In general, it can be noticed that the theoretical consideration of channel capacity is based on the array antennas at both transmitter and receiver but, the channel characteristic is composed of many angle parameters such as angle of arrival, angle of departure and angle spread. Therefore, it is interesting to investigate the performance of MIMO systems using the AB technique. Recently, Li, H., et.al, (2008) develop the channel estimation of MIMO-OFDM system based on AB technique consideration. The applicability of AB technique depends on the CSI available to the receiver. The design of suitable beamforming is proposed by facilitating the direct implementation. But, so far in literature, there is no work to illustrate the benefit of channel capacity using AB technique. Therefore, this thesis focuses on investigating the performance of channel capacity using AB technique. The reason is that the pre and post coding schemes of angle transformations decrease the complexity on both transmitter and receiver. Then, this thesis finds how to implement the AB and QB techniques in practice. Accordingly, the authors construct the MIMO systems employing AB and QB techniques by just inserting phase shifter

and microprocessor for choosing the set of steering vectors. The reason why microprocessor and phase shifter are chosen is because they are just a low-complexity hardware that can operate the AB and QB techniques. However, the AB and QB techniques have many beam directions when increase the number of feedback bits. Therefore, this thesis selects the beamforming vectors that give maximum SNR. Then, maximum SNR leads to maximum channel capacity.

1.2 Thesis objectives

- (i) To study the basic principles and theories of the channel capacity for the MIMO beamforming systems.
- (ii) To propose the new technique that its complexity is lower than QB technique.
- (iii) To investigate the performances of MIMO beamforming using the proposed technique.

1.3 Scope of and limitation of the study

- (i) In this thesis, the performances in terms of the channel capacity and simulation times for EB, QB and AB techniques are presented.
- (ii) All simulation results have been performing by MATLAB programming.
- (iii) The channel measurements operate in frequencies 2.4 GHz.
- (iv) The channel measurements have 4 array antennas at both transmitter and receiver.
- (v) The channel measurements are performed for only the AB and QB techniques.

1.4 Contributions

This thesis proposes the novel thinking of AB technique for MIMO beamforming which the outcome can be categorized into two major contributions.

- (i) AB technique is attractive to be practically implemented because it offers a low complexity that can decrease the processing times.
- (ii) This thesis has shown the construction of channel measurement for AB and QB techniques.

1.5 Thesis organization

The remainder of this thesis is organized as follows. Chapter II presents the literature review for MIMO systems. In literature review, MIMO systems can be categorized into two groups including open loop and closed loop which the MIMO beamforming in this thesis is in a group of closed loop.

Chapter III describes the background theory of channel capacity on wireless communication. This knowledge is important to be a useful tool for judging the merit of MIMO systems.

Chapter IV presents the details of MIMO beamforming including AB, QB and EB techniques. The contribution of this chapter falls into two main issues. The first contribution is on the comparisons in term of channel capacity. Secondly, the simulation times of how AB and QB techniques impact on the channel matrix are originally presented. This helps the reader to understand in a true benefit of AB technique.

Chapter V presents the practical channel measurement of MIMO beamforming systems. The full testbed is constructed. The component of MIMO beamforming

systems consists of array antennas, weighting networks, control devices, splitter, combiner and voltage multiplier.

In Chapter VI, the experimental setup and the obtained results are presented. This chapter shows the experiment carried out using AB and QB techniques. The channel measurements are undertaken in Telecommunication laboratory F4, SUT. Then, the channel capacities are simulated by utilizing measured channels.

In Chapter VII, it provides conclusion of the research work and suggestion for further study.



CHAPTER II

LITERATURE REVIEW

2.1 Introduction

This chapter presents literature review for the MIMO systems. The basic concept of MIMO systems is now divided into two main groups, open loop and closed loop. Then, algorithms of MIMO systems are presented. The categories of MIMO systems can be presented as a diagram in Figure 2.1.

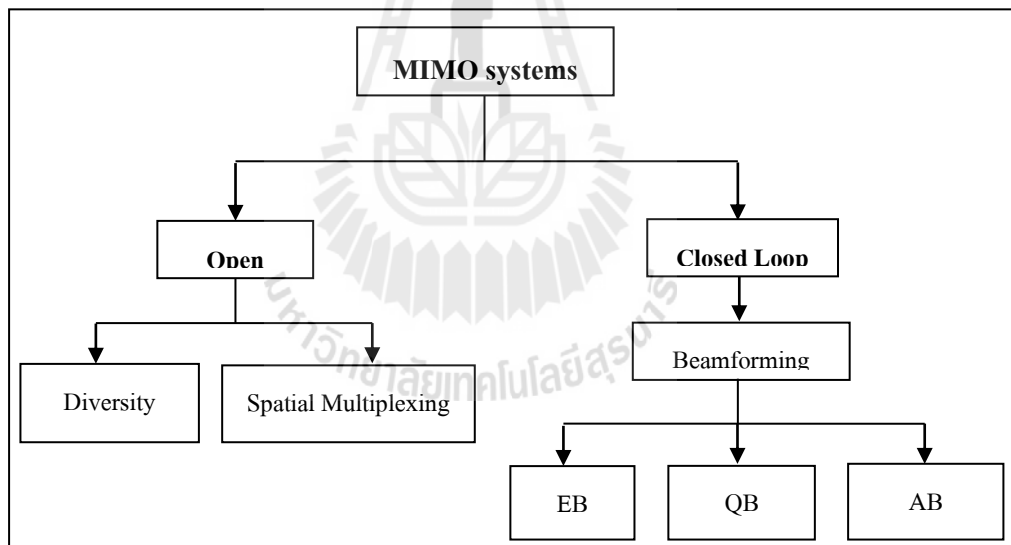


Figure 2.1 Categories of MIMO systems.

2.2 MIMO systems

MIMO systems are using multiple antennas at both the transmitter and receiver to improve communication performance. The terms of input and output refer to the radio channel carrying the signal. MIMO systems have attracted attention in

wireless communication because it offers significant increases in data throughput. It achieves an array gain that improves the spectral efficiency (bits per second per hertz of bandwidth).

MIMO technology has been developed and implemented in some standards, e.g. 802.11n products. In Single Input Single Output (SISO), both the transmitter and the receiver have one antenna. In Single Input Multiple Output (SIMO), there is one antenna at the transmitter and multiple antennas at the receiver. In Multiple Input Single Output (MISO), there are multiple antennas at the transmitter and one antenna at the receiver. Illustrations of SISO, MISO, SIMO and MIMO can be shown in Figure 2.2.

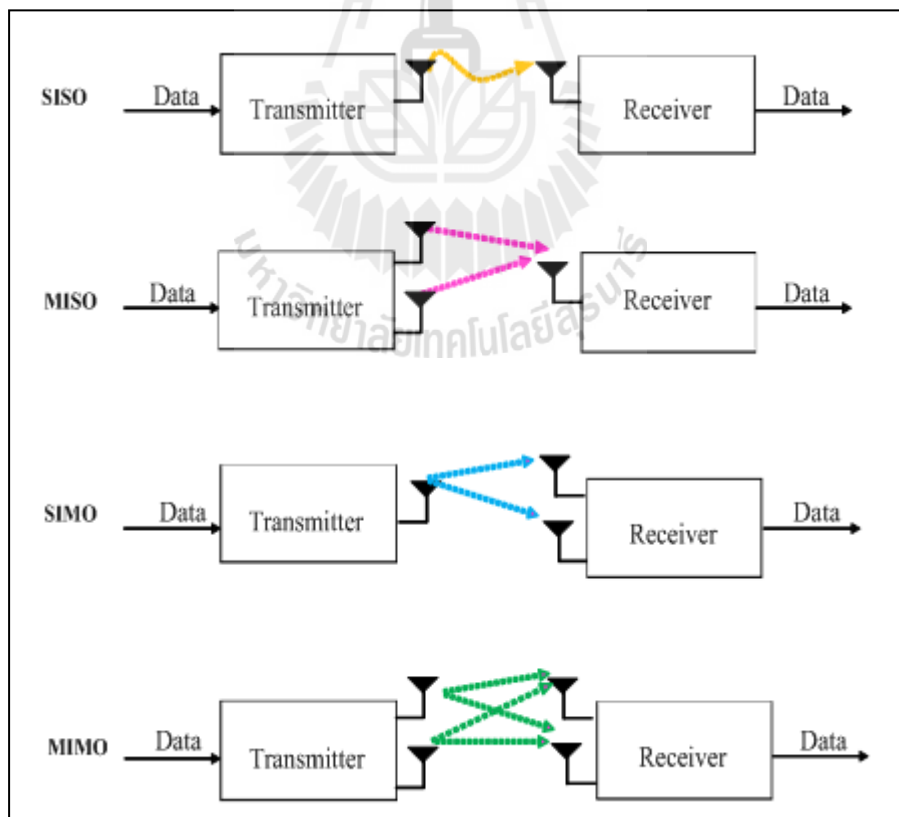


Figure 2.2 Illustrations of SISO, SIMO, MISO and MIMO.

2.2.1 Open loop systems

MIMO can be divided into two main categories, spatial multiplexing (SM) and diversity.

- **Spatial multiplexing** : SM is a technique for increasing channel capacity. The maximum number of spatial streams is limited by the less number of antennas at the transmitter or receiver. Each stream is transmitted from a different transmit antenna in the same frequency channel. SM can also be used for simultaneous transmission to multiple receivers. If these signals arrive at the receiver antenna array with sufficiently different spatial signatures, the receiver can separate these streams into parallel channels. The scheduling of receivers with different spatial signatures allows good separations that cause increasingly the channel capacity.

- **Diversity** : Diversity technique is transmitted a single stream. The signal is emitted from each of the transmitting antenna. Diversity can be divided into three groups including time diversity, frequency diversity and space diversity. Because time and frequency diversity have limitations and hardly to perform pre and post coding. Diversity coding exploits the independent fading in the multiple antenna links to enhance signal diversity.

Open loop system has disadvantage that offers the channel capacity less than closed loop system. Because Open loop system does not have feedback information that can improve the performances. At present, the demand of wireless communications is increasing. Therefore, this thesis use closed loop beamforming to increase the channel capacity. MIMO Beamforming knows CSI from feedback information.

2.2.2 Closed loop systems

The closed loop systems are considered to be spatial processing that occurs at the transmitter and receiver, so called MIMO beamforming. The beamforming signal is emitted from each transmitting antenna with appropriate phase weighting such that the signal power is maximized at the receiver input. The benefit of beamforming is to increase the received signal gain. Note that MIMO beamforming system uses CSI for selecting the beamforming vectors to obtain maximum SNR. Then, maximum SNR leads to maximum channel capacity. But, smart antenna does not uses CSI to find the beamforming vectors.

2.3 Literature Review

2.3.1 MIMO capacity

In general, MIMO systems consideration of channel capacity is based on the array antennas at both transmitter and receiver. Many works (Vieira, R. D., et.al (2006); Foschini, G. L., et.al (1998); Telatar, I. E. (1995) and Foschini, G. J. (1996)) have been proposed to enhance the channel capacity. Some studies have been focused on theoretical works and performed by measurements. Moreover, most of them develop the techniques to enhance the channel capacity through channel behaviour (Kermoal, J. P., et.al (2000); Stridh, R., et.al (2000) and Molisch, A. F., et.al (2002)) such as adjusting transmitted powers according to eigen value of channels so called as water filling method. In general, it can be noticed that the theoretical consideration of channel capacity is based on the array antennas at both transmitter and receiver, but the channel characteristic is composed of many angle parameters such as angle of arrival, angle of departure and angle spread. Therefore, it is interesting to investigate

the performance of MIMO systems using the AB instead of the conventional MIMO systems.

2.3.2 Angular beamforming technique

In literature, Li, H., et.al (2008) present technique that the angle spread are divided equally as shown in Figure 2.3. This paper divides the angle for channel estimation of MIMO-OFDM based on AB technique but, this paper has not used AB technique to operate MIMO beamforming. Therefore, this thesis originally adapts to AB technique to MIMO beamforming and also operates the channel capacity using 4 array antennas at both transmitter and receiver. This thesis applies the angles to determine beamforming vectors by selecting the beamforming vectors that give maximum SNR. Then, maximum SNR leads to maximum channel capacity.

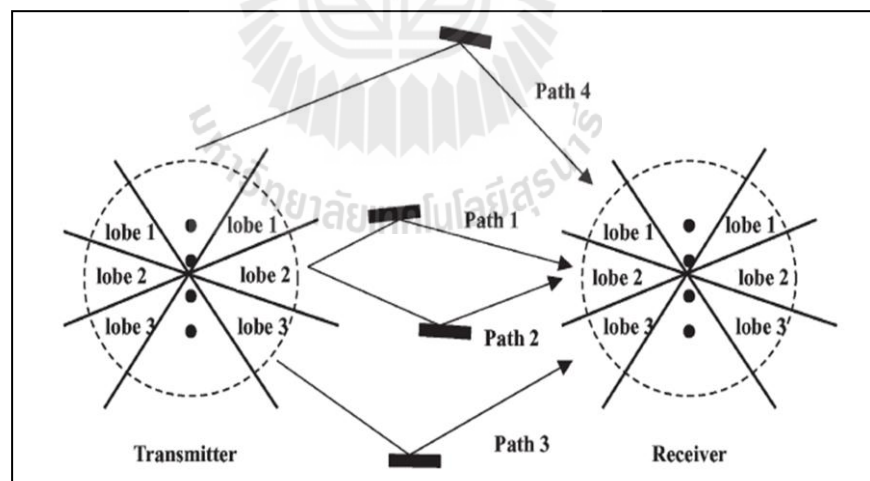


Figure 2.3 Schematic AB technique representation of a MIMO channel with four transmitting and four receiving antennas.

2.3.3 Quantized beamforming technique

The QB technique (Bishwarup, M., et.al (2006) and Zheng, X., et.al (2007)) has the process of feedback data shown in Figure 2.4, which has the beamforming vectors \mathbf{w}_t and \mathbf{w}_r . The suitable beamforming vector can be selected from the beamforming vectors that give maximum SNR. Unfortunately, the complexity of finding the beamforming vector is a drawback of QB technique. Therefore, this thesis proposed the AB technique to overcome such a drawback of QB technique which the number of beamforming vector of AB and QB techniques are equal. The AB technique offers a less computational complexity than QB technique.

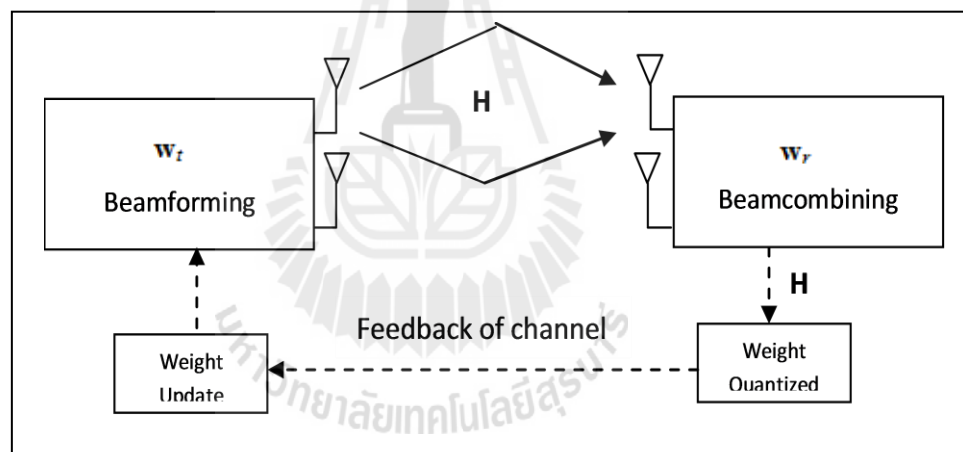


Figure 2.4 System overviews of QB technique.

2.3.4 Eigen beamforming technique

In the EB technique design, this thesis assumes that the transmitter has a perfect knowledge of CSI. This technique used singular value decomposition (SVD) to determine the beamforming matrices \mathbf{V} and \mathbf{B} shown in Figure 2.5. This thesis studies the formation of EB technique which many researches (Chu, Z., et.al (2007);

Sirikiat, L. A., et.al (2006) and Liang, S., et.al (2009)) consider only the channel capacity. These two beamforming matrices (\mathbf{V} and \mathbf{B}) are used as pre and post coding matrices at transmitter and receiver. Then, the beamforming vectors \mathbf{v} and \mathbf{b} are given by the first column of the beamforming matrices \mathbf{V} and \mathbf{B} .

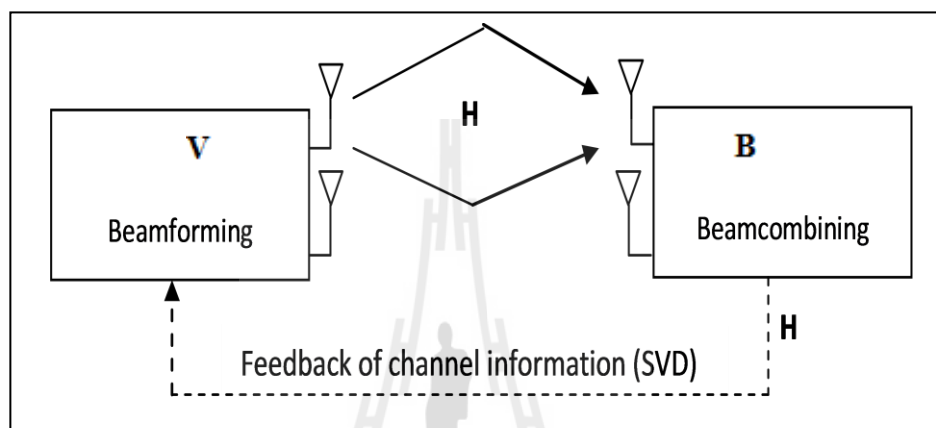


Figure 2.5 System overviews of EB technique.

2.4 Chapter summary

This chapter gives the details and literature surveys of MIMO systems. MIMO employs multiple antennas at both transmitter and receiver to improve communication performances. This chapter discusses the different types of MIMO systems including open loop and closed loop. Then, literature presents the channel capacity and beamforming techniques for MIMO systems. This thesis focuses on the beamforming including EB, QB and AB techniques. The first two types are unattractive to communication system because EB technique is impossible to fully know the CSI. Thus, EB technique has been studied as ideal technique and used as a reference to compare with other techniques. Then, QB technique has a drawback in the complexity

of finding the suitable beamforming vectors. Therefore, the AB technique has been presented to overcome such a drawback of QB technique.



CHAPTER III

BACKGROUND THEORY

3.1 Introduction

In this chapter, the multiple antennas at the transmitter and receiver are considered which this configuration is commonly referred as MIMO system. The multiple antennas can be used to increase data rates through multiplexing or to improve a diversity performance. In MIMO systems, the transmitting and receiving antennas can both be used for diversity gain. Multiplexing is obtained by exploiting the structure of the channel gain matrix to obtain independent signalling paths that can be used to send independent data. Indeed, the initial excitement about MIMO was sparked by the pioneering work of Winters, Foschini, Gans, and Telatar predicting remarkable spectral efficiencies for wireless systems with multiple transmitting and receiving antennas. This spectral efficiency gains often require accurate knowledge of the channel at the receiver and sometimes at the transmitter as well. The cost of the performance enhancements obtain through MIMO techniques. MIMO techniques are the added cost of deploying multiple antennas. The mathematics in this chapter uses several matrix theories.

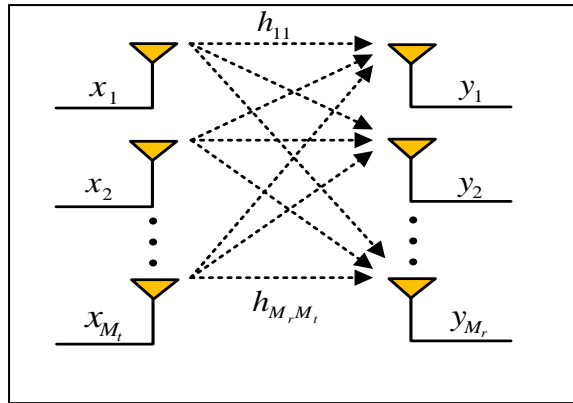


Figure 3.1 MIMO systems.

3.2 Narrowband MIMO Model

This thesis considers a narrowband MIMO channel. A narrowband point-to-point communication system of M_t transmitting and M_r receiving antennas is shown in Figure 3.1. This system can be represented by the following discrete time model:

$$\begin{bmatrix} y_1 \\ \vdots \\ y_{M_r} \end{bmatrix} = \begin{bmatrix} h_{11} & \cdots & h_{1M_t} \\ \vdots & \ddots & \vdots \\ h_{M_r 1} & \cdots & h_{M_r M_t} \end{bmatrix} \begin{bmatrix} x_1 \\ \vdots \\ x_{M_t} \end{bmatrix} + \begin{bmatrix} n_1 \\ \vdots \\ n_{M_r} \end{bmatrix} \quad (3.1)$$

Or simply as $\mathbf{y} = \mathbf{H}\mathbf{x} + \mathbf{n}$. Here \mathbf{x} represents the M_t -dimensional transmitted symbol, \mathbf{n} is the M_r dimensional noise vector, and \mathbf{H} is the $M_t \times M_r$ matrix of channel gains h_{ij} representing the gain from transmit antenna j to receive antenna i . This thesis assumes a channel bandwidth as B and complex gaussian noise with zero mean and covariance matrix as σ_n^2 . For simplicity, given a transmitting power constraint P . Assume the average SNR per receiving antenna under unity channel gain ρ equal to transmitting

power constraint P per noise σ_n^2 . This power constraint implies that the input symbols satisfy by

$$\sum_i^{M_i} E[x_i x_i^*] = \rho \quad (3.2)$$

Note that $Tr(R_x) = \rho$, where $Tr(R_x)$ is the trace of the input covariance matrix $R_x = E[xx^T]$. Different assumptions can be made about the knowledge of the channel gain matrix \mathbf{H} at the transmitter and receiver, referred to as channel side information at the transmitter (CSIT) and channel side information at the receiver (CSIR), respectively. For a static channel CSIR is typically assumed, since the channel gains can be obtained easily by sending a pilot sequence for channel estimation. If a feedback path is available Then, CSIR from the receiver can be sent back to the transmitter to provide CSIT: CSIT may also be available in time division duplexing systems without a feedback path by exploiting reciprocal properties of propagation. When the channel is not known at either the transmitter or receiver Then, some distribut,ion on the channel gain matrix must be assumed. The most common model for this distribut,ion is a zero-mean spatially white model, where the entries of \mathbf{H} assumed complex circularly symmetric Gaussian random variables. In general, different assumptions about CSI and about the distribut,ion of the \mathbf{H} entries lead to different channel capacities and different approaches to space-time signaling.

3.3 Parallel Decomposition of the MIMO Channel

The multiple antennas at the transmitter or receiver can be used for diversity gain. When both the transmitter and receiver have multiple antennas, there is another

mechanism for performance gain called multiplexing gain. The multiplexing gain of a MIMO systems results from the fact that a MIMO channel can be decomposed into a number R of parallel independent channels. By multiplexing independent data onto these independent channels get an R -fold increase in data rate in comparison to a system with just one antenna at the transmitter and receiver. This increased data rate is called the multiplexing gain. In this section, this thesis describes how to obtain independent channels from MIMO systems.

MIMO systems consider the channel matrix \mathbf{H} known to both the transmitter and the receiver. Let R_H denote the rank of \mathbf{H} . From matrix theory, for any matrix \mathbf{H} which can obtain its singular value decomposition (SVD) as

$$\mathbf{H} = \mathbf{U} \mathbf{\Sigma} \mathbf{V}^H \quad (3.3)$$

where the $M_r \times M_r$ matrix \mathbf{U} and the $M_t \times M_t$ matrix \mathbf{V} are unitary matrices and $\mathbf{\Sigma}$ is an $M_r \times M_t$ diagonal matrix of singular values σ_i of \mathbf{H} . These singular values have the property that $\sigma_i = \sqrt{\lambda_i}$ for λ_i the i th eigenvalue of $\mathbf{H}\mathbf{H}^H$, and R_H of these singular values are nonzero, where R_H is the rank of the matrix \mathbf{H} . Since R_H cannot exceed the number of columns or rows of \mathbf{H} , $R_H \leq \min(M_t, M_r)$. If \mathbf{H} is full rank, which is sometimes referred to as a rich scattering environment, Then, $R_H = \min(M_t, M_r)$. Other environments may lead to a low rank \mathbf{H} : a channel with high correlation among the gains in \mathbf{H} .

The parallel decomposition of the channel is obtained by defining a transformation on the channel input and output \mathbf{x} and \mathbf{y} through transmitting precoding and receiving postcoding. In transmitting precoding, the input to the

antennas x is generated through a linear transformation on input vector \tilde{x} as $x = \mathbf{V} \tilde{x}$. Receiving postcoding performs a similar operation at the receiver by multiplying the channel output y with \mathbf{U}^H as shown in Figure 3.2.

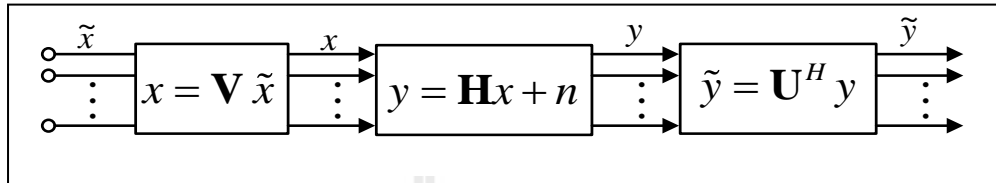


Figure 3.2 Transmitting precoding and receiving postcoding.

The transmitting precoding and receiving postcoding transform the MIMO channel into R_H parallel SISO channels with input \tilde{x} and output \tilde{y} , since from the SVD, this method can be written as

$$\begin{aligned}
 \tilde{y} &= \mathbf{U}^H (\mathbf{H}x + n) \\
 &= \mathbf{U}^H (\mathbf{U} \Sigma \mathbf{V}^H x + n) \\
 &= \mathbf{U}^H (\mathbf{U} \Sigma \mathbf{V}^H \mathbf{V} \tilde{x} + n) \\
 &= \mathbf{U}^H \mathbf{U} \Sigma \mathbf{V}^H \mathbf{V} \tilde{x} + \mathbf{U}^H n \\
 \tilde{y} &= \Sigma \tilde{x} + \tilde{n}
 \end{aligned} \tag{3.4}$$

where $\tilde{n} = \mathbf{U}^H n$ and Σ is the diagonal matrix of singular values of \mathbf{H} with σ_i on the i th diagonal. Note that multiplication by a unitary matrix does not change the distribution of the noise, n and \tilde{n} are identically distributed. Thus, the transmitting precoding and receiving postcoding transform the MIMO channel into R_H parallel

independent channels where the i th channel has input \tilde{x}_i , output \tilde{y}_i , noise \tilde{n}_i , and channel gain σ_i . Note that the σ_i are related all functions of \mathbf{H} . This parallel decomposition is shown in Figure 3.3. Since the parallel channels do not interfere with each other, the number of independent paths that need to be decoded. Moreover, by sending independent data across each of the parallel channels, the MIMO channel can support R_H times the data rate of a system with just one transmitting and receiving antenna, leading to a multiplexing gain of R_H . Note, however, that the performance on each of the channels will depend on its gain σ_i . The next section will more precisely characterize the multiplexing gain associated with the Shannon capacity of the MIMO channel.

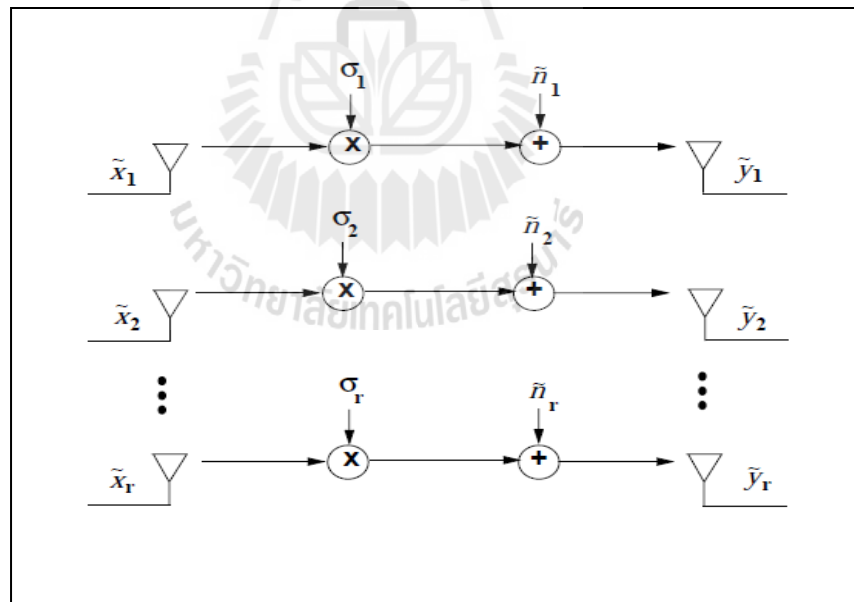


Figure 3.3 Parallel decomposition of the MIMO channel.

3.4 MIMO channel capacity

This section focuses on the Shannon capacity of a MIMO channel, which equals the maximum data rate that can be transmitted over the channel with arbitrarily small error probability. Capacity versus outage defines the maximum rate that can be transmitted over the channel with some nonzero outage probability. Channel capacity depends on channel gain matrix or its distribution at the transmitter and receiver. Throughout this section it is assumed that the receiver has knowledge of the channel matrix \mathbf{H} , since for static channels a good estimate of \mathbf{H} can be obtained fairly easily. First the static channel capacity will be given, which forms the basis for the subsequent section on capacity of fading channels.

3.4.1 Static channels

The capacity of a MIMO channel is an extension of the mutual information formula for a SISO channel. Specifically, the capacity is given in terms of the mutual information between the channel input vector x and output vector y as

$$C = \max I(X;Y) = \max [H(Y) - H(Y|X)] \quad (3.5)$$

The definition of entropy yields that $H(Y|X) = H(N)$, the entropy in the noise. Since this noise n has fixed entropy independent of the channel input, maximizing mutual information is equivalent to maximizing the entropy in y .

The mutual information of y depends on its covariance matrix, which for the narrowband MIMO model is given by

$$R_y = E[yy^H] = \mathbf{H}R_x\mathbf{H}^H + \mathbf{I}_{M_r} \quad (3.6)$$

Where R_x is the covariance of the MIMO channel input. It turns out that for all random vectors with a given covariance matrix R_y , the entropy of y is maximized when y is a zero-mean circularly symmetric complex gaussian random vector. Therefore, the resulting in the mutual information can be written as

$$I(x; y) = B \log_2 \det(\mathbf{I}_{M_r} + \mathbf{H}R_x\mathbf{H}^H) \quad (3.7)$$

The MIMO capacity is achieved by maximizing the mutual information (3.7) over all input covariance matrices R_x satisfying the power constraint:

$$C = \max_{R_x: \text{Tr}(R_x) = \rho} B \log_2 \det(\mathbf{I}_{M_r} + \mathbf{H}R_x\mathbf{H}^H) \quad (3.8)$$

Clearly, the optimization relative to R_x will depend on \mathbf{H} that known at the transmitter. This method considers this maximizing under different assumptions about transmitter CSI.

- **Channel known at transmitter: water filling**

The MIMO decomposition described in Section 3.3 allows a simple characterization of the MIMO channel capacity for a fixed channel matrix \mathbf{H} known at the transmitter and receiver. Specifically, the definition is identical for random vectors of capacities on each of the independent parallel channels with the transmit power optimally allocated between these channels. This optimization of transmit power across the independent channels results from optimizing the input covariance

matrix to maximize the capacity formula (3.9). Substituting the matrix SVD (3.3) into (3.8) and using properties of unitary matrices the method get the MIMO capacity with CSIT and CSIR as

$$C = \max_{\rho_i: \sum_i \rho_i \leq \rho} \sum_{i=1}^{R_H} \left[B \log_2 \left(1 + \sigma_i^2 \rho_i \right) \right] \quad (3.9)$$

Since $\rho = P/\sigma_n^2$, the capacity (3.9) can also be expressed in terms of the power allocation P_i to the i th parallel channel as

$$\begin{aligned} C &= \max_{P_i: \sum_i P_i \leq P} \sum_{i=\gamma_i \geq \gamma_0}^{R_H} \left[B \log_2 \left(1 + \frac{\sigma_i^2 P_i}{\sigma^2} \right) \right] \\ &= \max_{P_i: \sum_i P_i \leq P} \sum_{i=\gamma_i \geq \gamma_0}^{R_H} \left[B \log_2 \left(1 + \frac{P_i \gamma_i}{P} \right) \right] \end{aligned} \quad (3.10)$$

where $\rho_i = P_i/\sigma_n^2$ and $\gamma_i = \sigma_i^2 P / \sigma_n^2$ is the SNR associated with the i th channel at full power. Solving the optimization leads to a water-filling power allocation for the MIMO channel:

$$\frac{P_i}{P} = \begin{cases} \frac{1}{\gamma_0} - \frac{1}{\gamma_i} & ; \gamma_i \geq \gamma_0 \\ 0 & ; \gamma_i < \gamma_0 \end{cases} \quad (3.11)$$

For some cutoff value γ_i . The resulting capacity is Then,

$$C = \sum_{i=\gamma_i \geq \gamma_0} \left[B \log_2 \left(\frac{\gamma_i}{\gamma_0} \right) \right] \quad (3.12)$$

Capacity under perfect CSIT and CSIR can also be defined on channels where there is a single antenna at the transmitter and multiple receiving antennas (SIMO) or multiple transmitting antennas and a single receiving antenna (MISO). These channels can only obtain diversity gain from the multiple antennas. When both transmitter and receiver know the channel the capacity equals that of a SISO channel with the signal transmitted or received over the multiple antennas coherently combined to maximize the channel SNR.

- **Channel unknown at transmitter: uniform power allocation**

Suppose now that the receiver knows the channel but, the transmitter does not. Without channel information, the transmitter cannot optimize its power allocation or input covariance structure across antennas. If the distributions of \mathbf{H} channel gain is no bias in terms of the covariance of \mathbf{H} . Thus, it seems intuitive that the best strategy should be to allocate equal power to each transmitting antenna, resulting in an input covariance matrix equal to the scaled identity matrix:

$R_x = (\rho / M_t) \mathbf{I}_{M_t}$. For an M_t transmitting, M_r receiving antenna system, this yields mutual information given by

$$I(x; y) = B \log_2 \det \left(\mathbf{I}_{M_r} + \frac{\rho}{M_t} \mathbf{H} \mathbf{H}^H \right) \quad (3.13)$$

Using the SVD of \mathbf{H} which can express mutual information as

$$I(x; y) = \sum_{i=1}^{R_{\mathbf{H}}} \left[B \log_2 \left(1 + \frac{\gamma_i}{M_t} \right) \right] \quad (3.14)$$

where $\gamma_i = \sigma_i^2 \rho = \sigma_i^2 \bar{P} / \sigma^2$ and $R_{\mathbf{H}}$ is the number of nonzero singular values of \mathbf{H} . The mutual information of the MIMO channel (3.14) depends on the specific realization of the matrix \mathbf{H} , in particular its singular values σ_i . The average mutual information of a random matrix \mathbf{H} , averaged over the matrix distribution, depends on the probability distribution of the singular values of \mathbf{H} . In fading channels the transmitter can transmit at a rate equal to this average mutual information and insure correct reception of the data as discussed in the next section.

3.4.2 Fading channels

Now suppose that the matrix of channel gains experiences flat fading, so the gains h_{ij} vary with time. As in the case of the static channel, the capacity depends on what is known about the channel matrix at the transmitter and receiver.

With perfect CSIR and CSIT the transmitter can adapt to the channel fading and its capacity equals the average over all channel matrix realizations with optimal power allocation. With CSIR and no CSIT outage capacity is used to characterize the outage probability associated with any given channel rate. These different characterizations are described in more detail in the following sections.

- **Channel known at transmitter: water filling**

With CSIT and CSIR the transmitter optimizes its transmission strategy for each fading channel realization as in the case of a static channel. The capacity is Then, just the average of capacities associated with each channel realization, given by (3.9), with power optimally allocated. This average capacity is called the ergodic capacity of the channel. There are two possibilities for allocating

power under ergodic capacity. A short term power constraint assumes that the power associated with each channel realization must equal the average power constraint P .

In this case the ergodic capacity becomes

$$\begin{aligned}
 C &= E_{\mathbf{H}} \left[\max_{R_x: Tr(R_x)=\rho} \left[B \log_2 \det \left(\mathbf{I}_{M_r} + \mathbf{H} R_x \mathbf{H}^H \right) \right] \right] \\
 &= E_{\mathbf{H}} \left[\max_{P_i: \sum_i P_i \leq \bar{P}} \sum_i \left[B \log_2 \left(1 + \frac{P_i \gamma_i}{P} \right) \right] \right] \tag{3.15}
 \end{aligned}$$

Where $\gamma_i = \sigma_i^2 \bar{P} / \sigma^2$

- **Channel unknown at transmitter: ergodic capacity**

Now the time varying channel considers random matrix \mathbf{H} known at the receiver but, could not be known the transmitter. Ergodic capacity defines the maximum rate, averaged over all channel realizations that can be transmitted over the channel for a transmission strategy based only on the distribution of \mathbf{H} .

The optimization method of transmitter finds the optimum input covariance matrix to maximize ergodic capacity. Mathematically, the channel capacity can be written as:

$$C = \max_{R_x: Tr(R_x)=\rho} E_{\mathbf{H}} \left[B \log_2 \det \left(\mathbf{I}_{M_r} + \mathbf{H} R_x \mathbf{H}^H \right) \right] \tag{3.16}$$

3.4.3 Array domain processing

The representation of array domain processing for MIMO systems can be shown in Figure 3.4.

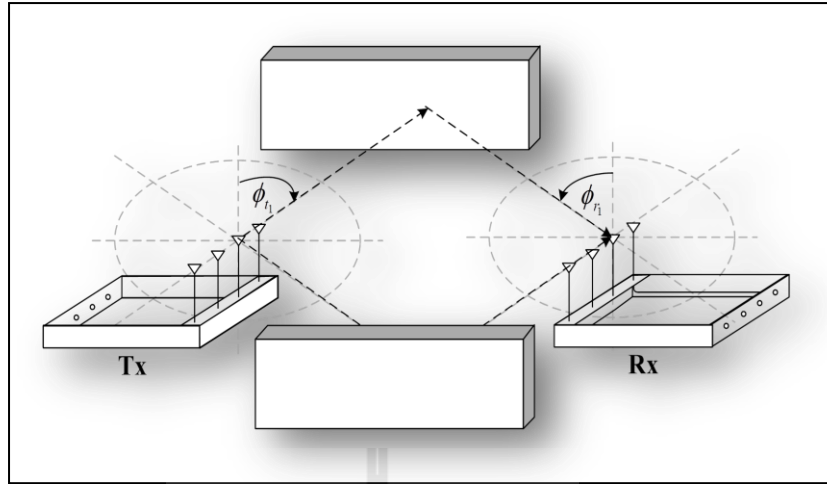


Figure 3.4 Array domain representations of MIMO channel with four transmitting and receiving antennas.

There is an arbitrary number of physical paths between the transmitter and receiver; the i th path having attenuation of a_i , makes an angle of ϕ_i ($\Omega_i := \cos \phi_i$) with the transmit antenna array and angle of ϕ_{ri} ($\Omega_{ri} := \cos \phi_{ri}$) with the receive antenna array. The channel matrix \mathbf{H} can be written as:

$$\mathbf{H} = \sum_i a_i^b \mathbf{e}_r(\Omega_{ri}) \mathbf{e}_t(\Omega_i)^* \quad (3.17)$$

$$a_i^b := a_i \sqrt{M_t M_r} \exp\left(\frac{j2\pi d_i}{\lambda_c}\right) \quad (3.18)$$

$$\mathbf{e}_t(\Omega) := \frac{1}{\sqrt{M_t}} \begin{bmatrix} 1 \\ \exp[j(2\pi\Delta_t\Omega)] \\ \vdots \\ \exp[j(N_t - 1)(2\pi\Delta_t\Omega)] \end{bmatrix} \quad (3.19)$$

$$\mathbf{e}_r(\Omega) := \frac{1}{\sqrt{M_r}} \begin{bmatrix} 1 \\ \exp[j(2\pi\Delta_r\Omega)] \\ \vdots \\ \exp[j(N_r-1)(2\pi\Delta_r\Omega)] \end{bmatrix} \quad (3.20)$$

Also, d_i is the distance between transmitting and receiving antennas along path i th. The vector $\mathbf{e}_t(\Omega)$ and the vector $\mathbf{e}_r(\Omega)$ are respectively the spatial signatures of transmitted and received units along the direction Ω , λ_c is the wavelength of the center frequency in the whole signal bandwidth. Δ_t is the normalized transmitting antenna and Δ_r is the normalized receiving antenna. When CSI is not available at the transmitter, the capacity of MIMO systems expressed in bits per second per hertz (bps/Hz) can be written as

$$C = \log_2 \det \left(\mathbf{I}_{M_r} + \frac{P_t}{P_N M_t} \mathbf{H} \mathbf{H}^* \right) \quad (3.21)$$

where \mathbf{I}_{M_r} is the identity matrix of size $M_r \times M_r$, \mathbf{H} is the channel matrix of size $M_r \times M_t$ with \mathbf{H}^* being its transpose conjugate, and P_t gives the average signal to noise ratio (SNR) per receiving branch.

3.4.4 Angular domain processing

The concept of angular domain can be represented by the transmitted and received signals. The signal arriving at a directional onto the receive antenna array is along the unit of spatial signature $\mathbf{e}_r(\Omega)$ given by (3.8). Hence, the M_r fixed vector is given by

$$\xi_r := \left\{ \mathbf{e}_r(0), \mathbf{e}_r\left(\frac{1}{L_r}\right), \dots, \mathbf{e}_r\left(\frac{M_r-1}{L_r}\right) \right\} \quad (3.22)$$

In (3.22), it can be noticed that there is a set of orthogonal basis for the received signal space. This basis provides the representation of received signals in the angular domain.

It is similarly defined for the angular domain representation of the transmitted signal. The signal transmitted at direction Ω is along the unit vector $\mathbf{e}_t(\Omega)$, defined in (3.22). The M_t fixed vector is given by

$$\xi_t := \left\{ \mathbf{e}_t(0), \mathbf{e}_t\left(\frac{1}{L_t}\right), \dots, \mathbf{e}_t\left(\frac{M_t-1}{L_t}\right) \right\} \quad (3.23)$$

Where $L_t = M_t \Delta_t$ and $L_r = M_r \Delta_r$ are the normalized antenna array lengths of the transmitter and receiver, respectively. Let \mathbf{U}_t and \mathbf{U}_r be the unitary matrices whose columns are the basis vectors in (3.22) and (3.23), respectively, can be written as:

$$\mathbf{U}_t = \frac{1}{\sqrt{M_t}} \exp\left(\frac{j2\pi kl}{M_t}\right) \quad k, l = 0, 1, \dots, M_t - 1. \quad (3.24)$$

$$\mathbf{U}_r = \frac{1}{\sqrt{M_r}} \exp\left(\frac{j2\pi kl}{M_r}\right) \quad k, l = 0, 1, \dots, M_r - 1. \quad (3.25)$$

The method can transform the array domain into the angular domain by

$$\mathbf{H}^A = \mathbf{U}_r^* \mathbf{H} \mathbf{U}_t \quad (3.26)$$

Thus, the capacity of MIMO systems is given by

$$C = \log_2 \det \left(\mathbf{I}_{N_r} + \frac{P_t}{P_N M_t} \mathbf{H}^A \mathbf{H}^{A*} \right) \quad (3.27)$$

Where \mathbf{I}_{M_r} is the identity matrix of size $M_r \times M_r$, \mathbf{H}^A is the channel matrix of size $M_r \times M_t$.

Figure 3.5 shows the simulated channel matrices from statistical modeling adopted by fundamentals of wireless communication book. The basis for the statistical modeling of MIMO fading channels is approximated by the physical paths partitioning into angularly resolvable bins and aggregated to form resolvable paths whose channel gains are \mathbf{H}^A . Assuming that a_i of the physical paths is independent. Then, this thesis use equations (3.18)-(3.20) to find channel matrix for array domain and equations (3.24)-(3.25) to find channel matrix for angular domain processing.

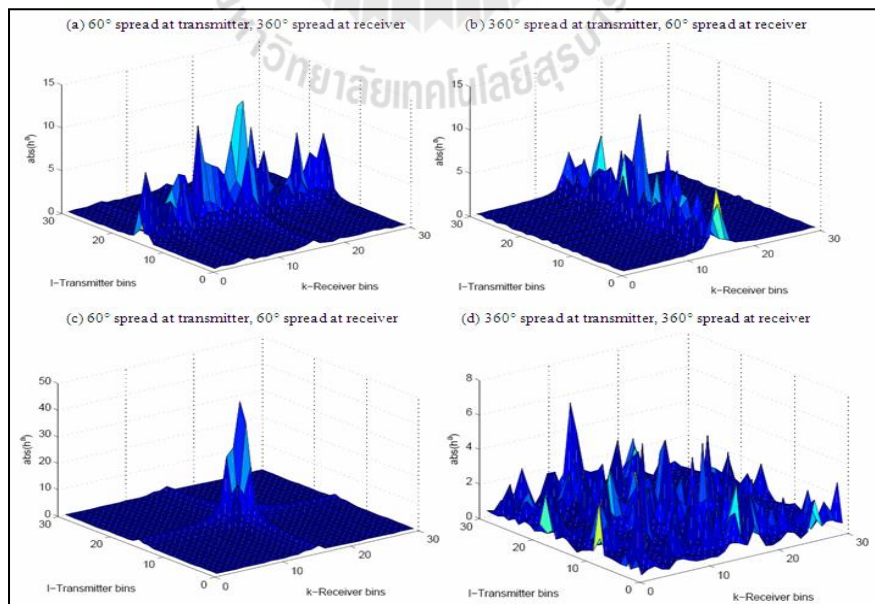


Figure 3.5 An example of \mathbf{H}^A with different angle spreads at transmitter/receiver.

3.5 Chapter summary

This chapter describes the background theory of MIMO systems. Then, this thesis considers narrowband model and many methods to find the channel capacity. In general, MIMO systems consider array domain processing with the reason that the array antennas experience the component of many angles such as angle of departure and angle of arrival. Therefore, this chapter uses angular domain processing for determining the channel capacity. The knowledge of this chapter is necessary to find the channel capacity of MIMO beamforming in the next chapter.



CHAPTER IV

MIMO BEAMFORMING

4.1 Introduction

This chapter describes the technique of MIMO beamforming which beamforming technique has gained a lot of attention. There are many techniques for improving the performance. Then, the popular techniques have been studied in this thesis including Eigen Beamforming (EB) and Quantized Beamforming (QB) techniques. The EB technique provides the best performance but, requiring full channel information. However, it is impossible to fully acquire the channel in a real fading environment. To overcome the limitations of the EB technique, the QB technique was proposed by using only some feedback bits instead of full channel information to calculate the suitable beamforming vectors. Unfortunately, the complexity of finding the beamforming vectors is the limitation of the QB technique. This thesis proposes a new technique named as Angular Beamforming (AB) to overcome drawbacks of QB technique. The proposed technique offers low computational complexity for finding the suitable beamforming vectors.

4.2 Angular beamforming technique

At the transmitter, the data symbol s is modulated by the beamforming vector \mathbf{u}_t and then, the signals are transmitted into a MIMO channel. At the receiver, there is the beamforming vector \mathbf{u}_r . Then, the receiving signals in Figure 4.1 is given by

$$y = \mathbf{u}_r^* [\mathbf{H} \mathbf{u}_t s + \mathbf{n}] \quad (4.1)$$

The beamforming vector \mathbf{u}_t at the transmitter and the beamforming vector \mathbf{u}_r at receiver in (4.1) are chosen to maximize the received SNR. Then, maximum the received SNR lead to maximum the receiving signals. Without loss of generality, this thesis assumes $\|\mathbf{u}_r\|^2 = 1$ and $E\{|s|^2\} = 1$. Then, the received SNR is expressed as

$$\rho = \frac{E\{\|\mathbf{u}_r^H \mathbf{H} \mathbf{u}_t s\|^2\}}{E\{\|\mathbf{u}_r^* \mathbf{n}\|^2\}} = \frac{\|\mathbf{u}_r^H \mathbf{H} \mathbf{u}_t\|^2}{\sigma_n^2} \quad (4.2)$$

The optimal transmitting beamformer is chosen as the eigen vector corresponding to the largest eigen value of $\mathbf{H} \mathbf{H}^H$. From (4.2), the maximized received SNR is $\rho = (\lambda_{\max}(\mathbf{H} \mathbf{H}^H)) / (\sigma_n^2)$. Note that λ_{\max} is the maximum eigen-value of a matrix and identically distributed complex gaussian random variable with zero-mean and variance σ_n^2 (X. Zheng, et.al, (2007)). This thesis applies the angles to determine beamforming vectors by selecting the beamforming vectors that give maximum SNR.

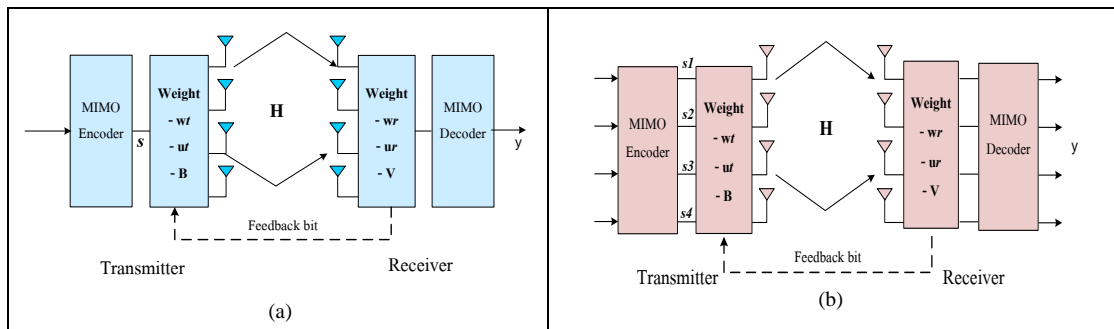


Figure 4.1 4x4 MIMO beamforming (a) 1 stream and (b) 4 streams.

Figure 4.1 shows 4x4 MIMO beamforming for (a) 1 stream and (b) 4 streams. In general, many researches consider 1 stream, but they have not illustrated multiple streams. In fact, the MIMO systems usually provide multiple streams. Therefore, this thesis considers both 1 stream and multiple streams.

The i th path having attenuation of a_i makes an angle of ϕ_{ti} ($\Omega_{ti} = \cos \phi_{ti}$) with the transmitting antenna array and an angle of ϕ_{ri} ($\Omega_{ri} = \cos \phi_{ri}$) with the receiving antenna array. The channel matrix \mathbf{H} can be written as:

$$\mathbf{H} = \sum_i a_i^b \mathbf{e}_r(\Omega_{ri}) \mathbf{e}_t(\Omega_{ti})^H \quad (4.3)$$

$$a_i^b = a_i \sqrt{N_t N_r} \exp\left(\frac{j2\pi d_i}{\lambda_c}\right) \quad (4.4)$$

$$\mathbf{e}_t(\Omega) = \frac{1}{\sqrt{N_t}} \begin{bmatrix} 1 \\ \exp[j(2\pi\Delta_t\Omega)] \\ \vdots \\ \exp[j(N_t-1)(2\pi\Delta_t\Omega)] \end{bmatrix} \quad (4.5)$$

$$\mathbf{e}_r(\Omega) = \frac{1}{\sqrt{N_r}} \begin{bmatrix} 1 \\ \exp[j(2\pi\Delta_r\Omega)] \\ \vdots \\ \exp[j(N_r-1)(2\pi\Delta_r\Omega)] \end{bmatrix} \quad (4.6)$$

Also, d_i is a distance between transmitting and receiving antennas along path i th. Note that $(.)^H$ is the conjugate and transpose operation. The vector $\mathbf{e}_t(\Omega)$ and $\mathbf{e}_r(\Omega)$ are the spatial signatures of transmitted and received units along the direction Ω ,

λ_c is the wavelength of the center frequency in a whole signal bandwidth. Assuming uniform linear array, the normalized separation between the transmitting antennas is Δ_t (antenna separation/ λ_c), and the normalized separation between receiving antennas is Δ_r (antenna separation/ λ_c). The reason of normalization is that the proposed technique can be worked in any frequency band. Hence, the normalization is made to neglect the unused parameter. The CSI is not available at the transmitter. The concept of AB technique can be represented by the transmitted and received signals. The low profile concept of AB technique, which is convenient for implementation, is proposed by just inserting \mathbf{u}_t and \mathbf{u}_r at both transmitter and receiver. The beamforming vectors depend on the angles of arrival and departure. The number of feedback bits defines the choice of angles (θ), $\theta \in [0, \pi)$. The angles are separation equally. The angle can be expressed as $N_i = 2^{B_i}$, N_i denoting the number of angle levels. B_i is the number of feedback bits. In comparing with QB technique, the procedure to find beamforming vectors of QB technique is more complexity than AB technique. The detail of QB technique is shown in the next section.

Let \mathbf{U}_t and \mathbf{U}_r be the beamforming matrices for multiple streams, but for 1 stream the \mathbf{U}_t and \mathbf{U}_r will be reduced to only the beamforming vectors. Beamforming matrices consist of a number of beamforming vectors according to the number of streams. In general, \mathbf{U}_t and \mathbf{U}_r can be written as:

$$\mathbf{U}_t = \frac{1}{\sqrt{M_t}} \exp(jlk\Delta_t \cos \theta); \quad l = 1, 2, \dots, M_t \quad (4.7)$$

$$\mathbf{U}_r = \frac{1}{\sqrt{M_r}} \exp(jmk\Delta_r \cos \theta); \quad m = 1, 2, \dots, M_r \quad (4.8)$$

Where $k = 2\pi / \lambda_c$. This thesis uses $\max \|\mathbf{U}_r^H \mathbf{H} \mathbf{U}_t\|^2$, which is maximum SNR, to find the maximum channel capacity. So, the maximum channel matrix of AB technique can be written as:

$$\mathbf{H}_{\max}^a = \mathbf{U}_{r\max}^H \mathbf{H} \mathbf{U}_{t\max} \quad (4.9)$$

Thus, the maximum channel matrix leads to maximum channel capacity. The maximum channel capacity (Tse D., et.al, (2005)) of AB technique is given by

$$C = \log_2 \det \left(\mathbf{I}_{M_r} + \frac{P_t}{P_N M_t} \mathbf{H}_{\max}^a \mathbf{H}_{\max}^{aH} \right) \quad (4.10)$$

where P_t is the transmitted power and P_N is the noise power in each branch of antennas at the receiver. Note that the signal to noise ratio (SNR) is defined as P_t/P_N .

\mathbf{I}_{M_r} is the identity matrix having $M_r \times M_r$ dimension, \mathbf{H} is the channel matrix having $M_r \times M_t$ dimension with H being its transpose conjugate. \mathbf{H}_{\max}^{aH} is the channel matrix of size $M_r \times M_t$ streams.

4.3 Quantized beamforming technique

The EB technique has the perfect knowledge on CSI. However, in many real systems, the CSI is hardly possible to be known exactly at the transmitter and receiver. Most of real systems realize the CSI by using feedback technique such as QB technique. The QB technique has been widely studied (M. Bishwarup, et.al, (2006) and X. Zheng, et.al, (2007)). This technique uses only some feedback bits

instead of all CSI to calculate the suitable beamforming vectors. The beamforming vector $\mathbf{w}_t(\theta_0, \theta_1, \dots, \theta_{M_t-1})$ is a function of M_t parameters $\{\theta_i, \theta_i \in [0, 2\pi)\}_{i=0}^{M_t-1}$ via simple manipulations.

$$\mathbf{w}_t(\theta_0, \theta_1, \dots, \theta_{M_t-1}) = \frac{1}{\sqrt{M_t}} e^{j\theta_0} \begin{bmatrix} 1 \\ e^{j\theta_1} \\ \vdots \\ e^{j\theta_{M_t-1}} \end{bmatrix} \quad (4.11)$$

Where $\|\mathbf{H}\mathbf{w}_t(\theta_0, \theta_1, \dots, \theta_{M_t-1})\|^2 = \|\mathbf{H}\mathbf{w}_t(\check{\theta}_1, \check{\theta}_2, \dots, \check{\theta}_{M_t-1})\|^2$.

This technique can be reduced by one parameter and quantize $\mathbf{w}_t(\check{\theta}_1, \check{\theta}_2, \dots, \check{\theta}_{M_t-1})$ instead of $\mathbf{w}_t(\theta_0, \theta_1, \dots, \theta_{M_t-1})$.

$$\mathbf{w}_t(\check{\theta}_1^{n_1}, \dots, \check{\theta}_{M_t-1}^{n_{M_t-1}}) = \frac{1}{\sqrt{M_t}} \begin{bmatrix} 1 \\ e^{j\check{\theta}_1^{n_1}} \\ \vdots \\ e^{j\check{\theta}_{M_t-1}^{n_{M_t-1}}} \end{bmatrix} \quad (4.12)$$

Where $\check{\theta}_i^{n_i} = (2\pi n_i)/(N_i)$, $0 \leq n_i \leq N_i - 1$, $i = 1, 2, \dots, M_t - 1$, with $N_i = 2^{B_i}$ and N_i is the number of quantization levels for feedback index $\check{\theta}_i$. B_i is the number of feedback bits for $\check{\theta}_i$. This technique quantizes the parameters $\check{\theta}_i$ to the round off grid point $\check{\theta}_i^{n_i}$, $i = 1, 2, \dots, M_t - 1$. Hence for this quantization scheme, this thesis needs to send the index set n_i from the receiver to the transmitter. Let \mathbf{w}_t and \mathbf{w}_r be the beamforming vector for 1 stream. For multiple streams, the notations of \mathbf{w}_t and \mathbf{w}_r

are the beamforming matrices. This requires $B = \sum_{i=1}^{M_r-1} B_i$ bits. The beamforming vector \mathbf{w}_r can be written as

$$\mathbf{w}_r = \frac{\mathbf{H}\mathbf{w}_t(\dot{\theta}_1^{n_i}, \dot{\theta}_2^{n_i}, \dots, \theta_{M_r-1}^{n_{M_r-1}})}{\left\| \mathbf{H}\mathbf{w}_t(\dot{\theta}_1^{n_i}, \dot{\theta}_2^{n_i}, \dots, \theta_{M_r-1}^{n_{M_r-1}}) \right\|} \quad (4.13)$$

The condition of maximum SNR can be used by $\max \left\| \mathbf{w}_r^* \mathbf{H} \mathbf{w}_t \right\|^2$ to find the maximum channel matrix of QB technique. Thus, the maximum channel matrix can be selected by the suitable beamforming vectors $\mathbf{w}_{t\max}$ at transmitting antennas and $\mathbf{w}_{r\max}$ at receiving antennas. The maximum channel matrix can be written as:

$$\mathbf{H}_{\max}^q = \mathbf{w}_{r\max}^H \mathbf{H} \mathbf{w}_{t\max} \quad (4.14)$$

Thus, the maximum channel matrix leads to maximum channel capacity. The maximum channel capacity (Tse D., et.al, (2005)) of QB technique is given by

$$C = \log_2 \det \left(\mathbf{I}_{M_r} + \frac{P_t}{P_N M_t} \mathbf{H}_{\max}^q \mathbf{H}_{\max}^{qH} \right) \quad (4.15)$$

Where \mathbf{I}_{M_r} is the $M_r \times M_r$ identity matrix and \mathbf{H}_{\max}^q is the $M_r \times M_t$ channel matrix of QB technique.

4.4 Eigen beamforming technique

The $M_r \times M_t$ channel matrix \mathbf{H} of MIMO systems can be separated by SVD technique which this technique can be called as the EB technique. Then, the channel matrix using SVD technique is given by

$$\mathbf{H} = \mathbf{B}\mathbf{S}\mathbf{V}^H \quad (4.16)$$

Where $M_t \times M_t$ matrix \mathbf{B} and the $M_r \times M_r$ matrix \mathbf{V} are unitary matrices, \mathbf{S} is $M_r \times M_t$ diagonal matrix. The beamforming vectors \mathbf{b} and \mathbf{v} can be found from unitary matrices \mathbf{B} and \mathbf{V} , respectively. The beamforming vectors are given by the first column of the unitary matrices. These two vectors are used to be the pre and post coding matrices at transmitter and receiver. So, the channel matrix of EB technique can be written as:

$$\mathbf{H}^e = \mathbf{b}^H \mathbf{H} \mathbf{v} \quad (4.17)$$

Thus, the channel capacity (Tse D., et.al, (2005)) of EB technique is given by

$$C = \log_2 \det \left(\mathbf{I}_{M_r} + \frac{P_t}{P_N M_t} \mathbf{H}^e \mathbf{H}^{eH} \right) \quad (4.18)$$

4.5 Simulation Results

The simulations are undertaken by MATLAB programming. The capacity results are evaluated by using (4.10), (4.15) and (4.18). Figure 4.2 has shown the average capacity versus SNR. This thesis increases the number of feedback bits and streams. Four cases are considered as (a) 1 stream at transmitter, 1 stream at receiver, (b) 2 streams at transmitter, 2 streams at receiver, (c) 3 streams at transmitter, 3 streams at receiver, (d) 4 streams at transmitter, 4 streams at receiver. The range of capacity enhancement depends on the number of feedback bits. To increase the number of feedback bits can improve the channel capacity. Also, to increase the number of streams can improve the channel capacity.

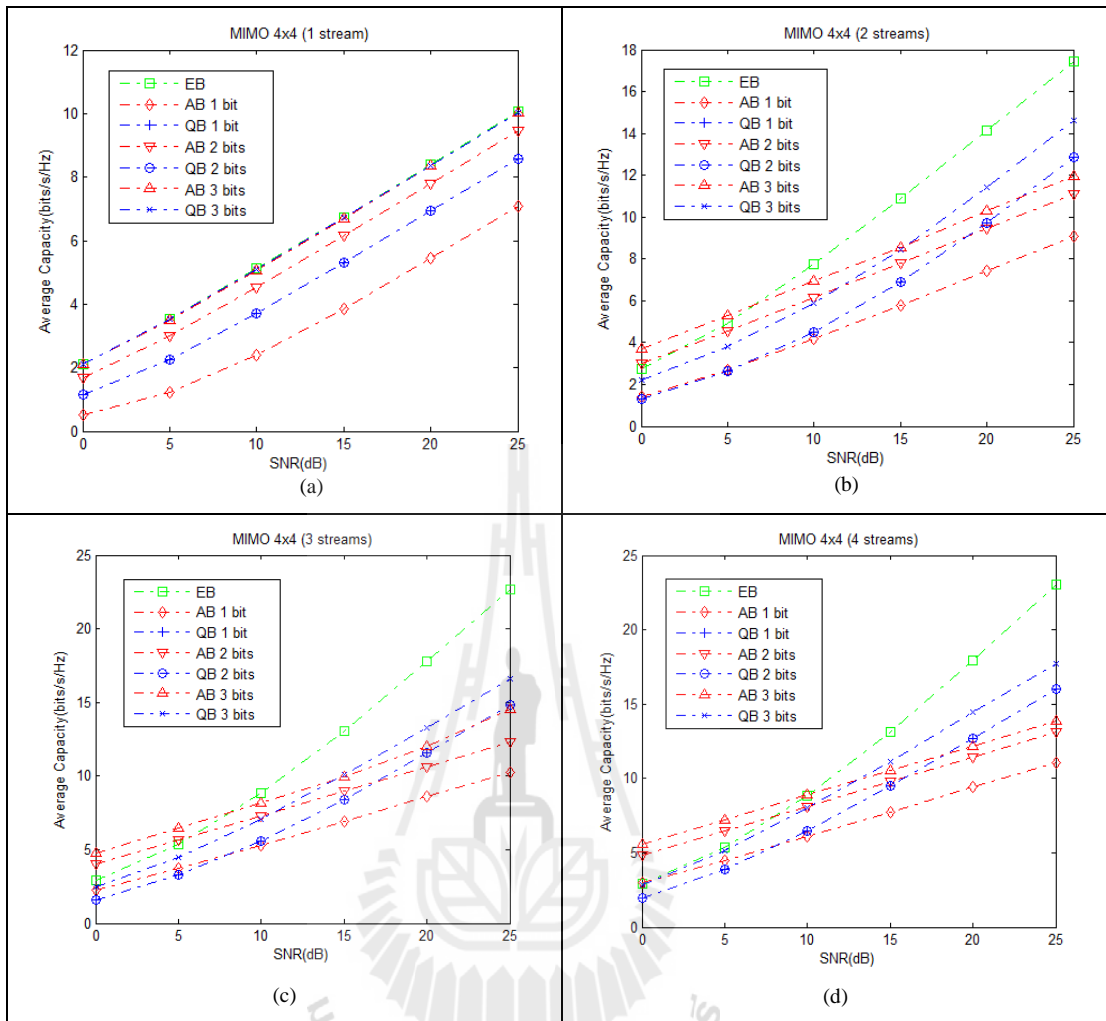


Figure 4.2 Capacity vs. SNR 1 stream, 2 streams, 3 streams and 4 streams.

The numeric values of average capacity at SNR = 10 dB are given in Table 4.1, 4.2, 4.3 and 4.4. It is obviously noticed that the benefit of AB technique is pronounced for all bits. Please remind that the improvement of MIMO capacity costs a little expense of inserting \mathbf{U}_t and \mathbf{U}_r at both transmitter and receiver without any extra complexity. The optimum EB technique offers better performance than QB and AB techniques. However, the implementation of AB technique is so easy that might be a good tradeoff in comparing with EB technique.

Table 4.5: The example of flop calculation for the QB technique.

QB	Flop
$N_i = 2^{B_i}$	$B-1$
$B_{a_1} = \lfloor B/(M_t-1) \rfloor$	2
$B_{a_2} = B_{a_1} + 1$	1
$N_s = B - B_{a_1} (M_t - 1)$	3
$\ddot{\theta}_i = \frac{2\pi n_i}{N_i}; 0 \leq n_i \leq N_i - 1$	2
Return loop $\theta_i^{n_i}$, which $\theta_i^{n_i}$ can be found by N_i	$B-1$
$\mathbf{w}_t(\ddot{\theta}_1^{n_1}, \dots, \theta_{M_t-1}^{n_{M_t-1}}) = \frac{1}{\sqrt{M_t}} \begin{bmatrix} 1 \\ e^{j\ddot{\theta}_1^{n_1}} \\ \vdots \\ e^{j\ddot{\theta}_{M_t-1}^{n_{M_t-1}}} \end{bmatrix}$	$s(M_t - 1)$
$\mathbf{w}_r = \frac{\mathbf{H}\mathbf{w}_t(\ddot{\theta}_1^{n_1}, \ddot{\theta}_2^{n_2}, \dots, \theta_{M_t-1}^{n_{M_t-1}})}{\ \mathbf{H}\mathbf{w}_t(\ddot{\theta}_1^{n_1}, \ddot{\theta}_2^{n_2}, \dots, \theta_{M_t-1}^{n_{M_t-1}})\ }$	$3s(M_t - 1)$
$h_s = \frac{1}{\sqrt{M_t}} \ \mathbf{w}_r^* \mathbf{H}\mathbf{w}_t\ ^2$	5
Return loop to find maximum channel from $N_i = 2^{B_i}$	$B-1$
Total	$2B^2 + B(4sM_t + 5) - 4sM_t - 7$

Many techniques define the complexity by big O notation. The big O notation describes the limiting behavior of a function when the argument tends towards a particular value in terms of simpler functions. It is a member of a larger family of notations. The big O notation considers the specifically largest of parameters but, this thesis cannot cut off some parameters. Because the complexity in this thesis depends

on many parameters and wants to analyze the delicacy of the information which the number of floating point operations (flops) can be used to replace big O notations. The computational complexity is calculated from a theoretical point of view, by giving the flop. A flop is here defined as one addition, subtraction, multiplication or division of two floating point numbers (Golub, G. H., et.al, (1989)). Therefore, this thesis uses flops for comparison between the performance of AB and QB techniques. Also, the flop can be related to the time delay in digital signal processing (DSP). The complexity of QB and AB techniques can be expressed in Table 4.5 and 4.6, respectively. It is clearly seen that the flop in Table 4.6 of AB technique is less than flop of QB technique presented in Table 4.5 which is shown in Figure 4.3. The method of calculating feedback bits in AB technique is so simpler than QB technique that the operating time of AB technique is shorter than QB technique which Figure 4.4 has shown the processing times for 4x4 MIMO beamforming 1, 2, 3 and 4 streams. The relations between Figure 4.3 and 4.4 can be discussed as follows. There is the same trend that the increase of flops will increase the processing times. However, the proportional value of increasing may not be exactly the same. Because the processing times in computer program calculate the times for all processings such as finding maximum SNR and keeping memory blocks for many factors. In turn, the flops ignore the time to manage with the memory blocks. Therefore, the number of flops is not the linear function of processing times.

Table 4.6: The example of flop calculation for the AB technique.

AB	Flop
$N_i = 2^{B_i}$	$B-1$
$\pi / 2^B$	1
Return loop θ , which θ can be found by N_i	$B-1$
$\mathbf{U}_t = \frac{1}{\sqrt{M_t}} \exp(jlk\Delta_t \cos \theta); l = 1, 2, \dots, M_t$	sM_t
$\mathbf{U}_r = \frac{1}{\sqrt{M_r}} \exp(jlk\Delta_r \cos \theta); l = 1, 2, \dots, M_r$	sM_r
$h_a = \frac{1}{\sqrt{M_t}} \ \mathbf{U}_r^* \mathbf{H} \mathbf{U}_t\ ^2$	5
Return loop to find maximum channel from $N_i = 2^{B_i}$	$B-1$
Total	$2B^2 + B(sM_t + sM_r + 3) - sM_t - sM_r - 5$

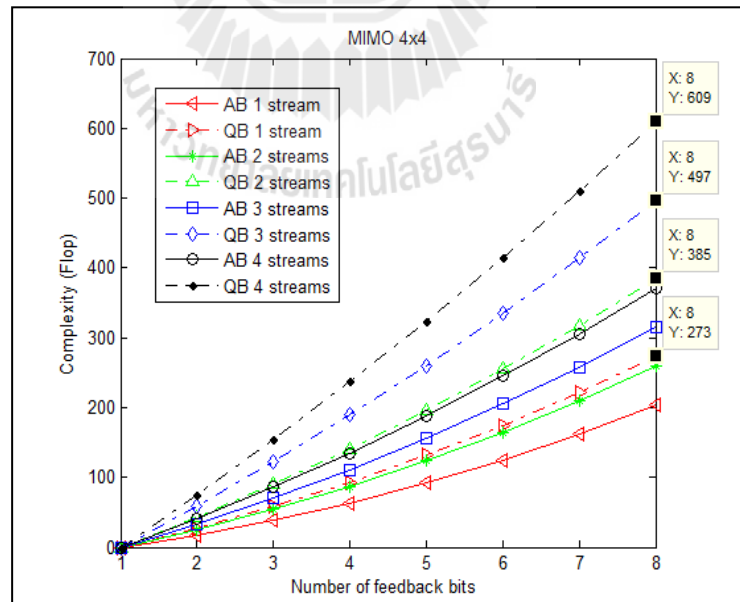


Figure 4.3 Complexity (flop) vs. number of feedback bits for 1, 2, 3 and 4 streams.

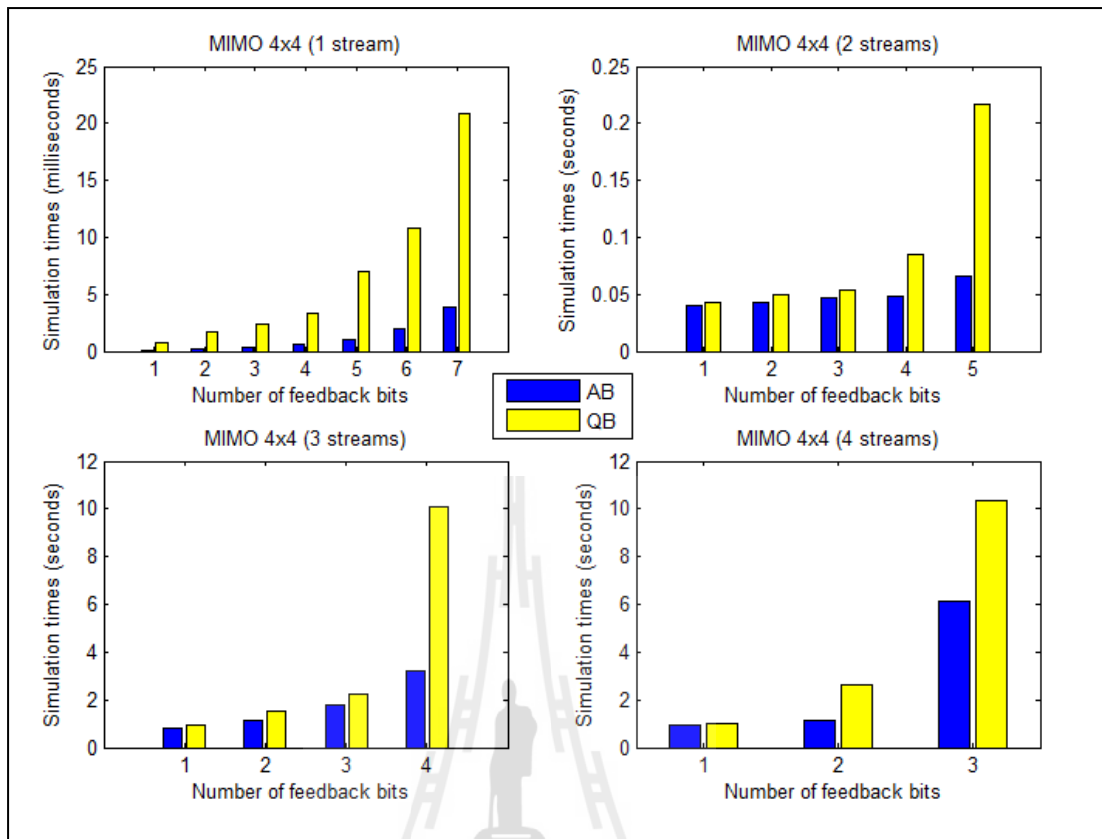


Figure 4.4 Simulation times vs. number of feedback bits for 1, 2, 3 and 4 streams.

4.6 Chapter summary

The contribution of this chapter falls into two main issues. The first contribution is the comparison offering the benefit to MIMO beamforming because it is easy to find the beamforming vectors. Secondly, the simulation times of AB and QB techniques are originally presented. It helps the reader to understand in a true benefit of AB technique that the QB technique has more complexity than AB technique, in terms of flops.

CHAPTER V

CHANNEL MEASUREMENT FOR MIMO

BEAMFORMING

5.1 Introduction

The previous chapter has focused on the concept of beamforming technique which the concept is confirmed by simulation results. But, the channel in simulations is not the real channel in practice because the channel model in simulations is randomly created by some specific paths. In turn, the multipath of real channel can not be known due to the different environments. Therefore, this chapter presents the construction of channel measurement for 4x4 MIMO beamforming techniques in order to validate the performance of proposed technique. The construction is designed for operating frequency 2.4 GHz. The block diagram of channel measurement for 4x4 MIMO beamforming is shown in Figure 5.1.

This chapter starts with the details of antenna. Next, the design of weighting network is discussed. This thesis uses phase shifter for weighting network. Finally, the part of control devices containing microprocessors to control components in weighting network is explained. The microcontroller is a digitally controlled beamforming system.

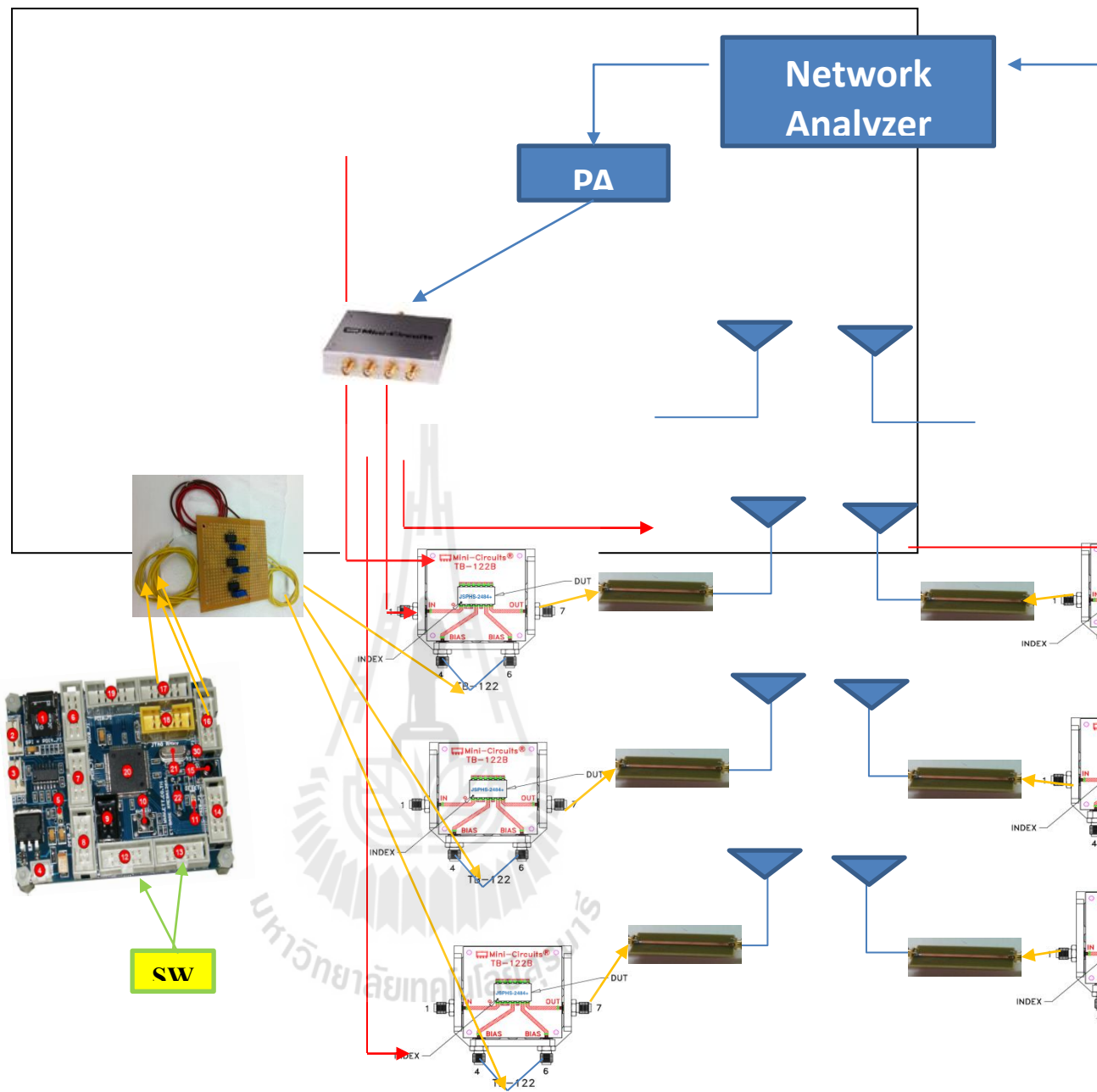


Figure 5.1 The block diagram of channel measurement for 4x4 MIMO beamforming.

5.2 Antennas

This section shows the array antennas followed by the monopole antenna. The monopole antenna works well in frequency 2.4 GHz. Also, it is compact enough to be

arranged to form the array having inter-element spacing of half wavelength. The geometrical configurations of monopole antennas are shown in Figure 5.2.

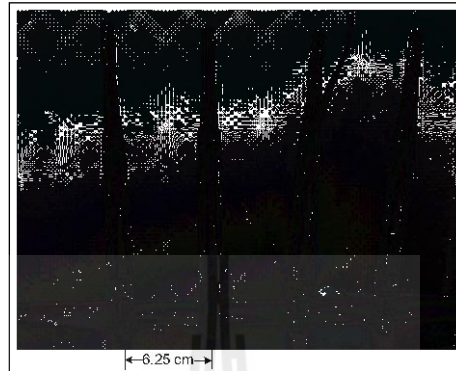


Figure 5.2 Monopole antenna structure.

5.3 Weighting networks

In the construction of channel measurement for MIMO beamforming, weighting networks consist of two major components: weighting systems and control devices which are explained in this section.

5.3.1 Weighting systems

The weighting systems consist of 3 components: phase shifters, power splitter/combiners and voltage multipliers. The details of each component are shown as follows:

(1) The first component is phase shifters. The receiving signals from each antenna are weighted by phase shifters which the systems are using phase shifters. The utilized phase shifters are a 50- Ω , offering a phase shifters range up to 15 volt with 0 volt serial interface. Each phase shifter operates very well over wide range of covering frequencies from 2.150 to 2.484 GHz. Operating Temperature - 40°C to 85°C. The operating frequency covers 2.4 GHz. The photograph of phase

shifters is shown in Figure 5.3 which is model number JSPHS-2484+ from minicircuit company. The operation of phase shifters can be explained using simplified schematic illustrated in Figure 5.4. The phase shifters state can be selected using different control volt as shown in Table 5.1.



Figure 5.3 Photograph of phase shifter.

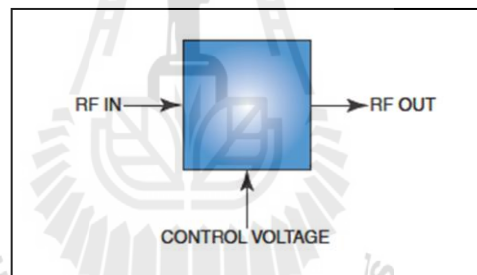


Figure 5.4 Simplified schematic of phase shifter

Table 5.1 Typical performance data for phase shifter

Control Voltage (V)	Phase Shift (Degrees)			
	2.15 GHz	2.30 GHz	2.40 GHz	2.484 GHz
0	0.01	0.00	0.00	0.00
1	5.06	4.69	4.93	4.22
2	10.50	9.70	10.50	8.68
3	17.42	16.05	17.26	14.29
4	27.60	25.25	25.39	22.27
5	42.79	38.72	35.37	33.71
6	63.72	56.65	48.73	48.52
7	89.57	77.62	76.29	65.24

8	119.07	99.77	89.25	82.32
9	151.83	122.45	112.71	99.06
10	187.02	145.74	135.37	115.49
11	222.21	169.98	157.44	135.24
12	254.14	195.10	178.14	148.56
13	280.85	220.25	198.82	165.52
14	302.85	244.62	217.94	183.15
15	320.70	266.91	236.41	201.15

The phase shifter is tested using network analyzer as shown in Figure 5.5 and the measurement result of attenuation factor for 0-15 volt at 2.4 GHz. Figure 5.6 is shown the example of measurement phase shifter at 2.4 GHz.

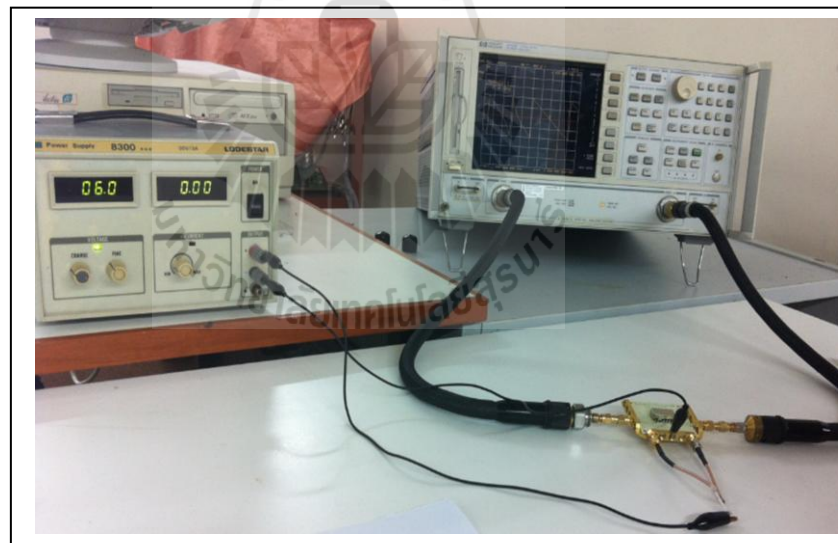


Figure 5.5 Set up for phase shifter testing.

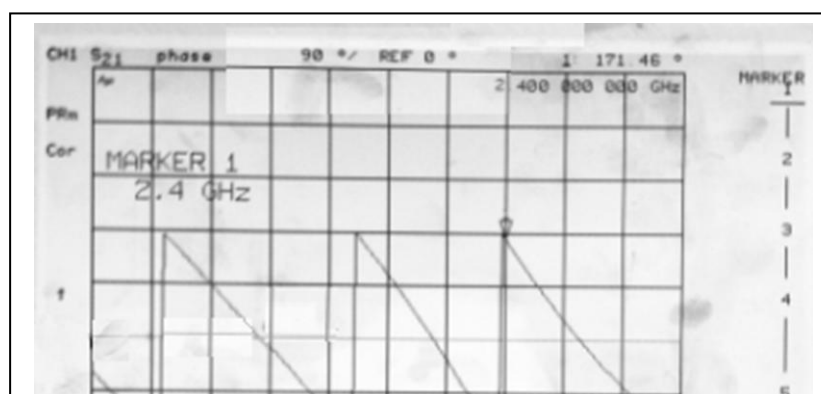


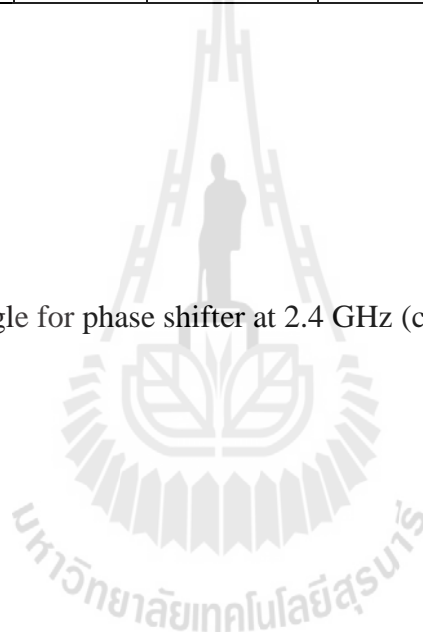
Figure 5.6 Measured phase shifter.

Table 5.2 Verified angle for phase shifter at 2.4 GHz

Number of feedback bits	Angle Number	Phase Shift		
		Beam direction (Degrees)	Phased of 2 nd antenna = Inter-element phasing (Degrees)	Control Voltage (V)
1	1	60	90	8
	2	120	270	8 + Phase 180
2	1	36	145.62	10
	2	72	55.62	6
	3	108	304.38	10 + Phase 180
	4	144	214.38	14
3	1	20	169.14	12
	2	40	137.89	10
	3	60	90	8
	4	80	31.26	5
	5	100	328.74	11 + Phase 180
	6	120	270	8 + Phase 180
	7	140	222.11	14
	8	160	190.86	13
4	1	10.59	176.93	12
	2	21.18	167.84	11
	3	31.77	153.03	11
	4	42.36	133.01	10

	5	52.95	108.45	9
	6	63.54	80.20	7
	7	74.13	49.22	6
	8	84.72	16.56	3
	9	95.31	343.34	11 + Phase 180
	10	105.9	310.69	10 + Phase 180
	11	116.49	279.71	9 + Phase 180
	12	127.08	251.47	6 + Phase 180
	13	137.67	226.93	15
	14	148.26	206.92	13
	15	158.85	192.12	13
	16	169.44	183.05	12

Table 5.2 Verified angle for phase shifter at 2.4 GHz (continued)



Number of feedback bits	Angle Number	Phase Shift		
		Beam direction (Degrees)	Phased of 2 nd antenna = Inter-element phasing (Degrees)	Control Voltage (V)
5	1	5.45	179.19	12
	2	10.9	176.75	12
	3	16.35	172.72	12
	4	21.8	167.13	11
	5	27.25	160.02	11
	6	32.7	151.47	11
	7	38.15	141.55	10
	8	43.6	130.35	10
	9	49.05	117.97	9
	10	54.5	104.53	9
	11	59.95	90.14	8
	12	65.4	72.93	7
	13	70.85	59.05	6
	14	76.3	42.63	6
	15	81.75	25.83	4
	16	87.2	8.79	2
	17	92.65	315.68	10 + Phase 180
	18	98.1	334.64	11 + Phase 180
	19	103.55	317.83	10 + Phase 180
	20	109	301.4	9 + Phase 180
	21	114.45	285.5	9 + Phase 180
	22	119.9	270.27	8 + Phase 180
	23	125.35	255.86	7 + Phase 180
	24	103.8	317.06	10 + Phase 180
	25	136.25	229.97	15
	26	141.7	218.74	14
	27	147.15	208.78	13
	28	152.6	200.19	13
	29	158.05	193.05	13
	30	163.5	187.41	12
	31	168.95	183.34	12
	32	174.4	180.86	12

Table 5.2 Verified angle for phase shifter at 2.4 GHz (continued)

Number of feedback bits	Angle Number	Phase Shift		
		Beam direction	Phased of 2 nd antenna = Inter-element phasing	Control Voltage

		(Degrees)	(Degrees)	(V)
	1	2.77	179.79	12
	2	5.54	179.16	12
	3	8.31	178.11	12
	4	11.08	176.64	12
	5	13.85	174.77	12
	6	16.62	172.48	12
	7	19.39	169.79	12
	8	22.16	166.70	11
	9	24.93	163.23	11
	10	27.7	159.37	11
	11	30.47	155.14	11
	12	33.24	150.55	11
	13	36.01	145.60	10
	14	38.78	140.32	10
	15	41.55	134.71	10
	16	44.32	128.78	10
	17	47.09	122.55	9
	18	49.86	116.04	9
	19	52.63	109.25	9
	20	55.4	102.21	9
	21	58.17	94.93	8
	22	60.94	87.43	8
	23	63.71	79.72	7
	24	66.48	71.83	7
	25	69.25	63.77	7
	26	72.02	55.56	6
	27	74.79	47.22	6
	28	77.56	38.78	5
	29	80.33	30.24	4
	30	83.1	21.62	4
	31	85.87	12.96	2
	32	88.64	4.72	1
	33	91.41	355.57	12 + Phase 180
	34	94.18	346.88	11 + Phase 180
	35	96.95	338.22	11 + Phase 180
	36	99.72	334.67	11 + Phase 180
	37	102.49	321.07	10 + Phase 180

6

Table 5.2 Verified angle for phase shifter at 2.4 GHz (continued)

Number of feedback bits	Angle Number	Phase Shift		
		Beam direction (Degrees)	Phased of 2 nd antenna = Inter-element phasing (Degrees)	Control Voltage (V)
6	38	105.26	312.62	10 + Phase 180
	39	108.03	304.29	10 + Phase 180
	40	110.8	296.08	9 + Phase 180
	41	113.57	288.02	9 + Phase 180
	42	116.34	280.13	8 + Phase 180
	43	119.11	272.43	8 + Phase 180
	44	121.88	264.93	8 + Phase 180
	45	124.65	257.66	7 + Phase 180
	46	127.42	250.62	7 + Phase 180
	47	130.19	243.84	15
	48	132.96	237.33	15
	49	135.73	231.11	15
	50	138.5	225.19	14
	51	141.27	219.58	14
	52	144.04	214.3	14
	53	146.81	209.37	13
	54	149.58	204.78	13
	55	152.35	200.56	13
	56	155.12	196.71	13
	57	157.89	193.24	13
	58	160.66	190.16	13
	59	163.43	187.48	12
	60	166.2	185.2	12
	61	168.97	183.33	12
	62	171.74	181.87	12
	63	174.51	180.83	12
	64	177.28	180.2	12

180° fixed phase shifters; the need of 180° fixed phase shifters is because the phase shifters from minicircuit company operate phase shift from 0-180 degrees. But, some weighting coefficients in this thesis require more than 180 degree phase shift. Therefore, this thesis must builds the 180° fixed phase shifter for shifting the phase around 360 degree. Then, this thesis uses 180 degree phase shifters to connect with phase shifter from minicircuit company. The 180 fixed phase shifters is designed by using FR-4 substrate. It can be calculated by

$$A = \frac{Z_0}{60} \sqrt{\frac{\varepsilon_r + 1}{2}} + \frac{\varepsilon_r - 1}{\varepsilon_r + 1} \left(0.23 + \frac{0.11}{\varepsilon_r} \right) \quad (5.1)$$

$$B = \frac{377\pi}{2(Z_0 \sqrt{\varepsilon_r})} \quad (5.2)$$

$$\frac{W}{d} = \begin{cases} \frac{8e^A}{e^{2A} - 2} & ; \frac{W}{d} < 2 \\ \frac{2}{\pi} \left[B - 1 \ln(2B - 1) + \frac{\varepsilon_r - 1}{2\varepsilon_r} \left\{ \ln(B - 1) + 0.39 - \frac{0.61}{\varepsilon_r} \right\} \right] & ; \frac{W}{d} > 2 \end{cases} \quad (5.3)$$

$$\varepsilon_e = \frac{\varepsilon_r + 1}{2} + \frac{\varepsilon_r - 1}{2} \frac{1}{\sqrt{1 + 12d/W}} \quad (5.4)$$

$$k_0 = \frac{2\pi}{\lambda} \quad (5.5)$$

$$\beta = \sqrt{\varepsilon_e} k_0 \quad (5.6)$$

$$\phi = \beta l \quad (5.7)$$

Where $Z_0 = 50 \Omega$, $f = 2.4$ GHz, $d = 1.6$ mm, $\varepsilon_r = 4.5$, $\phi = 180$ degree. Its size and dimension l can find from (5.7) = 7.4 cm. and $W = 3$ mm. which dimensions are shown in Figure 5.7. This component is utilized 180 degree to shift phase of the signal. The 180° fixed phase shifter can be connected to phase shifter from minicircuit company when some weighting coefficients require to shift the phase more than 180 degree. The phase shifter is manufactured as shown in Figure 5.8.

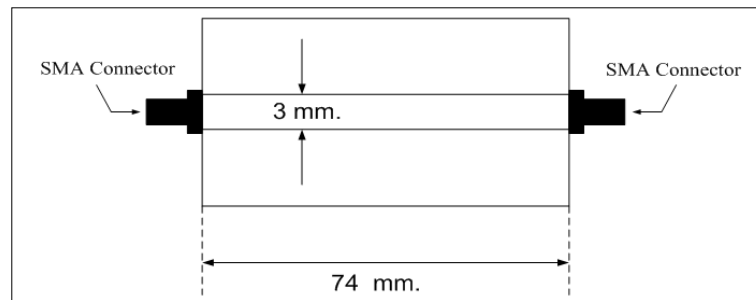


Figure 5.7 Diagram of phase shifter.



Figure 5.8 Photograph of phase shifter.

Figures 5.9 and 5.10 show the measured return loss for the phase shifter. The obtain results indicate that the return loss is lower than -10 dB over the designated band. This confirms that the designed phase shifter work well for proposed technique.

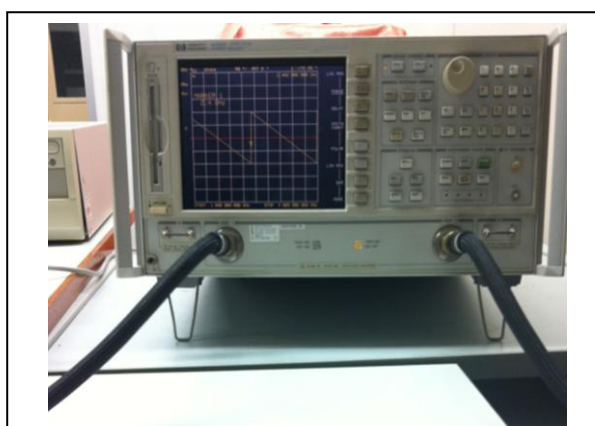


Figure 5.9 Photograph of measured return loss (S_{11}) of phase shifter.

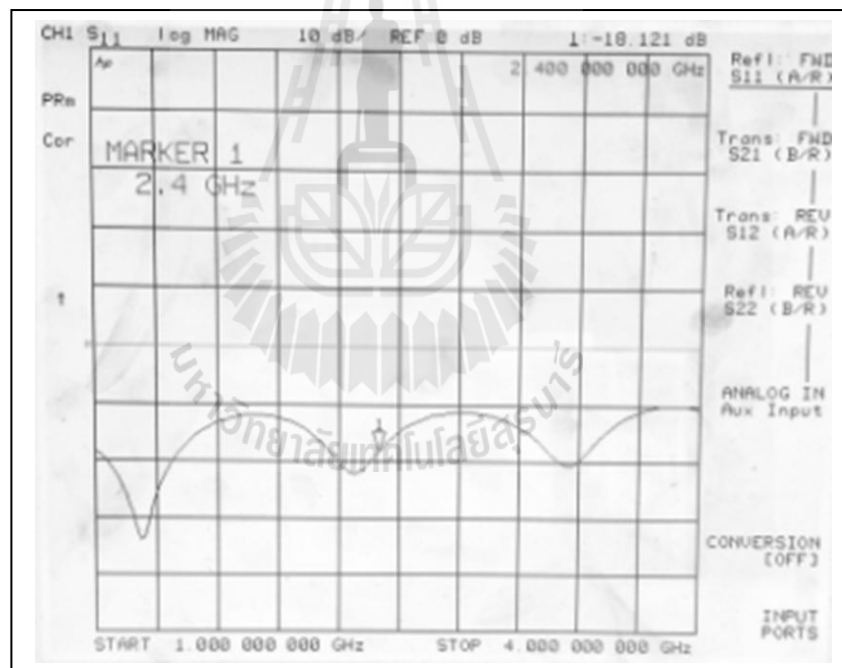


Figure 5.10 Measured return loss (S_{11}) of phase shifter Number 6 (Table 5.3).

In addition, Figure 5.11 shows that the designed phase shifter has a slight insertion loss throughout the designated band. Also, Figure 5.12 shows that output signal has 180° phase difference with input signal.

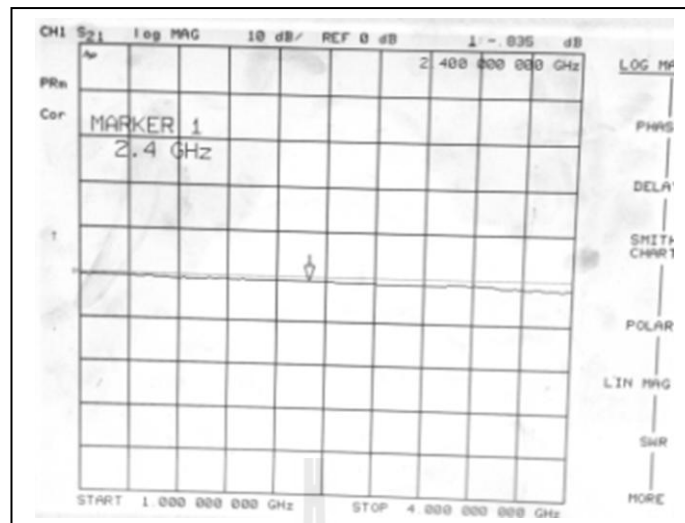


Figure 5.11 Measured insertion loss (S_{21}) of phase shifter Number 6 (Table 5.3).

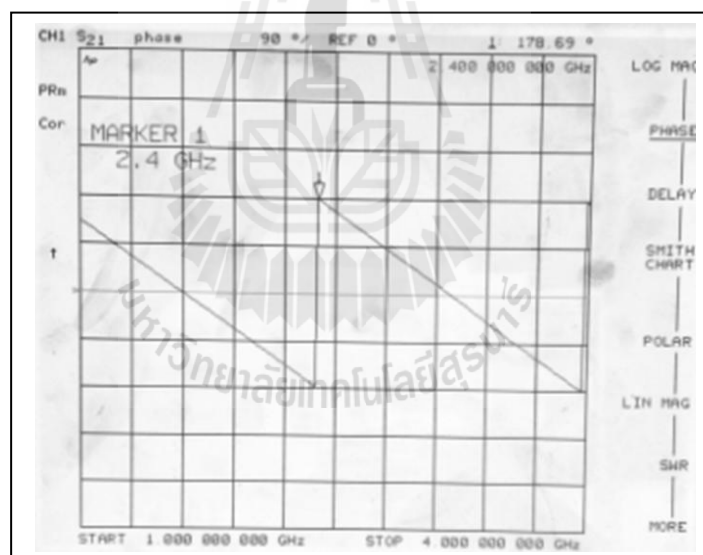


Figure 5.12 Phase difference between input and output signal of phase shifter Number 6 (Table 5.3).

The author builds 6 pieces for 180 degree phase shifter. The measurement parameters for phase shifter at 2.4 GHz are given in Table 5.3. It can be obviously

noticed that the 180 degree phase shifter of S_{21} (degree) are nearby 180 degree for all.

Table 5.3 Measured parameters for 180 degree phase shifter at 2.4 GHz

Number	S_{11} (dB)	S_{21} (dB)	S_{21} (degree)
1	-34.032	-0.780	179.89
2	-16.424	-1.034	179.28
3	-23.376	-0.709	179.89
4	-28.074	-0.669	-176.12
5	-32.274	-0.691	174.67
6	-18.121	-0.835	178.69

(2) The power splitter and combiner are designed for receiving signal from power amplifier and low noise amplifier, respectively. The photograph of power splitter/combiner number ZN4PD-272+ has shown in Figure 5.13. It operates the range of covering frequencies from 2.150 to 2.484 GHz.



Figure 5.13 Photograph of power splitter/combiner.

This product includes an internal control driver with 4-pin control and its circuit is shown in Figure 5.14. The RF control selects the electrical specifications at 25°C shown in Table 5.4

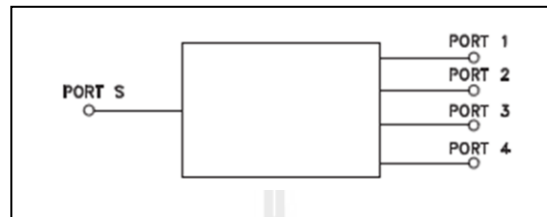


Figure 5.14 Electrical schematic of the power splitter/combiner.

Table 5.4 Electrical specifications at 25°C

Parameter	Frequency (MHz)	Min.	Typ.	Max.	Unit
Insertion Loss (above theoretical 6.0 dB)	500-1500	-	0.9	1.3	dB
	1500-2700	-	1.9	1.6	
Isolation	500-1500	15	25	-	dB
	1500-2700	15	22	-	
Phase Unbalance	500-1500	-	1.7	3	Degree
	1500-2700	-	3.1	6	
Amplitude Unbalance	500-1500	-	0.2	0.8	dB
	1500-2700	-	0.4	0.8	
VSWR (Port S)	500-1500	-	1.2	1.65	dB
	1500-2700	-	1.4	1.7	
VSWR Output (Port 1-4)	500-1500	-	1.2	1.6	dB
	1500-2700	-	1.2	1.5	

(3) A voltage multiplier is an electrical circuit that converts AC electrical power from a lower voltage to a higher DC voltage. Typically, the voltage multiplier uses a network of capacitors and diodes. Voltage multipliers can be used to generate a few volts up to purposing volts such as high energy. Figure 5.15 and 5.16 show diagram of voltage multiplier and the photograph of voltage multiplier, respectively. Then, the equation for calculating can be written as

$$V_{out} = \left(1 + \frac{R_f}{R_1}\right) V_{in} \quad (5.8)$$

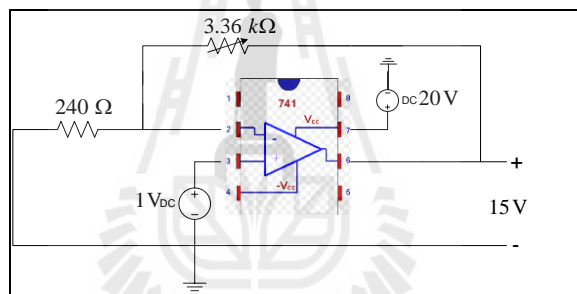


Figure 5.15 Diagram of voltage multiplier.

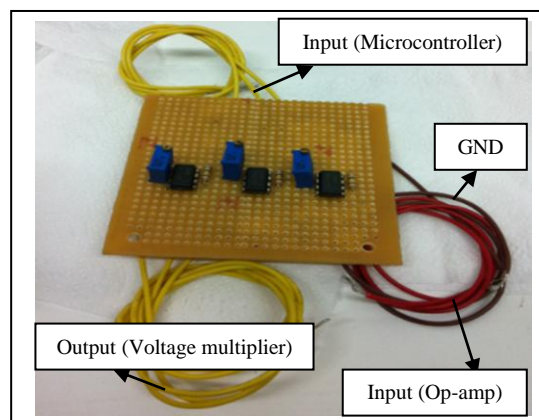


Figure 5.16 Photograph of voltage multiplier.

5.3.2 Control Device

Microcontroller of ATMEL is one of the most widespread microcontroller families. ATMEL has developed and improved capability of MCU to support various users' requirements. Moreover, ATMEL manufactures many chip MCU numbers; so, users have many choices to choose the most suitable MCU number for their proper applications easily and conveniently. Now, ATMEL improves and develops capability of the newest AVR MCU called "xMEGA" family that has more outstanding features and higher capability than the old AVR family. However, it still uses commands as same as the old AVR family. ATMEL has improved hardware system of the new version better and upgraded capability higher such as higher speed to process data, internal resource systems and low-power consumption. So, it is suitable for users who are familiar with AVR MAU because they will use the basic knowledge of the old AVR versions to develop xMEGA MCU easily. Board ET-BASE xMEGA128A1 are utilized to control phase shifter and switches. The reason to choose this type of control device is that it is low of cost but, able to meet the requirement in this thesis. Figure 5.17 demonstrates a Board ET-BASE xMEGA128A1. The Board ET-BASE xMEGA128A1 is a microcontroller board based on the ATmega128a1 which has 72 digital input/output pins. It has 4-channel 12bit DAC, a USB connection, a power jack, an ICSP header, and a reset button. It can be simply connected to a computer with a USB cable. Also, it can be powered with a AC-to-DC adapter or battery to get started. Table 5.5 shows summary of specification for xMEGA128A1.

- **No.19:** It is a connector GPIO (PC[0..7]).
- **No.20:** It is a MCU No.ATxMEGA128A1 (100Pin TQFP).
- **No.21:** It is a crystal 8MHz for Time Base of MCU.
- **No.22:** It is 32.768 KHz Crystal for Time Base for RTC internal MCU.

This thesis use No. 12 (AB method) and 13 (QB method) for input port that makes the number of feedback bit. The QB method use No.16 (PA2 and PA3) and 17 (PB2 and PB3) for output port that it can transfer analog to digital convertor transmission to phase shifter. The AB method use No.16 and 17 collaborating with voltage multiplier for transmission to phase shifter. Figure 5.18 shows the measurement voltages from microcontroller that support phase shifter for all feedback bits.

Table 5.5 Summary of specification of microcontroller “ET-BASExMEGA128A1

Parameters	Details
Operating Voltage	5V
2-Channel Circuit RS232	4-PIN
12 Bits DAC	4 channel
DC Current per I/O Pin	40 mA
DC Current for 3V Pin	50 mA
Flash Memory	128 KB (ATmega128a1) of which 8 KB used by boot loader
SRAM	8 KB
EEPROM	2 KB

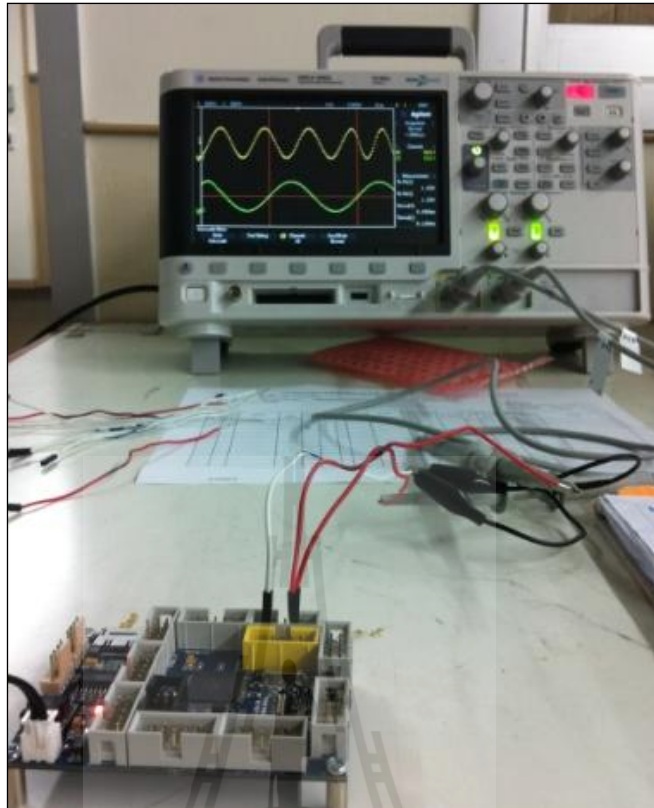


Figure 5.18 Measurement voltages from microcontroller.

5.4 Construction of channel measurement for MIMO beamforming

All parts discussed in section 5.3 are assembled to form a construction of channel measurement for 4×4 MIMO beamforming as shown in Figure 5.19. The power supply is located at the bottom of the shelf in order for microcontrollers and phase shifter.

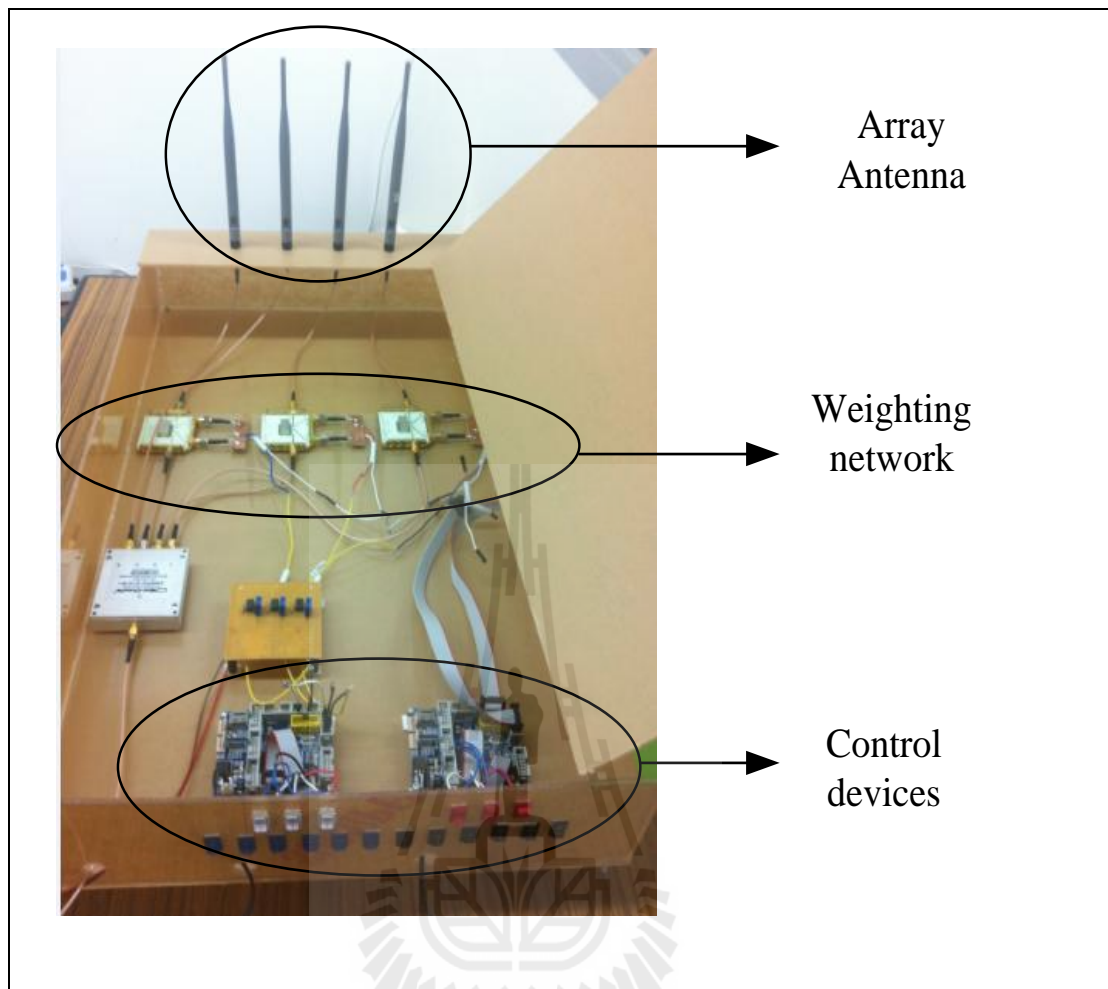


Figure 5.19 Photograph of full construction of channel measurement for MIMO beamforming.

5.5 Chapter summary

This chapter has shown the design and the construction of channel measurement for MIMO beamforming which consists of the three core components: antenna and weighting networks and control devices. Each components are discussed and some testing are confirmed the performances as expected.

CHAPTER VI

EXPERIMENTAL RESULTS

6.1 Introduction

The previous chapter has shown the design and construction of channel measurement for 4x4 MIMO beamforming. Then, this chapter presents the experimental results of channel measurement. The experimental results include the performance comparison between AB and QB techniques. Also, the beam direction of AB technique has been investigated in order to confirm the measured channel.

6.2 Experimental setup

First of all, the two microprocessors are programmed in order to control digital phase shifter and switches. Figure 6.1 shows the equipments of channel measurement for 4x4 MIMO beamforming.

Table 6.1 shows the weighting coefficients of AB techniques. The reason of chosen directions is the need of variation case between $\pm 360^\circ$ off bore sight direction. The receiving signals from each antenna are weighted by phase shifter from minicircuit company and 180° fixed phase shifter. The control voltages of each element are shown in Table 6.1.

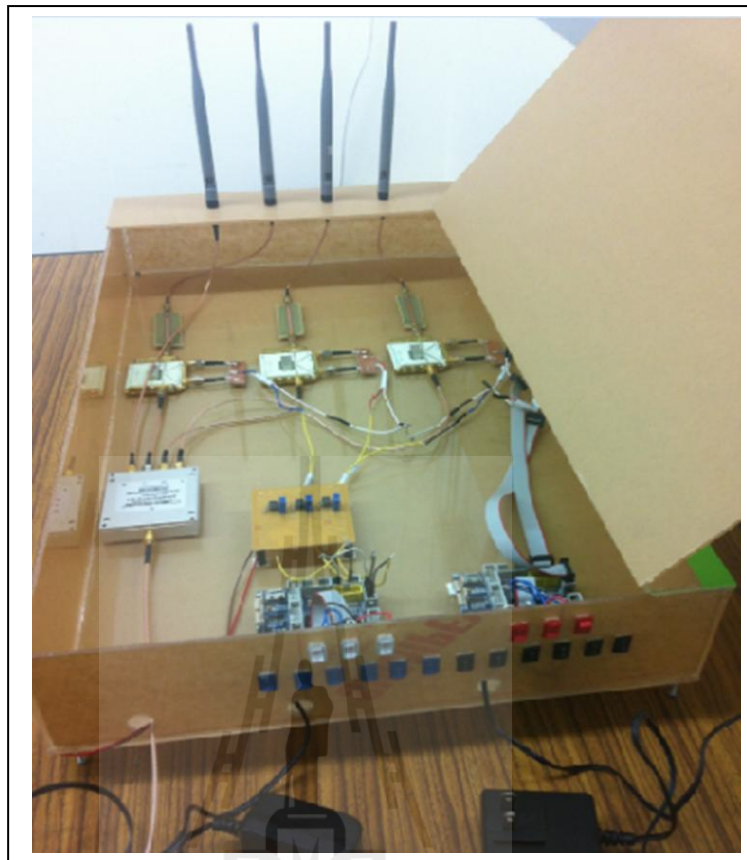


Figure 6.1 The equipments of channel measurement for 4×4 MIMO beamforming.

6.3 Experimental results and discussion

The measurement of beam directions is assembled as shown in Figure 6.2. This measurement is undertaken in chamber room. The beam directions are tested for confirming the construction of channel measurement. It can form the beam directions following the simulation results. Figure 6.3, 6.4 and 6.5 show the examples of the beam directions comparing between simulation and experimental results. There is a good agreement between simulation and measurement results. However, the shape and the level of null in measurement are different from simulations results. This may be caused by the loss in cable and connectors.

Table 6.1 Weighting coefficients of AB technique for 4×4 MIMO beamforming

Number of feedback bits	Angle number	Element number				Control voltage (V) of element number 2	Control voltage (V) of element number 3	Control voltage (V) of element number 4
		1 (Degree)	2 (Degree)	3 (Degree)	4 (Degree)			
1	1	0	90	180	270	8	12	8+ Phase 180
	2	0	270	180	90	8 + Phase 180	12	8
2	1	0	145.62	291.24	76.86	10	9+ Phase 180	7
	2	0	55.62	111.24	166.86	6	9	11
	3	0	304.83	248.76	192.74	10 + Phase 180	7+ Phase 180	13
	4	0	214.38	68.76	283.14	14	7	9+ Phase 180
3	1	0	169.14	338.28	147.42	12	11+ Phase 180	11
	2	0	137.89	275.78	53.67	10	8+ Phase 180	6
	3	0	90	180	270	8	12	8+ Phase 180
	4	0	31.26	62.52	93.78	5	6	8
	5	0	328.74	297.48	266.22	11 + Phase 180	9+ Phase 180	8 + Phase 180
	6	0	270	150	90	8 + Phase 180	12	8
	7	0	222.11	84.22	306.33	14	8	10+Phase 180
	8	0	190.86	21.72	212.58	13	4	5+ Phase 180
4	1	0	176.93	353.86	170.79	12	12+ Phase 180	12
	2	0	167.84	335.68	143.52	11	11+ Phase 180	10
	3	0	153.03	306.06	99.09	11	10+ Phase 180	8
	4	0	133.01	266.02	39.03	10	6+ Phase 180	5
	5	0	108.45	216.9	325.35	9	14	10+ Phase 180
	6	0	80.20	160.4	240.6	7	11	15
	7	0	49.22	98.44	147.66	6	8	11
	8	0	16.56	33.12	49.68	3	5	6
	9	0	343.34	326.68	310.02	11 + Phase 180	11+ Phase 180	10+ Phase 180
	10	0	310.69	216.38	212.07	10 + Phase 180	14	14
	11	0	279.71	199.42	119.13	9 + Phase 180	13	9
	12	0	251.47	142.94	34.41	6 + Phase 180	10	5
	13	0	226.93	93.86	320.79	15	8	10+ Phase 180
	14	0	206.92	53.84	260.76	13	6	7+ Phase 180
	15	0	192.12	24.24	216.36	13	4	14
	16	0	183.05	6.1	189.15	12	1	13

Table 6.1 Weighting coefficients of AB technique for 4×4 MIMO beamforming (continued)

Number of feedback bits	Angle number	Element number				Control voltage (V) of element number 2	Control voltage (V) of element number 3	Control voltage (V) of element number 4
		1 (Degree)	2 (Degree)	3 (Degree)	4 (Degree)			
5	1	0	179.19	358.38	177.57	12	12+ Phase 180	12
	2	0	176.75	353.5	170.25	12	12+ Phase 180	12
	3	0	172.72	345.44	158.16	12	12+ Phase 180	11
	4	0	167.13	334.26	141.39	11	11+ Phase 180	10
	5	0	160.02	320.04	120.06	11	10+ Phase 180	9
	6	0	151.47	302.94	94.41	11	9+ Phase 180	8
	7	0	141.55	283.1	64.65	10	9+ Phase 180	7
	8	0	130.35	260.7	31.05	10	7+ Phase 180	5
	9	0	117.97	235.94	353.91	9	15	12+ Phase 180
	10	0	104.53	209.06	313.59	9	13	10+ Phase 180
	11	0	90.14	180.28	270.42	8	12	8+ Phase 180
	12	0	72.93	145.86	218.79	7	10	14
	13	0	59.05	118.1	177.15	6	6	12
	14	0	42.63	85.26	127.89	6	8	10
	15	0	25.83	51.66	77.49	4	6	7
	16	0	8.97	17.58	26.37	2	3	4
	17	0	315.68	271.36	227.04	10 + Phase 180	8+ Phase 180	15
	18	0	334.64	309.28	283.92	11 + Phase 180	10+ Phase 180	9+ Phase 180
	19	0	317.83	275.66	233.49	10 + Phase 180	8+ Phase 180	15
	20	0	301.4	272.8	214.2	9 + Phase 180	8+ Phase 180	6+ Phase 180
	21	0	285.5	211	136.5	9 + Phase 180	14	10
	22	0	270.27	180.54	90.81	8 + Phase 180	12	8
	23	0	255.86	151.72	47.58	7 + Phase 180	11	6
	24	0	317.06	274.12	231.18	10 + Phase 180	8+ Phase 180	15
	25	0	229.97	99.94	329.91	15	8	11+ Phase 180
	26	0	218.74	77.48	296.22	14	7	9+ Phase 180
	27	0	208.78	57.56	266.34	13	6	8+ Phase 180
	28	0	200.19	40.38	240.57	13	5	15
	29	0	193.05	26.1	219.15	13	4	14
	30	0	187.41	14.82	202.23	12	3	13
	31	0	183.34	6.68	190.02	12	1	13
	32	0	180.86	1.72	182.58	12	1	12

Table 6.1 Weighting coefficients of AB technique for 4×4 MIMO beamforming (continued)

Number of feedback bits	Angle number	Element number				Control voltage (V) of element number 2	Control voltage (V) of element number 3	Control voltage (V) of element number 4
		1 (Degree)	2 (Degree)	3 (Degree)	4 (Degree)			
6	1	0	179.79	359.58	179.37	12	12+ Phase 180	12
	2	0	179.16	358.32	177.48	12	12+ Phase 180	12
	3	0	178.11	356.22	174.33	12	12+ Phase 180	11
	4	0	176.64	353.28	169.92	12	11+ Phase 180	11
	5	0	174.77	349.54	164.31	12	11+ Phase 180	11
	6	0	172.48	344.96	157.44	12	11+ Phase 180	11
	7	0	169.79	339.58	149.37	12	11+ Phase 180	11
	8	0	166.70	333.4	140.1	11	11+ Phase 180	10
	9	0	163.23	326.46	129.69	11	10+ Phase 180	10
	10	0	159.37	318.74	118.11	11	10+ Phase 180	9
	11	0	155.14	310.28	105.42	11	10+ Phase 180	9
	12	0	150.55	301.1	91.65	11	9+ Phase 180	8
	13	0	145.60	291.2	76.8	10	9+ Phase 180	7
	14	0	140.32	280.64	60.96	10	9+ Phase 180	6
	15	0	134.71	269.42	44.13	10	8+ Phase 180	5
	16	0	128.78	257.56	26.34	10	7+ Phase 180	4
	17	0	122.55	245.1	7.65	9	6+ Phase 180	1
	18	0	116.04	232.08	348.12	9	15	11+ Phase 180
	19	0	109.25	218.5	327.75	9	14	10+ Phase 180
	20	0	102.21	204.42	306.63	9	13	9+ Phase 180
	21	0	94.93	189.86	284.79	8	12	8+ Phase 180
	22	0	87.43	174.86	262.29	8	12	8+ Phase 180
	23	0	79.72	159.44	239.16	7	11	15
	24	0	71.83	143.66	215.59	7	10	14
	25	0	63.77	127.54	191.31	7	9	13
	26	0	55.56	111.12	166.68	6	9	11
	27	0	47.22	94.44	141.66	6	8	10
	28	0	38.78	77.56	116.34	5	7	9
	29	0	30.24	60.48	90.72	4	6	8
	30	0	21.62	43.24	64.86	4	6	6
	31	0	12.96	25.65	38.61	2	4	5
	32	0	4.72	9.44	14.16	1	2	3

Table 6.1 Weighting coefficients of AB technique for 4×4 MIMO beamforming (continued)

Number of feedback bits	Angle number	Element number				Control voltage (V) of element number 2	Control voltage (V) of element number 3	Control voltage (V) of element number 4
		1 (Degree)	2 (Degree)	3 (Degree)	4 (Degree)			
6	33	0	355.57	351.14	346.71	12 + Phase 180	12 + Phase 180	11 + Phase 180
	34	0	346.88	333.76	320.64	11 + Phase 180	11 + Phase 180	10 + Phase 180
	35	0	338.22	316.44	294.66	11 + Phase 180	10 + Phase 180	9 + Phase 180
	36	0	334.67	309.34	284.01	11 + Phase 180	10 + Phase 180	8 + Phase 180
	37	0	321.07	282.14	243.01	10 + Phase 180	9 + Phase 180	6 + Phase 180
	38	0	312.62	265.24	217.86	10 + Phase 180	8 + Phase 180	14
	39	0	304.29	248.58	192.87	10 + Phase 180	7 + Phase 180	13
	40	0	296.08	232.16	168.24	9 + Phase 180	15	11
	41	0	288.02	216.04	144.06	9 + Phase 180	14	10
	42	0	280.13	200.26	120.39	8 + Phase 180	13	9
	43	0	272.43	184.86	97.29	8 + Phase 180	11	8
	44	0	264.93	169.86	74.79	8 + Phase 180	11	7
	45	0	257.66	155.32	52.98	7 + Phase 180	10	6
	46	0	250.62	141.24	31.86	7 + Phase 180	10	5
	47	0	243.84	127.68	11.52	6 + Phase 180	9	2
	48	0	237.33	114.66	251.99	15	9	7 + Phase 180
	49	0	231.11	102.22	333.33	15	8	11 + Phase 180
	50	0	225.19	90.38	315.57	14	8	10 + Phase 180
	51	0	219.58	79.16	298.74	14	7	9 + Phase 180
	52	0	214.3	68.6	282.9	14	7	8 + Phase 180
	53	0	209.37	58.69	268.01	13	7	8 + Phase 180
	54	0	204.78	49.56	254.34	13	6	7 + Phase 180
	55	0	200.56	41.12	241.68	13	6	6 + Phase 180
	56	0	196.71	33.42	230.13	13	5	15
	57	0	193.24	26.48	219.72	13	4	14
	58	0	190.16	20.32	210.48	13	3	13
	59	0	187.48	14.96	202.44	12	3	13
	60	0	185.2	10.4	195.6	12	2	12
	61	0	183.33	6.66	189.99	12	2	12
	62	0	181.87	3.74	185.61	12	1	12
	63	0	180.83	1.66	182.49	12	1	12
	64	0	180.2	0.4	180.6	12	1	12



Figure 6.2 Assembly of MIMO beamforming tested in chamber room.

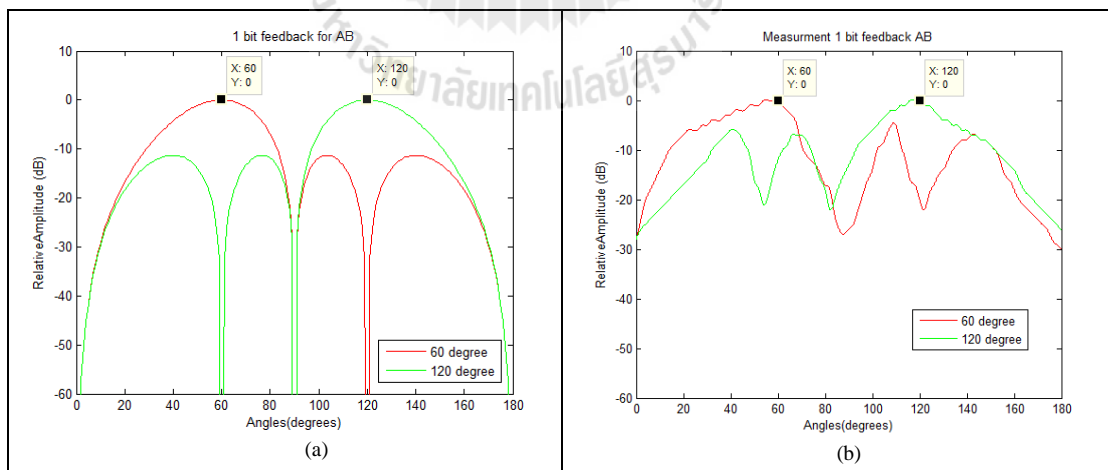


Figure 6.3 (a) Simulated and (b) measured beam directions using AB technique

for 1 bit feedback when the beam directions are 60° and 120°

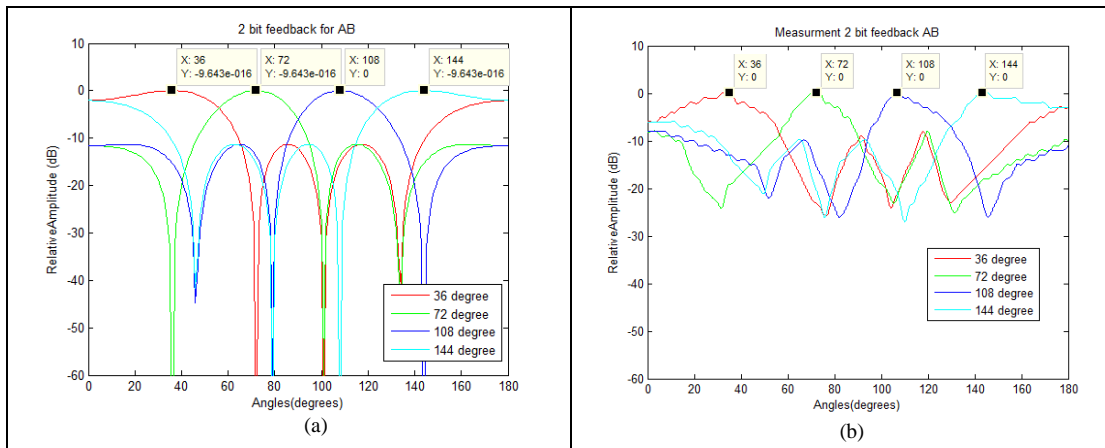


Figure 6.4 (a) Simulated and (b) measured beam directions using AB technique for 2 bit feedback when the beam directions are 36° , 72° , 108° and 144° .

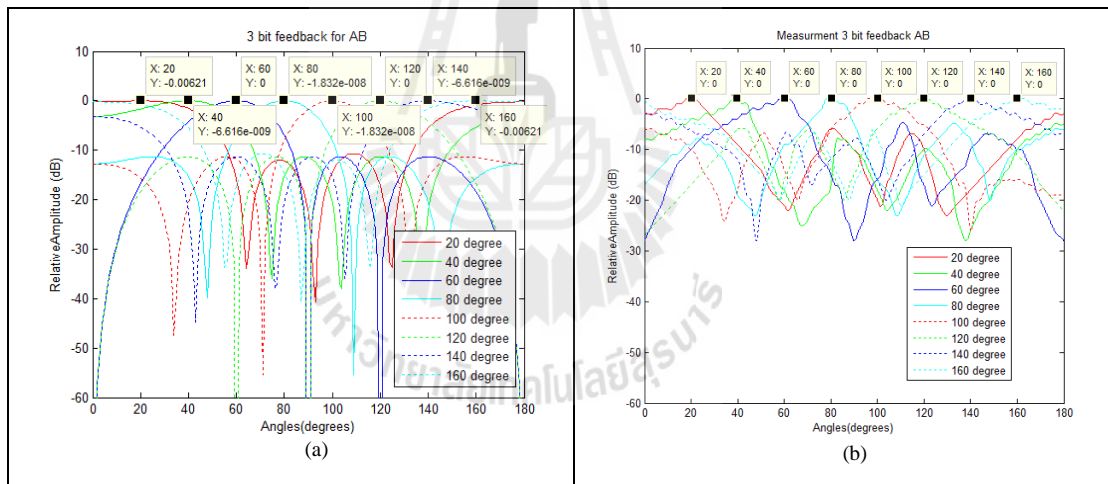


Figure 6.5 (a) Simulated and (b) measured beam directions using AB technique for 3 bit feedback when the beam directions are 20° , 40° , 60° , 80° , 100° , 120° , 140° and 160° .

The channel measurements can be described as follows. Figure 6.6 shows measurement scenarios. This thesis chooses a large room to provide various test conditions. The location of the transmitter is fixed as shown by rectangular symbol. There are five measured locations for the receiver represented by circular symbols. The four array antennas at both transmitter and receiver are used. The center frequency (λ_c) is 2.4 GHz. The separation between transmit and receiving antenna (Δ_t, Δ_r) are $\lambda_c / 2$. The distance between transmitters (Tx) and receiver (Rx) location 1, 2, 3, 4 and 5 are 1.9, 6.8, 13.5, 6.3 and 8.7 meters, respectively. Figure 6.7 shows a block diagram of channel measurement for 4×4 MIMO beamforming. It is easy to measure both QB and AB techniques by using switches. The measurement results achieved by network analyzer are used as a channel response in MIMO systems. The network analyzer is used for measuring channel coefficients in magnitude and phase. The power amplifier (PA) is used at transmitter to provide more transmitted power. The low noise amplifier (LNA) is used at the receiver to increase the appropriated received signal level. Therefore, the measured channels can be directly compared to each other as presented in the following. Figure 6.8 shows the photograph of measurement set up for location 1. The channel matrices \mathbf{H}^{AB} and \mathbf{H}^{QB} can be realized by measured data from network analyzer. The measured channels are collected by changing locations of the receiver. This thesis also believes that the mismatches among RF circuits in transmitting/receiving components and mutual coupling effects are included in the measured channel. The simulations are undertaken by utilizing measured data into MATLAB programming. This thesis considers 4 streams. The capacity results are evaluated by using (4.10) and (4.15) for AB and QB techniques, respectively.

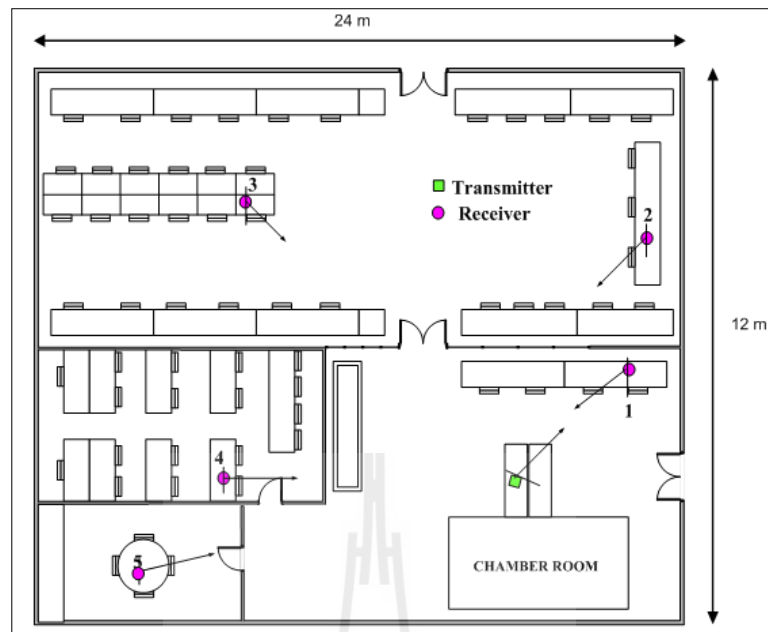


Figure 6.6 Measurement scenarios.

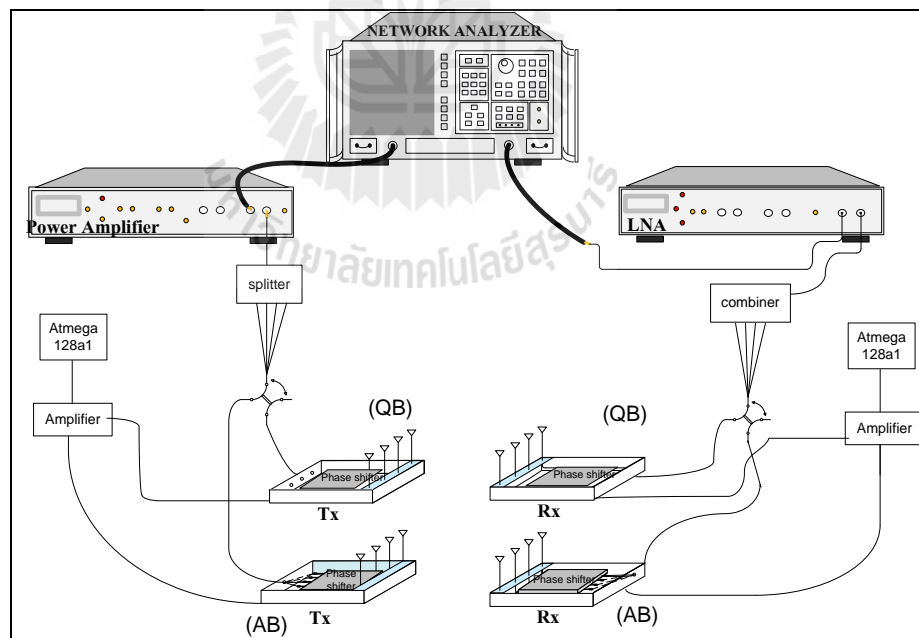


Figure 6.7 Block diagram of channel measurement for 4x4 MIMO beamforming.



Figure 6.8 The photograph of measurement set up for location 1.

Figure 6.9 shows the capacity versus SNR for AB technique at each location. Six cases are considered as (a) location 1, (b) location 2, (c) location 3, (d) location 4, (e) location 5 and (f) all locations in Figure 6.9. In the same way, Figure 6.10 shows the capacity versus SNR for QB technique at each location. The capacities in Figure 6.9 and 6.10 are considered at 4 streams. The changing locations lead to change the channels which give changing the performance. The range of capacity enhancement depends on the number of feedback bits. Figure 6.9 and Figure 6.10 have the same trend at all locations. The results also indicate that to increase the number of feedback bits will increase the channel capacity.

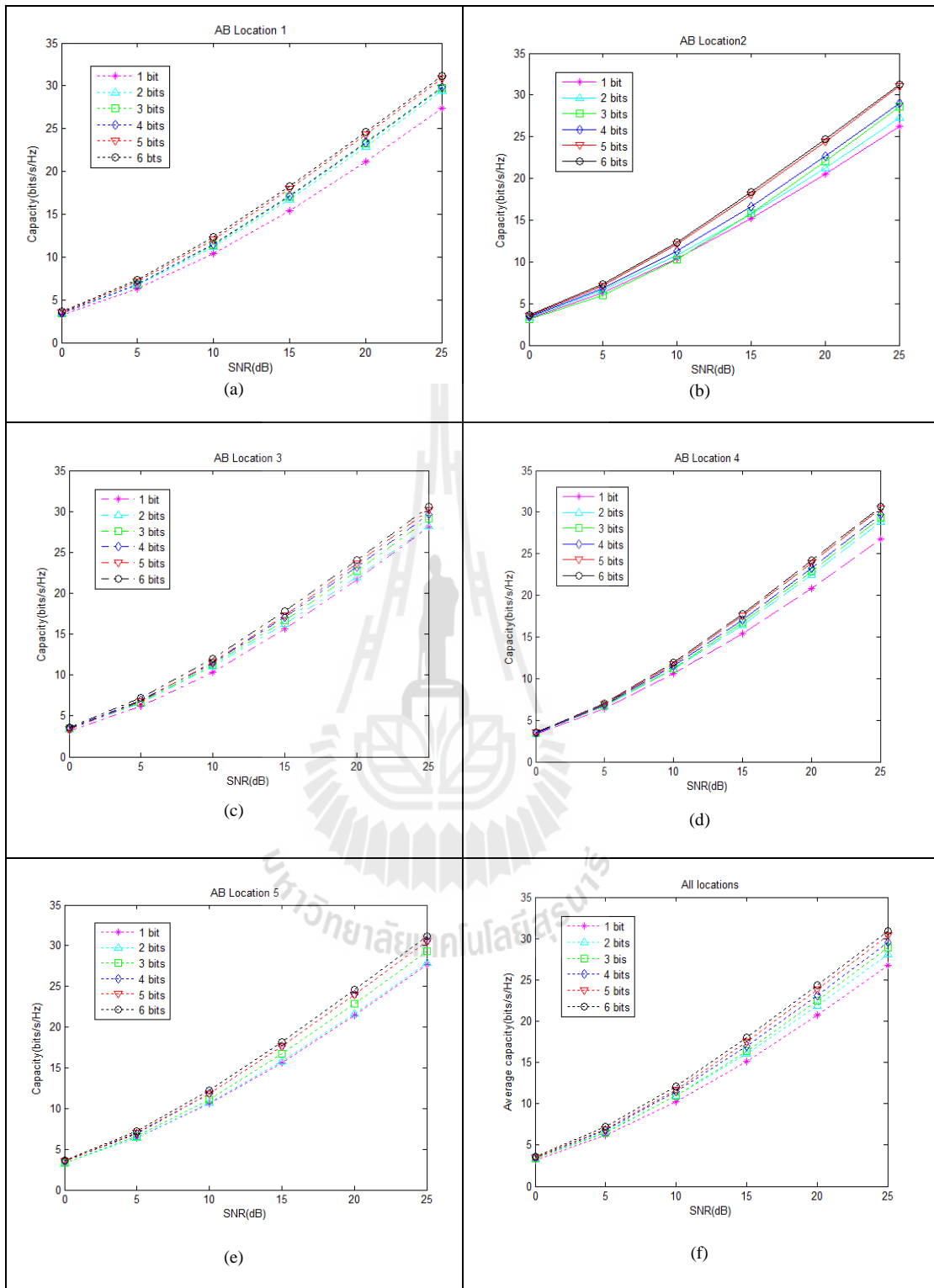


Figure 6.9 The capacity versus SNR for AB technique at each location.

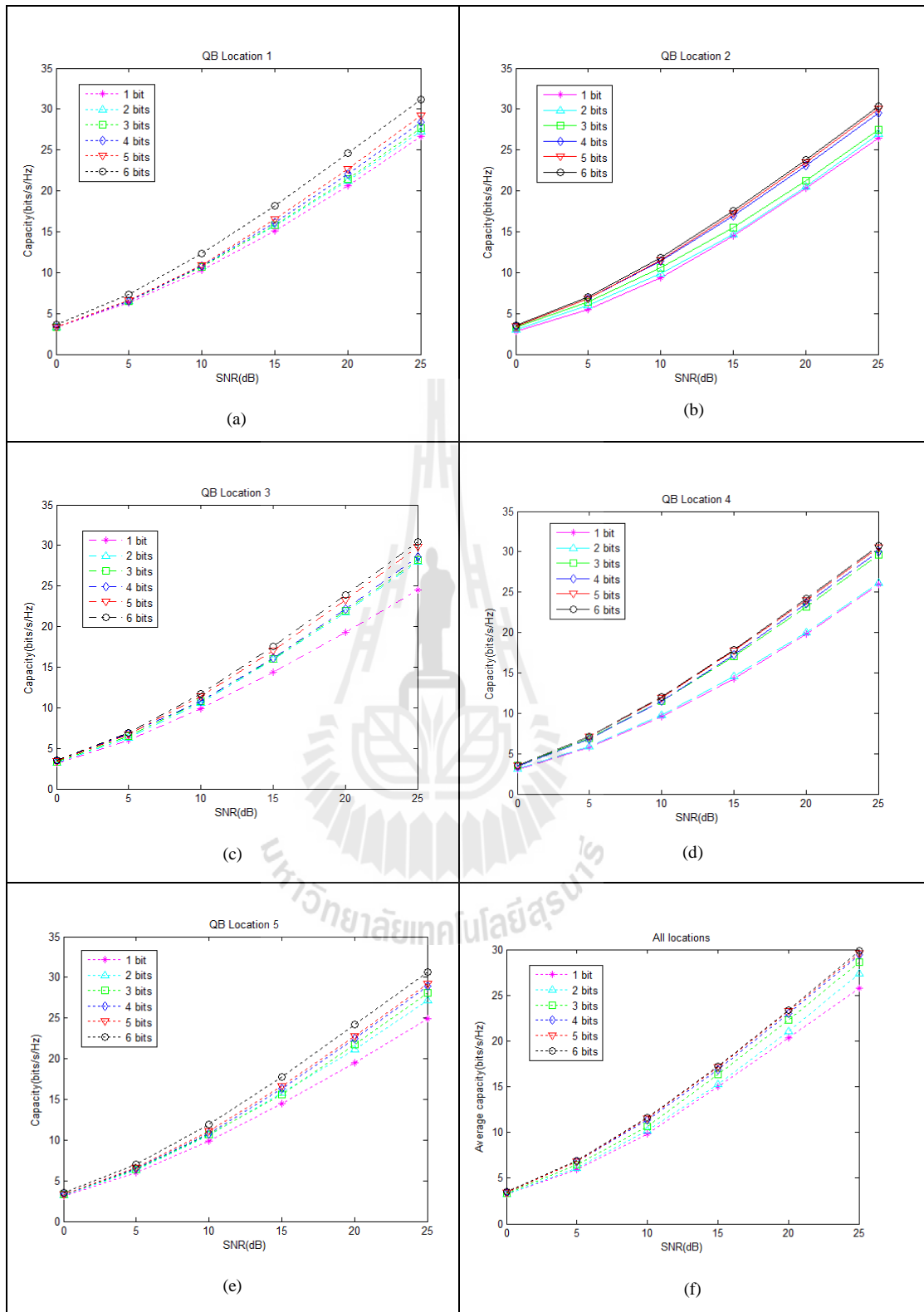


Figure 6.10 The capacity versus SNR for QB technique at each location.

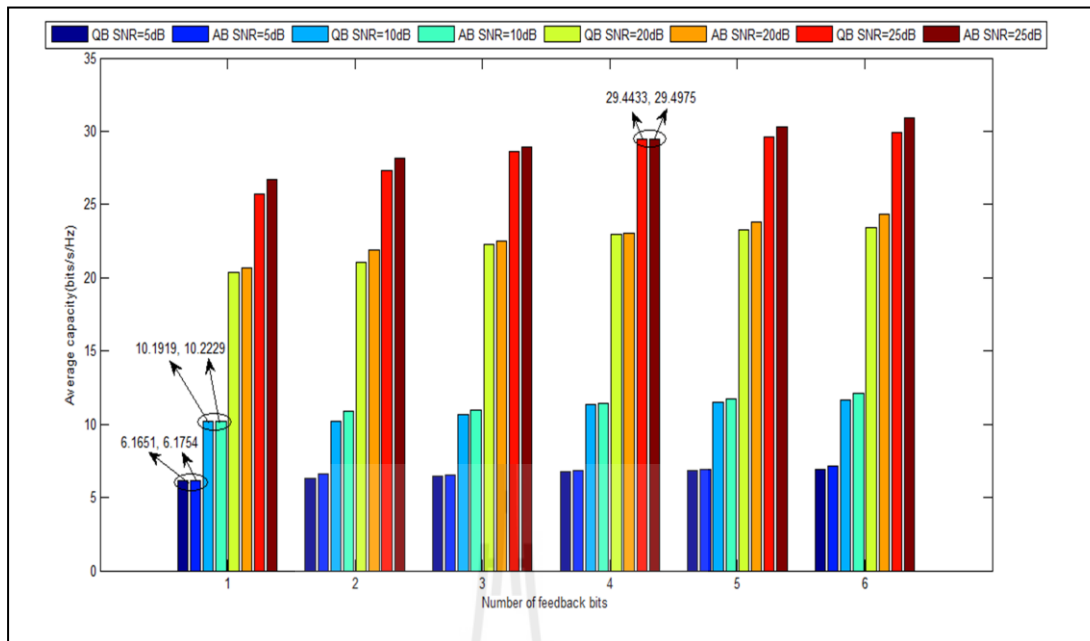


Figure 6.11 The average capacity versus number of feedback bits for 4x4 MIMO beamforming using AB and QB techniques.

Figure 6.11 presents the average capacity at all locations for 4 streams. The AB and QB techniques are fixed SNR at 5, 10, 20 and 25 dB. The results reveal that the increase number of feedback bit can increase the channel capacity. It is obviously noticed that the benefit of the AB technique outperforms the QB technique. The reason is that the channels of AB technique provide more eigen value than QB technique. From the theory, the optimal transmitting beamformer is chosen as the eigen vector corresponding to the largest eigen value of $\mathbf{H}\mathbf{H}^H$ that give maximum SNR. Then, the maximum SNR leads to maximum channel capacity. That is why the capacity of AB technique is higher than QB technique. Note that, the channel in simulations is not the real channel in practice because the channel model in simulations is randomly created by some specific paths. In turn, the multipath of real

channel cannot be known due to the different environments. Therefore, the results from simulation (Chapter IV) and experimental results (Chapter VI) cannot be compared. However, there is the same trend that the increase number of feedback bits will increase the channel capacity.

The measurement results at number of 4 feedback bits show that the AB technique offers a slightly better capacity than QB technique. The reason is that this thesis applies the angles to determine beamforming vectors by selecting the beamforming vectors to maximize SNR. Then, the optimal beamforming of AB technique provides the nearby performance as QB technique. Therefore, AB and QB techniques have the similar capacity. However, if we change locations, it has an effect on channel matrix. Consequently, the capacity might not be similar.

According to this issue, the author has performed more simulations to compare between the radiation patterns of AB and QB techniques as shown in Figure 6.12. It can be noticed that AB technique can provide more coverage than QB technique. Hence it can be predicted that AB technique always receives a good signal quality and could not offer a less capacity than QB technique

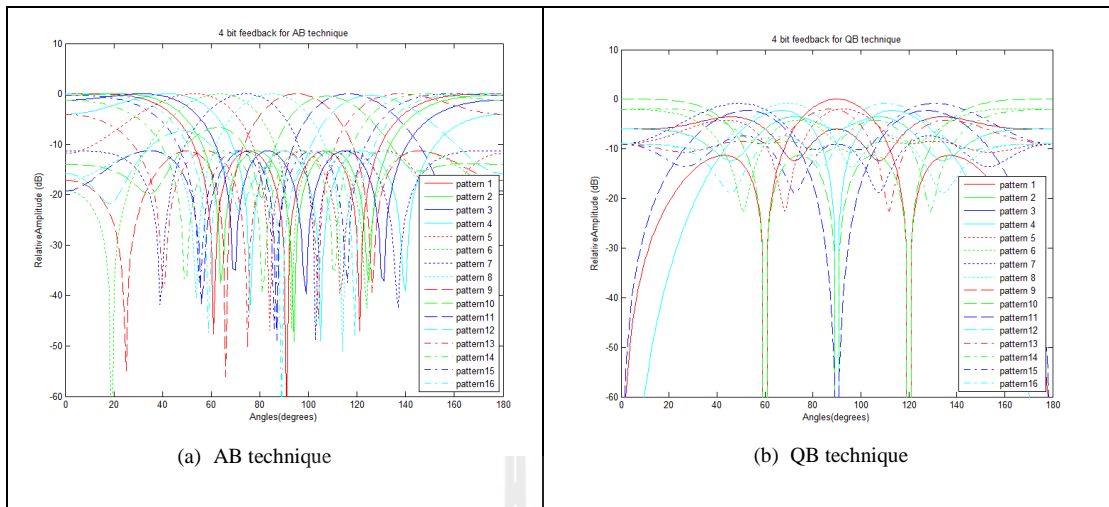


Figure 6.12 The radiation patterns comparison between AB and QB techniques for 4 feedback bits.

6.4 Chapter summary

This chapter presents the experimental results of MIMO beamforming systems using the measured channel of QB and AB techniques. The results reveal that the proposed system offers a slightly better capacity than QB technique while it offers a low complexity.

CHAPTER VII

THESIS CONCLUSION

7.1 Conclusion

MIMO systems employ multiple antennas at both transmitter and receiver to improve communication performances. This thesis discusses the different types of MIMO systems including open loop and closed loop systems. This thesis focuses on closed loop systems for applying the MIMO beamforming including EB, QB and AB techniques. The first two types are unattractive for communication system because EB technique is impossible to fully know the CSI. Thus, EB technique has been studied as ideal technique and used as a reference to compare with other techniques. Then, QB technique has a drawback in the complexity of finding the suitable beamforming vectors. Therefore, the AB technique has been originally proposed to overcome such a drawback of QB technique. In order to study the AB technique, the background theories of MIMO systems are presented for calculating the channel capacity. The knowledge of the channel capacity is necessary to be the figure of merit for MIMO beamforming systems.

This thesis presents the performance of MIMO beamforming systems using EB, QB and AB techniques based on simulation. The EB technique has used the maximum eigen value for finding channel capacity. The result reveals that the proposed system, AB technique is attractive to be practically implemented because it offers a low complexity while keeping the similar performance as QB technique.

This thesis has shown the design and construction of MIMO beamforming. Two main components consist of weighting networks and control devices by using microcontroller and phase shifter. The performance of MIMO beamforming systems using QB and AB techniques are compared. The channel measurements of AB and QB techniques have been performed for 4x4 MIMO systems. Then, the channel capacity can be calculated by using the channel from measurements. The capacity results have revealed that the AB technique provided the performance like the QB technique while keeping a low complexity.

In summary, the contributions of this thesis have proposed the novel thinking of AB technique for MIMO beamforming which the outcome can be categorized into two major contributions. At first, the AB technique is attractive to be practically implemented because it offers a low complexity that can decrease the processing times. Secondly, this thesis has shown the construction of channel measurement for AB and QB techniques.

7.2 Future studies

Based on the knowledge learned and acquired over this research, some recommendations for future wireless communication design should be presented. In this thesis, the design examples of AB technique have used microcontroller matching with phase shifter. It was found that when we have changed weighting, the beam direction characteristics are also changed. In the future study, we can change the weight for various main beams in order to provide variety of weighting characteristics. In applying the techniques of AB and QB techniques to analyze MIMO systems, it is necessary to know several vectors associated with a beam

direction. This thesis needs a systematical approach to obtain these derivatives. Therefore, a few general and useful formulas in various geometries should be reviewed. Full implementation of AB technique based on the upcoming standard should be taken.



REFERENCES

- Andrea, G. (2005). **Wireless Communications**, Cambridge University Press, ch. 10.
- Bakhshi, G., Saadat, R., Shahtalebi, K. (2008). **A Modified Two-Ring Reference Model for MIMO Mobile to Mobile Communication Channels**. International Symposium on Telecommunications, pp 409 - 413.
- Bishwarup, M. and Robert, W. H. (2006). **Performance analysis of quantized beamforming MIMO systems**. IEEE Transactions on Signal Processing, vol. 54, no. 12, pp. 4753-4766.
- Foschini, G. J. (1996). **Layered space time for wireless communication in a fading environment when using multielement antennas**. Bell Labs Tech. J., no. 2, pp. 41-59.
- Foschini, G. L. and Gans, M. J. (1998). **On limit of wireless communications in a fading environment when using multiple antennas**. Wireless Personal Communications, vol. 06, no 03, pp. 311-335.
- Georgy, L., Sergey, L. (2008). **On the Outage Capacity Distribution of Correlated Keyhole MIMO Channels**. IEEE Transactions on Information Theory, pp. 3232 - 3245.
- Golub, G. H. and Loan, C. F. V. (1989). **Matrix Computations**, Baltimore: The Johns Hopkins University Press, 2nd ed.
- Kermoal, J. P., Mogensen, P. E., Jensen, S. H., Andersen, J. B., Frederiksen, Sorensen, F. T. B. and Pedersen, K. I. (2000). **Experimental investigation of multipath richness for multi-element transmit and receive antenna array**.

- IEEE 51st Vehicular Technology conference-Spring Tokyo, vol. 3, pp. 2004-2008.
- Liang, S., Matthew, R. Mc. and Shi, J. (2009). **Analytical Performance of MIMO Multichannel Beamforming in the Presence of Unequal Power Cochannel Interference and Noise.** IEEE Transactions on Signal Processing, vol. 57, no.7, pp. 2721-2735.
- Liberti, J. C. and Rappaport, J. T. S. (1999). **Smart Antennas for Wireless Communications**, IS-95 and Third Generation CDMA Applications, ch.3.
- Li, H., Bergmans, J. W. M. and Willems, F. M. J. (2007). **Pilot-aided angle-domain channel estimation techniques for MIMO-OFDM system.** IEEE Transactions Vehicular Technology, vol. 57, no. 2, pp. 906-920.
- Ming, K. and Alouini, M. S. (2003). **Impact of correlation on the capacity of MIMO channels.** IEEE International Conference on Communications 11-15 May, vol. 4, pp. 2623-2627.
- Molisch, A. F., Steinbauer, M., Toeltsch, M., Bonek, E., and Thoma, R. S. (2002). **Capacity of MIMO systems based on measured wireless channel.** IEEE Journal on Selected Areas in Communications, vol. 20, no. 3, April, pp. 561-569.
- Promsuvana, N. and Uthansakul, P. (2008). **Feasibility of adaptive 4×4 MIMO systems using channel reciprocity in FDD mode.** Proceedings of the 14th Asia-Pacific Conference on Communications (*APCC '08*), pp. 1–5
- Ratnarajah, T. (2006). **Spatially correlated multiple-antenna channel capacity distributions.** IEE Proceedings: Communications, vol. 2, pp. 263-271.

- Shi, J., Xiqi, G. and Xiaohu Y. (2007). **On the Ergodic Capacity of Rank-1 Ricean-Fading MIMO Channels**. IEEE Transactions on Information Theory 2007: vol. 53, no. 2, pp. 502-517.
- Sirikiat, Lek, A., Zheng, J., Eric, O. and Joonsuk, K. (2006). **Subspace beamforming for near-capacity performance**. IEEE Transactions on Signal Processing, vol. 56, no. 11, pp. 5729-5733.
- Stridh, R., Ottersten, B. and Karlsson, P. (2000). **MIMO channel capacity of a measured indoor radio channel at 5.8 Ghz**. Conference Record of the Thirty-Fourth Asilomar Conference on Signals, Systems and Computers, vol. 1, pp. 733-737.
- Telatar, I. E. (1995). **Capacity of multi-antenna Gaussian channels**. AT&T Bell Laboratories, Tech. Memo., June.
- Tse, D. and Viswanath, P. (2005). *Fundamentals of Wireless Communication*, Cambridge, UK, ch. 7.
- Uthansakul, P. (2009) **Adaptive MIMO systems Explorations for Indoor Wireless Communications**, Appendix D.
- Vieira, R. D., Brandao, J. C. B. and Siqueira, G. L. (2006). **MIMO measured channels: Capacity results and analysis of channel parameters**. International Telecommunications Symposium, pp. 152–157.
- Xiayu, Z., Yao. X., Jian, L. and Petre, S. (2007). **MIMO transmit beamforming under uniform Elemental Power Constraint**. IEEE Transactions on Signal Processing, vol. 55, no. 11, pp. 5395-5406.

APPENDIX A
PUBLICATIONS



List of Publications

International Conference Paper

Innok, A., Uthansakul P., Wongsan, R. and Uthansakul, M., (2012). **Angular Beamforming Technique for MIMO Beamforming System.** Electrical /Electronics Engineering, Computer Engineering, Telecommunications Engineering and Information Technology International Conference, Thailand May 16-18, 4 pages.

International Journal Paper

Innok, A., Uthansakul, P. and Uthansakul, M. (2011). **Open-Loop Beamforming Technique for MIMO systems and Its Practical Realization.** International Journal of Antennas and Propagation, Volume 2011, Article ID 723719, 13 pages. (ISI Impact factor 0.5)

Innok, A., Uthansakul, P. and Uthansakul, M. (2012). **Angular Beamforming Technique for MIMO Beamforming System.** International Journal of Antennas and Propagation, Volume 2012, Article ID 638150, 10 pages. (ISI Impact factor 0.683)

Angular Beamforming Technique for MIMO Beamforming System

A. Innok, P. Uthansakul and M. Uthansakul
 School of Telecommunication Engineering, Suranaree University of Technology,
 Nakhon Ratchasima, Thailand 30000
 E-Mail: apinya_in@hotmail.com, {uthansakul, mtp}@sut.ac.th

Abstract- For MIMO beamforming, the Eigen Beamforming (EB) technique provides the best performance with the expense of knowing full channel information. To reduce such an expense, the Quantized Beamforming (QB) has been presented by using only some feedback bits to calculate the suitable beamforming vectors. However, QB has a drawback in the complexity of finding the beamforming vectors and it is more difficult for a lot of feedback bits. In this paper, the new technique named as Angular Beamforming (AB) has been presented to overcome such a drawback of QB. The investigations are undertaken by sending multiple data streams into 4x4 MIMO system. The effect of different data streams and number of feedback bits are studied. The simulation results indicate that AB technique performs very well and its performance is as good as QB.

Keywords- MIMO capacity; Eigen Beamforming; Angular Beamforming; Quantized beamforming

I. INTRODUCTION

MIMO (Multiple-Input-Multiple-Output) systems provide a promising quality of service including a great channel capacity. Many works have proposed the method of EB and QB technique [1]-[4] to improve the capacity. The EB technique utilizes the properties of estimated channels by performing Singular Value Decomposition (SVD) on channel matrix. Then the eigenvectors compositing of channel matrix are considered as pre and post coding schemes for MIMO systems. For QB technique, it used weight for pre and post coding by forming beams at transmitter and receiver. This technique can find the weight from the uniform elemental power constraint [3]. This technique efficiently attempts to feedback the transmit beamformer from the receiver to the transmitter via a feedback channel, which is assumed to be error free. The problem formulated by QB is on the design of high complex common codebook. However, the drawbacks of these techniques are the requirement of feedback channel information which increases the overhead of data transmission and the expense of data processing.

In addition, the QB complexity of pre and post coding is so difficult that it is unattractive to be implemented for real application. Therefore, the search of new technique instead of EB and QB techniques is still on focus.

In this paper, the simple technique based on the concept of AB is introduced. This is because AB is low complexity in feedback channel for pre and post coding schemes. We apply the steering vectors for pre and post coding at transmitter and receiver. The number of feedback bits is used to define the spacing between

beams. The angle of departure or arrival is so equally spaced that it is easy to be implemented by either hardware or software. In turn, the implementation of QB beamforming vectors is more complex and harder for a lot of feedback bits. Although the performance of AB cannot be superior to EB and QB but the ease of implementation might be a good tradeoff to take an attention from MIMO researcher.

The remainder of this paper is organized as follows. In section II, the details of three techniques for MIMO beamforming system are described. Three techniques include AB, EB and QB. Section III provides the simulation results comparing the capacity performance of three techniques. Finally in section IV, the conclusion of this paper is given.

II. MIMO BEAMFORMING

A. Angular Beamforming (AB)

At the transmitter, the data symbol s is modulated by the beamformer U_t and the transmitted into a MIMO channel. At the receiver, after processing with the beamforming vector U_r in [3]. Then the relation between transmitted and received signal is given by

$$y = U_r^* [H U_t s + n] \quad (1)$$

The transmit beamforming vector U_t and the receive beamforming vector U_r in (1) are usually chosen to maximize the receive SNR. Without loss of generality, we assume that $\|U_r\|^2 = 1$, $E\{|s|^2\} = 1$. Then the received SNR is expressed as

$$\rho = \frac{E\{\|U_r^* H U_t s\|^2\}}{E\{\|U_r^* n\|^2\}} = \frac{\|U_r^* H U_t\|^2}{\sigma_n^2} \quad (2)$$

To maximize the received SNR, the optimal transmit beamformer is chosen as the eigenvector corresponding to the largest eigen-value of HH^H singular value can find form SVD technique in MATLAB programming. Thus the maximized received SNR is $\rho = (\lambda_{\max}(HH^H))/(\sigma_n^2)$. By λ_{\max} is the maximum eigen-value of a matrix and identically distributed (i.i.d.) complex Gaussian random variables with zero-mean and variance σ_n^2 .

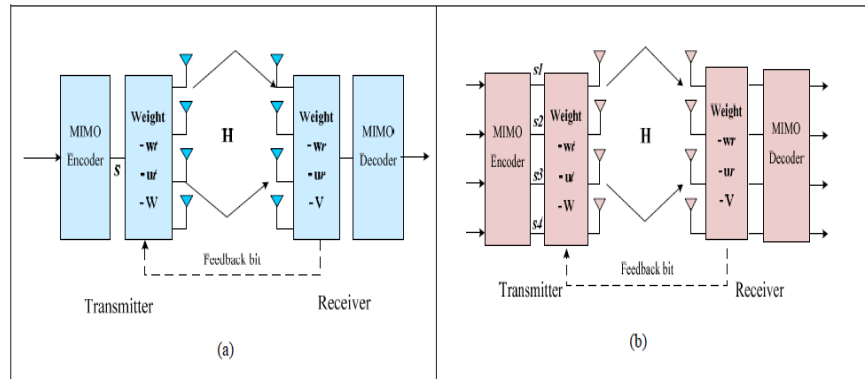


Figure 1. 4x4 MIMO Beamforming (a) 1 stream and (b) 4 streams.

Fig.1 show 4x4 MIMO beamforming for (a) 1 stream and (b) 2 streams. There is an arbitrary number of physical paths between the transmitter and receiver [5], the i th path having attenuation of a_i , makes an angle of ϕ_n ($\Omega_n = \cos \phi_n$) with the transmit antenna array and an angle of ϕ_r ($\Omega_r = \cos \phi_r$) with the receive antenna array. The channel matrix \mathbf{H} can be written as:

$$\mathbf{H} = \sum_i a_i^b \mathbf{e}_r(\Omega_r) \mathbf{e}_t(\Omega_n)^* \quad (3)$$

where

$$a_i^b = a_i \sqrt{N_t N_r} \exp\left(-\frac{j2\pi d_i}{\lambda_c}\right) \quad (4)$$

$$\mathbf{e}_r(\Omega) = \frac{1}{\sqrt{N_r}} \begin{bmatrix} 1 \\ \exp[-j(2\pi\Delta_r\Omega)] \\ \vdots \\ \exp[-j(N_r-1)(2\pi\Delta_r\Omega)] \end{bmatrix} \quad (5)$$

$$\mathbf{e}_t(\Omega) = \frac{1}{\sqrt{N_t}} \begin{bmatrix} 1 \\ \exp[-j(2\pi\Delta_t\Omega)] \\ \vdots \\ \exp[-j(N_t-1)(2\pi\Delta_t\Omega)] \end{bmatrix} \quad (6)$$

Where, d_i is the distance between transmit and receive antennas along path i th. The vector $\mathbf{e}_t(\Omega)$ and $\mathbf{e}_r(\Omega)$ are, respectively, the transmitted and received unit spatial signatures along the direction Ω , λ_c is the wavelength of the center frequency in the whole signal bandwidth. Δ_t is the normalized transmit antenna separation and Δ_r is the normalized receive antenna separation.

The concept of AB can be represented by the transmitted and received signals. The low profile concept of AB which is convenient for implementation is proposed by just inserting \mathbf{U}_t and \mathbf{U}_r at both transmitter and receiver which the beamforming vectors depend on angle of arrival or departure. The number of

feedback bits are defined the angle (θ) $\theta \in [0, 2\pi)$. The angles are dividing equally. The angle can be expressed as $N_i = 2^{B_i}$, N_i denoting the number of angle levels. B_i is the number of feedback bits. In comparing with QB, the procedure to find beamforming vectors of QB is more complexity than AB. The detail of QB is shown in the next section.

Let \mathbf{U}_t and \mathbf{U}_r be the beamforming matrices for multiple streams. For 1 stream, the \mathbf{U}_t and \mathbf{U}_r will be reduced to only the beamforming vectors. Beamforming matrices consist of number of beamforming vectors according to the number of streams. In general, \mathbf{U}_t and \mathbf{U}_r can be written as:

$$\mathbf{U}_t = \frac{1}{\sqrt{N_t}} \exp(jlk\Delta_t \cos \theta); \quad l=1, 2, \dots, N_t \quad (7)$$

$$\mathbf{U}_r = \frac{1}{\sqrt{N_r}} \exp(jmk\Delta_r \cos \theta); \quad m=1, 2, \dots, N_r \quad (8)$$

where $k = 2\pi/\lambda_c$. We can use $\max \|\mathbf{U}_r^* \mathbf{H} \mathbf{U}_t\|^2$ will be maximum \mathbf{U}_t and \mathbf{U}_r . So the channel matrix of AB can be written as:

$$\mathbf{H}_{\max}^a = \mathbf{U}_{r,\max}^* \mathbf{H} \mathbf{U}_{t,\max} \quad (9)$$

Thus, the capacity of MIMO systems using AB given by

$$C = \log_2 \det \left(\mathbf{I}_{N_r} + \frac{P_t}{P_r N_t} \mathbf{H}_{\max}^a \mathbf{H}_{\max}^{a*} \right) \quad (10)$$

where \mathbf{I}_{N_r} is the identity matrix of size $N_r \times N_r$, \mathbf{H}_{\max}^a is the channel matrix of size $N_r \times N_t$ streams.

B. Quantized Beamforming (QB)

In the EB designs, we have assumed that the transmitter has perfect knowledge on CSI. However, in many real systems, having the CSI known exactly at the transmitter is hardly possible. The channel information is usually provided by the receiver through a bandwidth-limited finite-rate feedback channel, and quantization method, which have been widely studied for source coding [3], can be used to

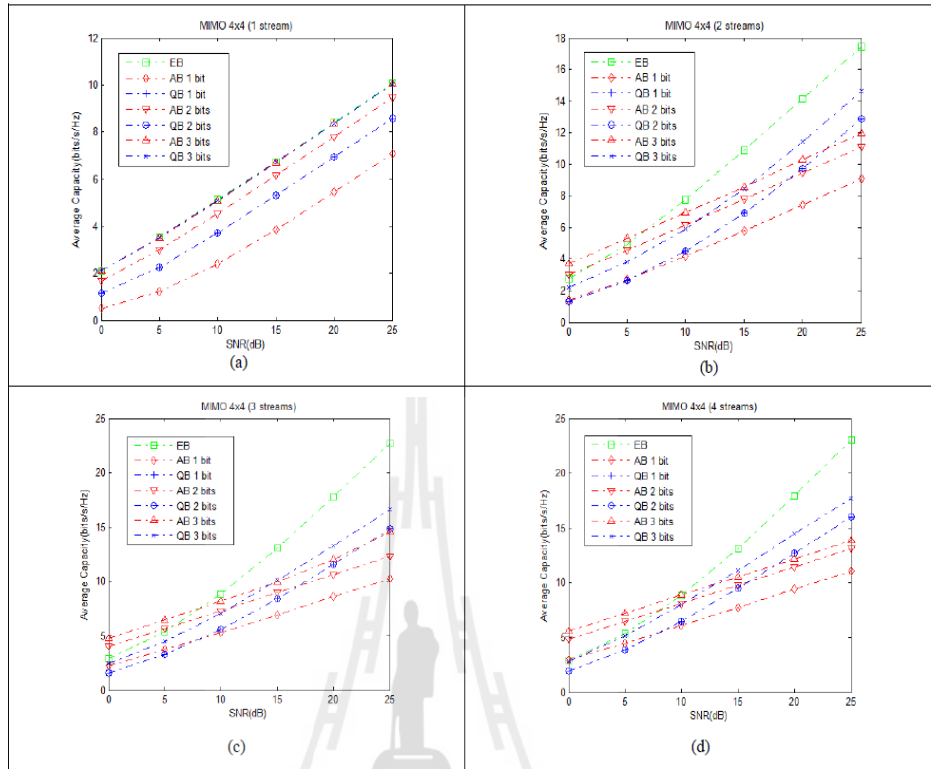


Figure 2. Capacity vs. SNR (a) 1 stream, (b) 2 streams, (c) 3 streams and (d) 4 streams.

provide the feedback information. We assume herein that the receiver has perfect CSI. The transmit beamforming vector \mathbf{w}_t for QB is used under the uniform elemental power constraint. The transmit beamformer $\mathbf{w}_t(\theta_0, \theta_1, \dots, \theta_{N_t-1})$ is a function of N_t parameters $\{\theta_i, \theta_i \in [0, 2\pi)\}_{i=0}^{N_t-1}$ via simple manipulations, we obtain

$$\mathbf{w}_t(\theta_0, \theta_1, \dots, \theta_{N_t-1}) = \frac{1}{\sqrt{N_t}} e^{j\theta_0} \begin{bmatrix} 1 \\ e^{j\theta_1} \\ \vdots \\ e^{j\theta_{N_t-1}} \end{bmatrix} \quad (11)$$

Where $\tilde{\theta}_i = \theta_i - \theta_0$, $\theta_i \in [0, 2\pi)$, $i = 1, 2, \dots, N_t - 1$.

Since $\|\mathbf{H}\mathbf{w}_t(\theta_0, \theta_1, \dots, \theta_{N_t-1})\|^2 = \|\mathbf{H}\mathbf{w}_t(\tilde{\theta}_1, \tilde{\theta}_2, \dots, \tilde{\theta}_{N_t-1})\|^2$, we can reduce one parameter and quantize $\mathbf{w}_t(\theta_1, \theta_2, \dots, \theta_{N_t-1})$ instead of $\mathbf{w}_t(\theta_0, \theta_1, \dots, \theta_{N_t-1})$

Denote

$$\mathbf{w}_t(\tilde{\theta}_1^n, \dots, \tilde{\theta}_{N_t-1}^n) = \frac{1}{\sqrt{N_t}} \begin{bmatrix} 1 \\ e^{j\tilde{\theta}_1^n} \\ \vdots \\ e^{j\tilde{\theta}_{N_t-1}^n} \end{bmatrix} \quad (12)$$

where $\tilde{\theta}_i^n = (2\pi n_i)/(N_t)$, $0 \leq n_i \leq N_t - 1$, $i = 1, 2, \dots, N_t - 1$, with $N_t = 2^{B_i}$ and N_t denoting the number of quantization levels and feedback index of $\tilde{\theta}_i$, respectively, and where B_i is the number of feedback bits for $\tilde{\theta}_i$. We quantize the parameters $\tilde{\theta}_i$ to the round off grid point $\tilde{\theta}_i^n$, $i = 1, 2, \dots, N_t - 1$. Hence for this quantization scheme, we need to send the index set n_i from the receiver to the transmitter. Let \mathbf{w}_t and \mathbf{w}_r be the beamforming vector for 1 stream. For multiple streams, the notations of \mathbf{W}_t and \mathbf{W}_r are the beamforming matrices. This requires $B = \sum_{i=1}^{N_t-1} B_i$ bits. The receive beamformer \mathbf{w}_r can be written as

$$\mathbf{w}_r = \frac{\mathbf{H}\mathbf{w}_t(\tilde{\theta}_1^n, \tilde{\theta}_2^n, \dots, \tilde{\theta}_{N_t-1}^n)}{\|\mathbf{H}\mathbf{w}_t(\tilde{\theta}_1^n, \tilde{\theta}_2^n, \dots, \tilde{\theta}_{N_t-1}^n)\|} \quad (13)$$

We can use $\max \|\mathbf{w}_t^* \mathbf{H}\mathbf{w}_t\|^2$ will be maximum \mathbf{w}_t and \mathbf{w}_r . Then, the channel matrix QB when applying the maximum transmits beamforming (\mathbf{W}_{\max}) and the maximum receive combining vector ($\mathbf{w}_{r,\max}$) can be written as:

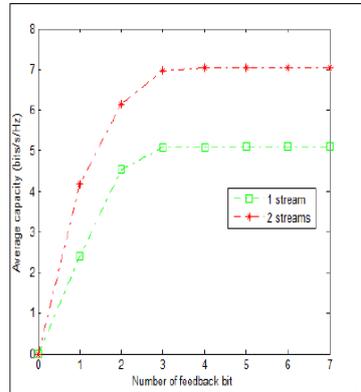


Figure 3. Average capacity vs. number of feedback bits for 4x4 MIMO beamforming using AB technique.

$$\mathbf{H}_{\max}^q = \mathbf{w}_{r\max}^* \mathbf{H} \mathbf{w}_{r\max} \quad (14)$$

Thus, the capacity [6] of MIMO system using QB given by

$$C = \log_2 \det \left(\mathbf{I}_{N_r} + \frac{P_t}{P_N N_t} \mathbf{H}_{\max}^q \mathbf{H}_{\max}^{q*} \right) \quad (15)$$

where \mathbf{I}_{N_r} is the identity matrix of size $N_r \times N_r$, \mathbf{H}_{\max}^q is the channel matrix of size $N_r \times N_t$.

C. Eigen Beamforming (EB)

Considering a MIMO channel with $N_r \times N_t$ channel matrix \mathbf{H} that is known to both the transmitter and the receiver, the eigen vectors can be found by applying SVD technique to channel matrix as shown below

$$\mathbf{H} = \mathbf{W} \mathbf{S} \mathbf{V}^* \quad (16)$$

Where $N_r \times N_r$ matrix \mathbf{W} and the $N_t \times N_t$ matrix \mathbf{V} are unitary matrices, \mathbf{S} is an $N_r \times N_r$ diagonal matrix. These two matrices are used as pre and post coding matrices at transmitter and receiver, respectively. So the channel matrix of EB can be written as:

$$\mathbf{H}^e = \mathbf{W}^e \mathbf{H} \mathbf{V} \quad (17)$$

Thus, the capacity of MIMO system using EB is given by

$$C = \log_2 \det \left(\mathbf{I}_{N_r} + \frac{P_t}{P_N N_t} \mathbf{H}^e \mathbf{H}^{e*} \right) \quad (18)$$

where \mathbf{I}_{N_r} is the identity matrix of size $N_r \times N_r$, \mathbf{H}^e is the channel matrix of size $N_r \times N_t$.

III. RESULTS AND DISCUSSIONS

The simulations are undertaken by MATLAB programming and the capacity results are evaluated by using (10), (15) and (18). Figure 2 shows the average capacity versus SNR. We increase the number of feedback bits and streams. Four cases are considered as (a) 1 stream at transmitter, 1 stream at receiver, (b)

2 streams at transmitter, 2 streams at receiver, (c) 3 streams at transmitter, 3 streams at receiver, (d) 4 streams at transmitter, 4 streams at receiver. The range of capacity enhancement depends on the number of feedback bits. The number of feedback bits can improve the channel capacity. Also, the number of streams can improve the channel capacity too. The optimum EB offers better performance than QB and AB. However, the implementation is so easy that might be a good tradeoff to take an attention from MIMO researcher.

In Figure 3, the average capacity versus number of feedback bits for 4x4 MIMO beamforming using AB technique is presented. This figure shows 1 stream and 2 streams. The number of 2 streams offers better performance than 1 stream. It is obviously seen that there is a steady state of capacity increase at the certain point of feedback bits. The results indicate that it is not necessary to use many feedback bits. For both results, it seems that 3 bits is an optimal bit requirement for feedback channel. This is helpful in practice to make the system successful.

IV. CONCLUSION

This paper presents the performance of MIMO beamforming systems using EB, QB and AB techniques. The result reveals that the proposed system, AB technique, is attractive to be practically implemented because it offers a low complexity while keeps the similar performance as QB. Also the results show that only 3 bits feedback is sufficient for AB technique.

ACKNOWLEDGEMENT

This work is financially supported by Suranaree University of Technology, Thailand and the Royal Golden Jubilee Program of Thailand Research Fund, Thailand.

REFERENCES

- [1] M. Bishwarup and W.H. Robert, "Performance analysis of quantized beamforming MIMO systems," *IEEE Transactions on Signal Processing*, vol. 54, no. 12, 2006, pp. 4753-4766.
- [2] A.S. Lek, Jun Zheng, O. Eric and J. Kim, "Subspace beamforming for near-capacity performance," *IEEE Transactions on Signal Processing*, vol. 56, no. 11, 2006, pp. 5729-5733.
- [3] Xiayu Zheng, Yao Xie, Jian Li, Petre S., MIMO transmit beamforming under uniform Elemental Power Constraint, *IEEE Transactions on Signal Processing*, vol. 55 no. 11, 2007, pp. 5395-5406.
- [4] Liang Sun, Matthew R. Mc., Shi Jin, Analytical Performance of MIMO Multichannel Beamforming in the Presence of Unequal Power Cochannel Interference and Noise, *IEEE Transactions on Signal Processing*, vol. 57, no.7, 2009, pp. 2721-2735.
- [5] D. Tse, and P. Viswanath, *Fundamentals of Wireless Communication*, Cambridge University Press, United Kingdom, 2005.
- [6] [11] R. G. Tsoulos, *MIMO systems Technology for Wireless Communications*. The electrical engineering and applied signal processing Series., ch. 4.

Research Article

Open-Loop Beamforming Technique for MIMO System and Its Practical Realization

Peerapong Uthansakul, Apinya Innok, and Monthippa Uthansakul

School of Telecommunication Engineering, Suranaree University of Technology, Muang, Nakhon Ratchasima 30000, Thailand

Correspondence should be addressed to Apinya Innok, apinya_in@hotmail.com

Received 21 February 2011; Accepted 19 May 2011

Academic Editor: Miguel Ferrando

Copyright © 2011 Peerapong Uthansakul et al. This is an open access article distributed under the Creative Commons Attribution License, which permits unrestricted use, distribution, and reproduction in any medium, provided the original work is properly cited.

The concept of close-loop beamforming for MIMO system was well known proposed the singular value decomposition on channel matrix. This technique can improve the capacity performance, but the cost of feedback channel and the complexity processing discard the interest of implementation. Therefore, this paper aims to investigate the benefit of using an open-loop beamforming for MIMO system in practical approaches. The low-profile concept of open-loop beamforming which is convenient for implementation is proposed by just inserting Butler matrices at both transmitter and receiver. The simulation and measurement results indicate that the open-loop beamforming with Butler matrix outperforms the conventional MIMO system. Although, the close-loop beamforming offers a better performance than open-loop beamforming technique, the proposed system is attractive because it is low cost, uncomplicated, and easy to implement.

1. Introduction

The MIMO (Multiple-input-multiple-output) system is a good quality of service such as channel capacity. In general, MIMO systems consideration of channel capacity is based on the array antennas at both transmitter and receiver. Many works have proposed the method of eigen-beamforming technique [1–5]. This technique utilizes the properties of estimated channels by performing singular value decomposition on channel matrix. Then eigenvectors compositing of channel matrix are considered as pre- and postcoding schemes for MIMO systems. This technique can improve the capacity performance, but both transmitter and receiver have to perfectly know the channel information, named as close loop MIMO system. However, there are many unattractive issues of using eigen-beamforming in practice such as a requirement of high system complexity and many procedures for channel feedback transmission. In turn, for open loop beamforming, the transmitter sends independent information symbols from multiple transmit antenna elements to the receiver. The received channels are not sent back to the transmitter. So, the transmitter does not know the channel information. The pre- and postcoding

schemes do not require any additional complexity like close loop system. Therefore, the study of using open loop is focused on in this paper.

In the research areas of MIMO system, many works such as [6–9] have been proposed to enhance the channel capacity in order to satisfy the user demand for high data rate applications. Some studies have been focused on theoretical works and some have been performed by measurements. Nevertheless, most of them develop the technique to enhance the channel capacity through channel behavior [10–12] such as adjusting transmitted powers according to eigenvalue of channels as so-called water filling method. In general, it can be noticed that the theoretical consideration of channel capacity is based on the array antennas at both transmitter and receiver, but the channel characteristic is composed of many angle parameters such as angle of arrival, angle of departure, and angle spread. Therefore, it is interesting to investigate the performance of MIMO system using the open loop beamforming instead of the conventional MIMO system. Recently, the authors in [13, 14] developed the channel estimation of MIMO-OFDM system based on open loop beamforming consideration. The applicability

of open loop beamforming technique is dependent on the channel stochastic information available to the receiver. The design of suitable pilots is proposed by facilitating the direct implementation of open loop beamforming and analyzing the performances of different channel estimation techniques. Although the significant improvement on MIMO capacity can be expected by using open loop beamforming, so far in the literature, there is no work to illustrate the capacity benefit of using open loop beamforming. The reason is that the pre- and postcoding schemes of angle transformations increase the complexity on both transmitter and receiver. Hence, it is challenging to find the technique with low cost and complexity matching with the concept of open loop beamforming. In [15], the proposed scheme uses a discrete fourier transformation (DFT) to receive a signal vector in RF domain. This can be realized by placing a Butler matrix between the antenna elements and the receiver switch. This paper presents only the simulations results. There is no measurement result presented in this paper. Clearly the difference between [15] and our paper is on the measurements. In [16], the authors investigate the correlation coefficients (line of sight and nonline of sight) via both simulation and measurement results. However, the analysis of correlation coefficients has not been analytically discussed yet. This is the claim of our novelty, that our paper presents the analytical analysis of correlation coefficients. Moreover, the additional measurements have been done by rotating the array direction for many degrees. These measurements are different from [16] and give more insight of using Butler matrix. We used the method of open loop beamforming in [17] investigated the capacity performance of compared with conventional MIMO system by computer simulations. The results in [17] confirm the advantages of using open loop beamforming. In this paper, the analytical analysis of how open loop beamforming impacts on the channel matrix is explained. Then, it gives a reason why using open loop beamforming for MIMO system provides a better performance over a conventional MIMO system. Also, further work from [17] is carried out by manufacturing a Butler matrix and performing the experimental results due to the fact that only simulation results cannot claim the use of the proposed system in practice. The reason why Butler matrix is chosen is because Butler matrix is just a low-complexity hardware that can offer the open loop beamforming. In general, there are infinite choices to choose the set of orthogonal steering vectors to form an open loop beamforming. Therefore, it is hard to justify whether Butler matrix provides the best performance among others. To focus on hardware complexity, the other methods to form open loop beamforming might need 16 phase shifters to simultaneously form 4 beams while Butler matrix approach uses only one low-cost printed circuit board. Thus, the authors construct the 4×4 MIMO system employing an open loop beamforming by Butler matrix which is a low-profile concept and convenient for implementation. This matrix simultaneously forms multiple departure or arrival angles into four directions. By only inserting Butler matrix next to antenna arrays, the conventional MIMO systems can be transformed into the MIMO systems with open loop

beamforming without the need of additional burden on processing units at both transmitter and receiver.

In summary, the contribution of this paper falls into three main issues. At first, the analytical analysis of how open loop beamforming impacts on the channel matrix is originally provided. This helps the reader to understand in a true benefit of open loop beamforming. Secondly, the practical realization of open loop beamforming for 4×4 MIMO systems has been demonstrated. The third contribution is on the experimental comparisons in terms of channel capacity. All contributions confirm either new concept or actual benefit of employing MIMO with open loop beamforming. The paper is organized as follows. In Section 2, the details of SISO system, conventional MIMO system, close loop beamforming, and open loop beamforming technique are described. Then in Section 3, the analytical analysis of using open loop beamforming is explained. The feature of Butler matrix to apply for open loop beamforming is given in Section 4. Section 5 describes the details of channel measurements. Section 6 provides the simulation and measurement results of open loop beamforming realized by Butler matrix in comparing with conventional MIMO system. Finally in Section 7, the conclusion of this paper is given.

2. System Model

2.1. SISO System. For a memoryless SISO (single-input-single-output) system, the Shannon capacity is given by [8]

$$C = \log_2 \left(1 + \frac{P_t h}{P_N} \right), \quad (1)$$

where P_t is the transmitted power, h is the wireless channel coefficient, and P_N is the noise power in each branch of antennas at the receiver. Note that the signal-to-noise-power ratio (SNR) is defined as P_t/P_N .

2.2. Conventional MIMO System. We consider the narrow-band MIMO channel. Let \mathbf{x} be a vector of the transmitted signals with N_t transmitted antennas and let \mathbf{y} be a vector of the received signals with N_r received antennas. Then the relation between transmitted and received signals is given by

$$\mathbf{y} = \mathbf{H}\mathbf{x} + \mathbf{n}, \quad (2)$$

where \mathbf{n} is an $N_r \times 1$ noise vector and \mathbf{H} is an $N_r \times N_t$ channel matrix. In this paper, the channel matrix is modelled by using the concept of geometrical two-ring model. This model is based on the extension of single-bounce two-ring scattering model for flat fading channels [19]. With this notation, channel output sequence can be written in matrix form as the following expressions:

$$\begin{bmatrix} y_1 \\ y_2 \\ \vdots \\ y_{N_r} \end{bmatrix} = \begin{bmatrix} h_{11} & h_{12} & \cdots & h_{1N_t} \\ h_{21} & h_{22} & \cdots & h_{2N_t} \\ \vdots & \vdots & \ddots & \vdots \\ h_{N_r,1} & h_{N_r,2} & \cdots & h_{N_r,N_t} \end{bmatrix} \begin{bmatrix} x_1 \\ x_2 \\ \vdots \\ x_{N_t} \end{bmatrix} + \begin{bmatrix} n_1 \\ n_2 \\ \vdots \\ n_{N_r} \end{bmatrix}. \quad (3)$$

Figure 1(a) shows the conventional 4×4 MIMO systems. There is an arbitrary number of physical paths between the transmitter and receiver [20]; the i th path having attenuation of a_i , makes an angle of $\phi_{ti}(\Omega_{ti} := \cos \phi_{ti})$ with the transmit antenna array and angle of $\phi_{ri}(\Omega_{ri} := \cos \phi_{ri})$ with the receive antenna array. The channel matrix \mathbf{H} can be written as the following expressions:

$$\mathbf{H} = \sum_i a_i^b \mathbf{e}_r(\Omega_{ri}) \mathbf{e}_t(\Omega_{ti})^*, \quad (4)$$

where

$$a_i^b := a_i \sqrt{N_t N_r} \exp\left(-\frac{j2\pi d_i}{\lambda_c}\right), \quad (5)$$

$$\mathbf{e}_t(\Omega) := \frac{1}{\sqrt{N_t}} \begin{bmatrix} 1 \\ \exp[-j(2\pi\Delta_t\Omega)] \\ \vdots \\ \exp[-j(N_t-1)(2\pi\Delta_t\Omega)] \end{bmatrix}, \quad (6)$$

$$\mathbf{e}_r(\Omega) := \frac{1}{\sqrt{N_r}} \begin{bmatrix} 1 \\ \exp[-j(2\pi\Delta_r\Omega)] \\ \vdots \\ \exp[-j(N_r-1)(2\pi\Delta_r\Omega)] \end{bmatrix}. \quad (7)$$

Also, d_i is the distance between transmit and receive antennas along path i th. Note that $(\cdot)^*$ is the conjugate and transpose operation. The vector $\mathbf{e}_t(\Omega)$ and $\mathbf{e}_r(\Omega)$ are, respectively, transmitted and received unit spatial signatures along the direction Ω , λ_c is the wavelength of the center frequency in a whole signal bandwidth. Assuming uniform linear array, the normalized separation between the transmit antennas is Δ_t (antenna separation/ λ_c) and the normalized separation between receive antennas is Δ_r (antenna separation/ λ_c). Note that the reason of normalization is because this proposed system can work in any frequency band. Hence, the normalization is made to neglect the unused parameter. When channel state information (CSI) is not available at the transmitter, the capacity of MIMO systems [21] expressed in bits per second per hertz (bps/Hz) can be written as

$$C = \log_2 \det\left(\mathbf{I}_{N_r} + \frac{P_t}{P_N N_t} \mathbf{H} \mathbf{H}^*\right), \quad (8)$$

where \mathbf{I}_{N_r} is the identity matrix having $N_r \times N_r$ dimension, \mathbf{H} is the channel matrix having $N_r \times N_t$ dimension with \mathbf{H}^* being its transpose conjugate. In this paper, the channel matrix \mathbf{H} is normalized by $\|\mathbf{H}\|_F^2 = N_r N_t$.

2.3. MIMO System with Close Loop Beamforming Technique. Figure 1(b) showed the close loop beamforming representation of MIMO systems. We can refer to eigen-beamforming technique. Considering an MIMO channel with $N_r \times N_t$ channel matrix \mathbf{H} that is known to both the transmitter and the receiver, the eigenvectors can be found by applying SVD technique to channel matrix as shown below:

$$\mathbf{H} = \mathbf{W} \mathbf{S} \mathbf{V}^*, \quad (9)$$

where $N_r \times N_r$ matrix \mathbf{W} and the $N_t \times N_t$ matrix \mathbf{V} are unitary, and \mathbf{S} is an $N_r \times N_t$ diagonal matrix. These two matrices are used as pre- and postcoding matrices at transmitter and receiver, respectively. So the channel matrix when applying pre and post matrices can be written as follows:

$$\mathbf{H}^e = \mathbf{W}^* \mathbf{H} \mathbf{V}. \quad (10)$$

Thus, the capacity of MIMO system is given by

$$C = \log_2 \det\left(\mathbf{I}_{N_r} + \frac{P_t}{P_N N_t} \mathbf{H}^e \mathbf{H}^{e*}\right). \quad (11)$$

2.4. MIMO System with Open Loop Beamforming Technique.

Figure 1(c) showed the open loop beamforming representation of MIMO systems. The open loop beamforming can be represented by the transmitted and received signals. The signal arriving at a directional cosine Ω into the receive antenna array is along the unit spatial signature $\mathbf{e}_r(\Omega)$ given by (7). Hence, the particularly fixed sequence of Ω can form a special set of $N_r \times 1$ vectors given as

$$\xi_r := \left\{ \mathbf{e}_r(0), \mathbf{e}_r\left(\frac{1}{L_r}\right), \dots, \mathbf{e}_r\left(\frac{N_r-1}{L_r}\right) \right\}. \quad (12)$$

In (12), it can be noticed that there is a set of orthogonal basis for the received signal space. This basis provides the representation of received signals in the open loop beamforming.

It is similarly defined for the open loop beamforming representation of the transmitted signal. The signal transmitted at direction Ω is along the unit vector $\mathbf{e}_t(\Omega)$, defined in (6). The set of $N_t \times 1$ sequential vectors is given as

$$\xi_t := \left\{ \mathbf{e}_t(0), \mathbf{e}_t\left(\frac{1}{L_t}\right), \dots, \mathbf{e}_t\left(\frac{N_t-1}{L_t}\right) \right\}, \quad (13)$$

where $L_t = N_t \Delta_t$ and $L_r = N_r \Delta_r$ are the normalized antenna array lengths of the transmitter and receiver, respectively. Let \mathbf{U}_t and \mathbf{U}_r be the unitary matrices whose columns are the basis vector in (13) and (12), respectively, which can be written as

$$\mathbf{U}_t = \frac{1}{\sqrt{N_t}} \begin{bmatrix} 1 & 1 & \dots & 1 \\ 1 & e^{-j2\pi/N_t} & \dots & e^{-j2\pi(N_t-1)/N_t} \\ \vdots & \vdots & \ddots & \vdots \\ 1 & e^{-j2\pi(N_t-1)/N_t} & \dots & e^{-j2\pi(N_t-1)(N_t-1)/N_t} \end{bmatrix}, \quad (14)$$

$$\mathbf{U}_r = \frac{1}{\sqrt{N_r}} \begin{bmatrix} 1 & 1 & \dots & 1 \\ 1 & e^{-j2\pi/N_r} & \dots & e^{-j2\pi(N_r-1)/N_r} \\ \vdots & \vdots & \ddots & \vdots \\ 1 & e^{-j2\pi(N_r-1)/N_r} & \dots & e^{-j2\pi(N_r-1)(N_r-1)/N_r} \end{bmatrix}. \quad (15)$$

We can transform the conventional MIMO system into the open loop beamforming by the following expression:

$$\mathbf{H}^a := \mathbf{U}_r^* \mathbf{H} \mathbf{U}_t. \quad (16)$$

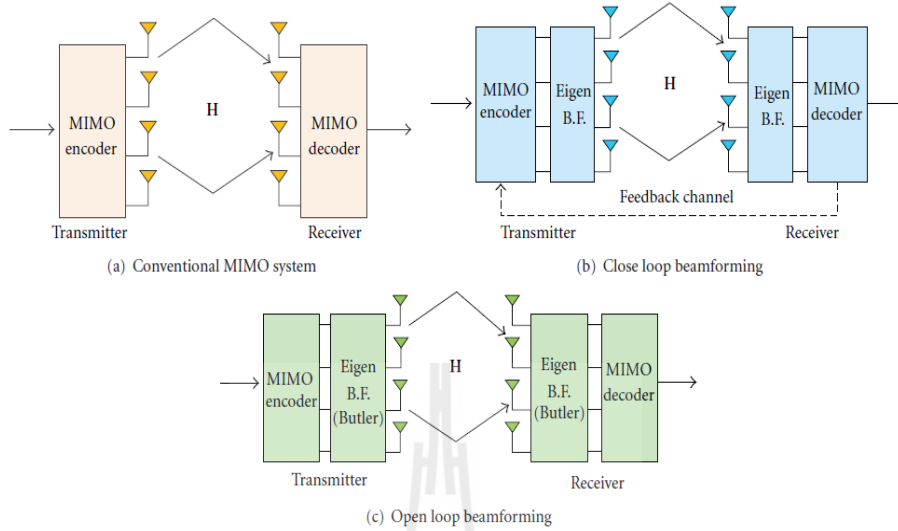


FIGURE 1: System overviews.

Thus, the capacity of MIMO systems can be given by

$$C = \log_2 \det \left(\mathbf{I}_{N_r} + \frac{P_t}{P_N N_t} \mathbf{H}^a \mathbf{H}^{a*} \right), \quad (17)$$

where \mathbf{I}_{N_r} is the identity matrix having $N_r \times N_r$ dimension, \mathbf{H}^a is the channel matrix having $N_r \times N_t$ dimension.

Figure 2 shows the simulated channel matrices from statistical modeling adopted by [20]. The basis for the statistical modeling of MIMO fading channels is approximated by the physical paths partitioning into angularly resolvable bins and aggregated to form resolvable paths, whose channel gains are $\mathbf{H}_{k,l}^a$. Assuming that a_i of the physical paths is independent. We use (4)–(7) to find channel matrix for conventional MIMO and (14)–(16) to find channel matrix for open loop beamforming.

3. Analytical Analysis of Open Loop Beamforming

It has been demonstrated in the literatures [22–27] that the channel capacity depends on the channel correlation. The large amplitude of correlation coefficient degrades the capacity performance. In this section, the analytical analysis of how open loop beamforming improves the channel capacity is described by showing the impact of using open loop beamforming on the channel correlation.

Let the channel matrix be modeled as

$$\mathbf{H} = \Psi_r^{1/2} \mathbf{H}_{iid} \Psi_t^{1/2}, \quad (18)$$

where \mathbf{H}_{iid} is the complex random matrix in which its entries are identically independent distribution, Ψ_r and Ψ_t represent the matrices of channel correlation at receiver and transmitter, respectively.

Using Conventional MIMO System. According to (4), the (k,l) th entry of correlation matrix at receiver is able to be given as

$$\Psi_r|_{k,l} = E \left\{ \left(\sum_i a_i^b e^{-j2\pi k \Delta_r \Omega_{ri}} \mathbf{e}_t(\Omega_{ri})^* \right) \times \left(\sum_r a_r^b e^{-j2\pi l \Delta_r \Omega_{ri}} \mathbf{e}_t(\Omega_{ri})^* \right)^* \right\}, \quad (19)$$

where $E\{\cdot\}$ is the expectation operation. Assuming all the propagation paths are independent from each other, the correlation element in (19) can be reduced to

$$\Psi_r|_{k,l} = \sum_i |a_i^b|^2 e^{-j2\pi(k-l)\Delta_r \Omega_{ri}}. \quad (20)$$

Same as the receiver, the (k,l) th entry of correlation matrix at transmitter is given by

$$\Psi_t|_{k,l} = \sum_i |a_i^b|^2 e^{j2\pi(k-l)\Delta_r \Omega_{ri}}. \quad (21)$$

In literatures, the degradation of channel capacity depends on the magnitude of correlation coefficient. As seen in (20) and (21), the magnitude is varied by multipath attenuation factors and angle of arrival or departure. However, in order to provide more insight on correlation coefficient, this paper assumes the Gaussian distribution for the attenuation a_i and the uniform distribution for the directional cosine within the range of angle spread σ . As a result, the mean of correlation coefficient at receiver is given by

$$\bar{\Psi}_r|_{k,l} = \int \sum_i |a_i^b|^2 e^{-j2\pi(k-l)\Delta_r \Omega_{ri}} \text{prob}(a_i^b, \Omega_{ri}) da_i^b d\Omega_{ri}. \quad (22)$$

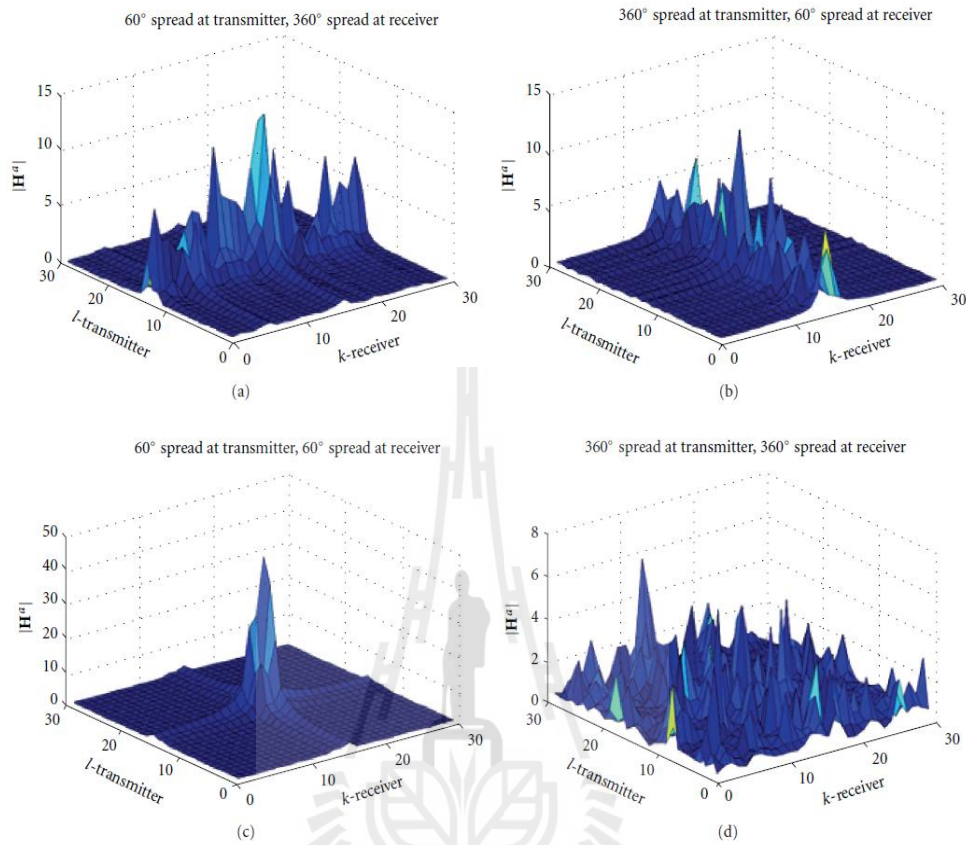


FIGURE 2: Examples of H^e with different angle spreads at transmitter and receiver.

Because the property of each path is independent from each other and also the attenuation is independent from the directional cosine, then

$$\bar{\Psi}_r|_{k,l} = \sum_i |\bar{a}_i^b|^2 e^{-j2\pi(k-l)\Delta_r \bar{\Omega}_{ri}} \frac{\sin(\pi(k-l)\Delta_r \sigma_{ri})}{\pi(k-l)\Delta_r \sigma_{ri}}, \quad (23)$$

where \bar{a}_i^b is the mean value of a_i^b and $\bar{\Omega}_{ri}$ is the mean value of Ω_{ri} .

In (23), it can be noticed that the mean of correlation coefficient depends on the angle spread. This mean correlation is close to 0 when the angle spread is large. If the angle spread is very small and assuming the same mean of directional cosine for all paths, then the magnitude of mean correlation can be given by

$$|\bar{\Psi}_r| = \sum_i |\bar{a}_i^b|^2. \quad (24)$$

With the same derivation as receiver, the mean of correlation coefficient at transmitter is given by $|\bar{\Psi}_t| = \sum_i |\bar{a}_i^b|^2$.

Using Open Loop Beamforming. According to (16) and (18), the correlation matrices of open loop beamforming can be formed as

$$\mathbf{H}^a = \mathbf{\Psi}_r^{a(1/2)} \mathbf{H}_{iid} \mathbf{\Psi}_t^{a(1/2)}. \quad (25)$$

Then, the (k,l) th entry of correlation matrix at the receiver is expressed by

$$\begin{aligned} \Psi_r^a|_{k,l} = E \left\{ \left(\mathbf{e}_r \left(\frac{k}{L_r} \right)^* \left(\sum_i a_i^b \mathbf{e}_r(\Omega_{ri}) \mathbf{e}_t(\Omega_{ti})^* \right) \mathbf{U}_t \right) \right. \\ \left. \times \left(\mathbf{e}_r \left(\frac{l}{L_r} \right)^* \left(\sum_{i'} a_{i'}^b \mathbf{e}_r(\Omega_{ri'}) \mathbf{e}_t(\Omega_{ti'})^* \right) \mathbf{U}_t \right)^* \right\}. \end{aligned} \quad (26)$$

Assuming all the propagation paths are independent,

$$\Psi_r^a|_{k,l} = \sum_i |a_i^b|^2 \left(\mathbf{e}_r \left(\frac{k}{L_r} \right)^* \mathbf{e}_r(\Omega_{ri}) \right) \left(\mathbf{e}_r \left(\frac{l}{L_r} \right)^* \mathbf{e}_r(\Omega_{ri}) \right)^*. \quad (27)$$

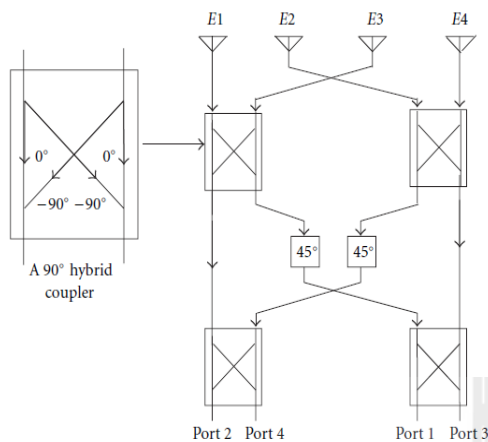


FIGURE 3: Block diagram of Butler matrix [18].

For the mean value of open loop beamforming, the same assumption with conventional MIMO has been used. From (26), the mean of correlation coefficient at receiver is given by

$$\begin{aligned} \bar{\Psi}_r|_{k,l} &= \int \sum_i |a_i^b|^2 \left(\mathbf{e}_r \left(\frac{k}{L_r} \right)^* \mathbf{e}_r(\Omega_{ri}) \right) \\ &\quad \times \left(\mathbf{e}_r \left(\frac{l}{L_r} \right)^* \mathbf{e}_r(\Omega_{ri}) \right)^* \text{prob}(a_i^b, \Omega_{ri}) da_i^b d\Omega_{ri}. \end{aligned} \quad (28)$$

Due to the independent property, then

$$\begin{aligned} \bar{\Psi}_r|_{k,l} &= \sum_i |a_i^b|^2 \int \frac{1}{N_r} \sum_{n=0}^{N_r-1} e^{(j2\pi n \Delta_r ((k/L_r) - \Omega_{ri}))} \frac{1}{N_r} \\ &\quad \times \sum_{n'=0}^{N_r-1} e^{(-j2\pi n' \Delta_r ((l/L_r) - \Omega_{ri}))} \text{prob}(\Omega_{ri}) d\Omega_{ri} \\ &= \sum_i |a_i^b|^2 \frac{1}{N_r^2} \sum_{n=0}^{N_r-1} \sum_{n'=0}^{N_r-1} e^{(j2\pi \Delta_r ((nk - n'l)/L_r))} \\ &\quad \times e^{-j2\pi(n-n')\Delta_r \bar{\Omega}_{ri}} \frac{\sin(\pi(n-n')\Delta_r \sigma_{ri})}{\pi(n-n')\Delta_r \sigma_{ri}}. \end{aligned} \quad (29)$$

For a small angle spread,

$$\begin{aligned} \bar{\Psi}_r|_{k,l} &= \sum_i |a_i^b|^2 \left(\frac{1}{N_r} \cdot \frac{1 - e^{(j2\pi N_r \Delta_r ((k/L_r) - \bar{\Omega}_{ri}))}}{1 - e^{(j2\pi \Delta_r ((k/L_r) - \bar{\Omega}_{ri}))}} \right) \\ &\quad \times \left(\frac{1}{N_r} \cdot \frac{1 - e^{(j2\pi N_r \Delta_r ((l/L_r) - \bar{\Omega}_{ri}))}}{1 - e^{(j2\pi \Delta_r ((l/L_r) - \bar{\Omega}_{ri}))}} \right)^* \end{aligned}$$

$$\begin{aligned} &= \sum_i |a_i^b|^2 e^{(j\pi(N_r-1)(k-l)/N_r)} \\ &\quad \times \left(\frac{\sin(\pi N_r \Delta_r ((k/L_r) - \bar{\Omega}_{ri}))}{N_r \sin(\pi \Delta_r ((k/L_r) - \bar{\Omega}_{ri}))} \right) \\ &\quad \times \left(\frac{\sin(\pi N_r \Delta_r ((l/L_r) - \bar{\Omega}_{ri}))}{N_r \sin(\pi \Delta_r ((l/L_r) - \bar{\Omega}_{ri}))} \right). \end{aligned} \quad (30)$$

For the transmitter, the mean of correlation coefficient can be given as

$$\begin{aligned} \bar{\Psi}_t|_{k,l} &= \sum_i |a_i^b|^2 e^{(-j\pi(N_r-1)(k-l)/N_r)} \\ &\quad \times \left(\frac{\sin(\pi N_t \Delta_t ((k/L_t) - \bar{\Omega}_{ti}))}{N_t \sin(\pi \Delta_t ((k/L_t) - \bar{\Omega}_{ti}))} \right) \\ &\quad \times \left(\frac{\sin(\pi N_t \Delta_t ((l/L_t) - \bar{\Omega}_{ti}))}{N_t \sin(\pi \Delta_t ((l/L_t) - \bar{\Omega}_{ti}))} \right). \end{aligned} \quad (31)$$

Due to the fact that

$$\begin{aligned} &(\sin(\pi N_t \Delta_t ((k/L_t) - \bar{\Omega}_{ti}))/N_t \sin(\pi \Delta_t ((k/L_t) - \bar{\Omega}_{ti}))) \\ &= \begin{cases} 1 & k/L_t = \Omega_{ti} \\ < 1 & k/L_t \neq \Omega_{ti}. \end{cases} \end{aligned} \quad (32)$$

The magnitude of mean correlation, for $k \neq l$, at the receiver when using open loop beamforming is given by

$$|\bar{\Psi}_r| = |\bar{\Psi}_t| < \sum_i |a_i^b|^2. \quad (33)$$

Comparing between (24) and (33), the magnitude of mean correlation achieved by using open loop beamforming is less than using conventional MIMO system. Therefore, according to the results in the literature [22–27], it can be implied that the capacity of MIMO system can be improved when applying open loop beamforming instead of conventional MIMO.

4. Practical Realization Using Butler Matrix

Figure 3 shows a block diagram of Butler matrix [18] which is applied to the concept of open loop beamforming for 4×4 MIMO systems. It is constituted by four 90° hybrid couplers, 2 phase shifters 45° , and a crossover. The fixed beamforming matrix is a bidirectional transmission. Hence, it can be used for either receiver or transmitter.

It is easily shown that the weight vectors corresponding to each port presented in Table 1 are mutually orthogonal. Therefore, instead of using (14) and (15), the unitary matrix

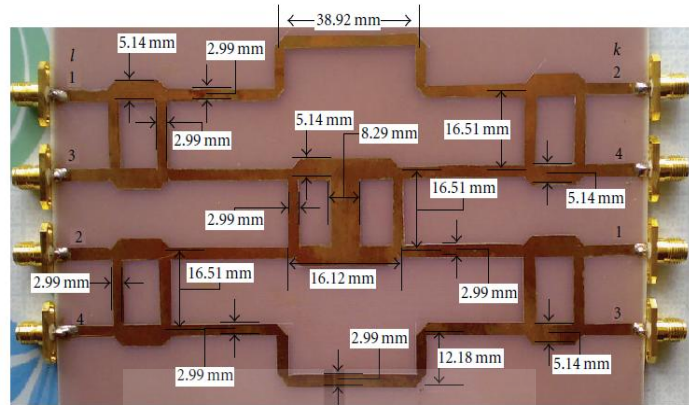


FIGURE 4: Configuration of manufactured Butler matrix.

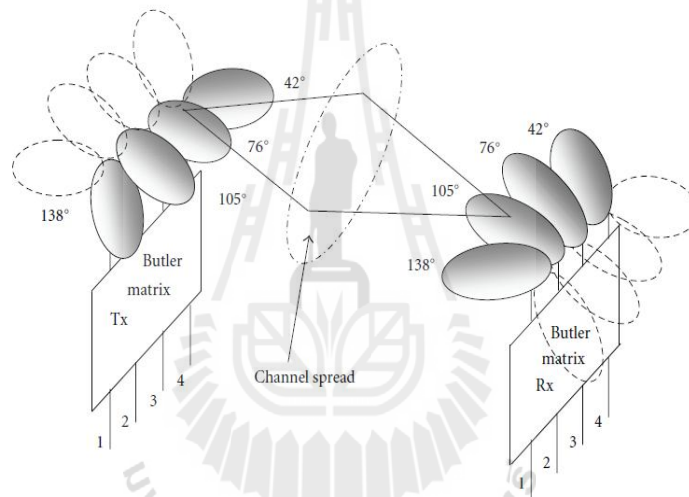
FIGURE 5: Illustration of applying Butler matrix for 4×4 MIMO systems.

TABLE 1: Element phasing, beam direction, and interelement phasing for the Butler matrix shown in Figure 3 (conceptual).

θ_{kl}	$E1 (l=1)$	$E2 (l=2)$	$E3 (l=3)$	$E4 (l=4)$	Beam direction	Inter-element phasing
Port 1 ($k=1$)	-45°	-180°	45°	-90°	138.6°	-135°
Port 2 ($k=2$)	0°	-45°	-90°	-135°	104.5°	-45°
Port 3 ($k=3$)	-135°	-90°	-45°	0°	75.5°	45°
Port 4 ($k=4$)	-90°	45°	-180°	-45°	41.4°	135°

TABLE 2: Element phasing, beam direction, and interelement phasing for the Butler matrix shown in Figure 4 (manufactured).

θ_{kl}	$E1 (l=1)$	$E2 (l=2)$	$E3 (l=3)$	$E4 (l=4)$	Beam direction	Inter-element phasing (average)
Port 1 ($k=1$)	158°	25°	-112°	118°	138°	-130°
Port 2 ($k=2$)	-87°	-137°	176°	137°	105°	-42°
Port 3 ($k=3$)	132°	178°	-139°	-98°	76°	50°
Port 4 ($k=4$)	136°	-90°	40°	176°	42°	138°

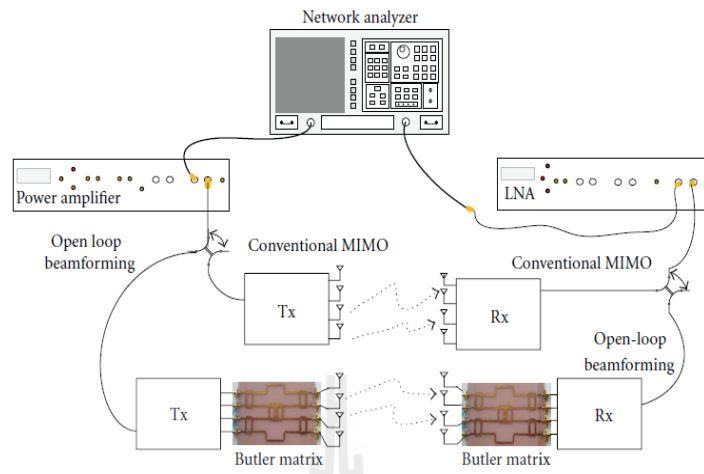


FIGURE 6: Block diagram of measurement setup.

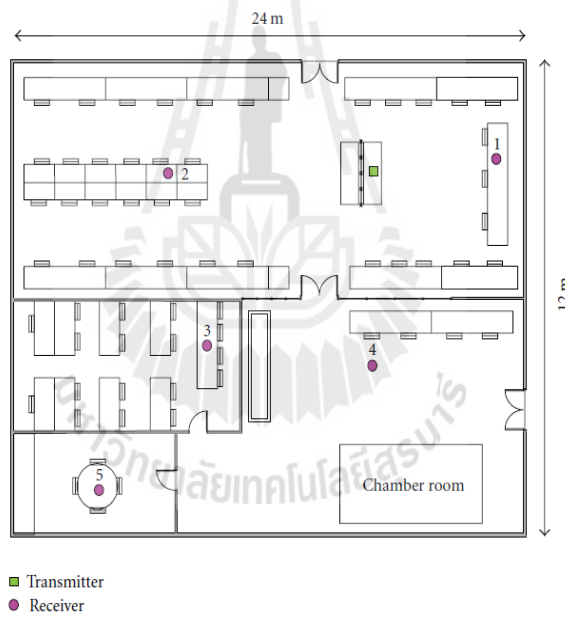


FIGURE 7: Measurement scenarios.

of applying Butler matrix can be written by the following expressions:

$$B_t = \frac{1}{\sqrt{N_t}} \begin{bmatrix} e^{-j(-45^\circ)} & e^{-j(-180^\circ)} & e^{-j(45^\circ)} & e^{-j(-90^\circ)} \\ e^{-j(0^\circ)} & e^{-j(-45^\circ)} & e^{-j(-90^\circ)} & e^{-j(-135^\circ)} \\ e^{-j(-135^\circ)} & e^{-j(-90^\circ)} & e^{-j(-45^\circ)} & e^{-j(0^\circ)} \\ e^{-j(-90^\circ)} & e^{-j(45^\circ)} & e^{-j(-180^\circ)} & e^{-j(-45^\circ)} \end{bmatrix},$$

$$B_r = \frac{1}{\sqrt{N_r}} \begin{bmatrix} e^{-j(-45^\circ)} & e^{-j(-180^\circ)} & e^{-j(45^\circ)} & e^{-j(-90^\circ)} \\ e^{-j(0^\circ)} & e^{-j(-45^\circ)} & e^{-j(-90^\circ)} & e^{-j(-135^\circ)} \\ e^{-j(-135^\circ)} & e^{-j(-90^\circ)} & e^{-j(-45^\circ)} & e^{-j(0^\circ)} \\ e^{-j(-90^\circ)} & e^{-j(45^\circ)} & e^{-j(-180^\circ)} & e^{-j(-45^\circ)} \end{bmatrix}. \quad (34)$$

Figure 4 shows a configuration of manufactured Butler matrix. The dimensions of Butler matrix can be calculated

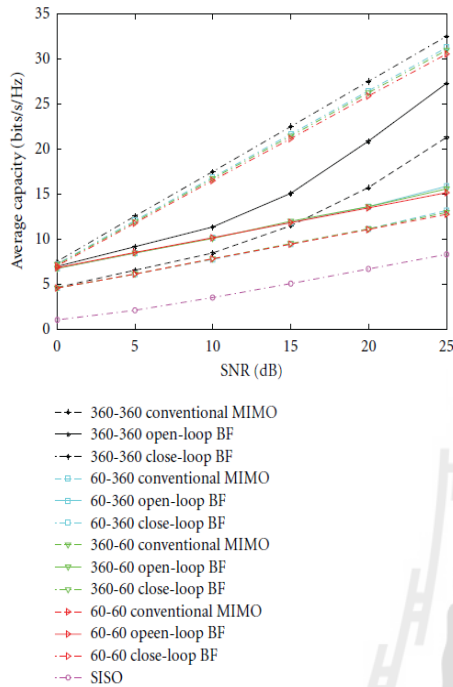


FIGURE 8: Average capacity (bits/s/Hz) versus SNR (dB) for 4 conditions of angle spread, $\Delta_t = \Delta_r = 0.5$.

from transmission line theory. The manufactured product is also confirmed by measuring inter-element phasing and beam direction which are shown in Table 2. In this table, the distributions of all inter-element phasing are similar to conceptual Butler matrix but they are slightly deviated by ± 10 degree. However, the beam direction is deviated by only 0.6 degree. All parameters used for experiments are presented in Table 3.

Figure 5 illustrates the beam direction of applying Butler matrix to both transmitter and receiver. It is interesting to see that the concept of open loop beamforming is successfully achieved by simply adding Butler matrices next to antenna elements. Then, the channel matrix realized by Butler matrix can be written as

$$\mathbf{H}^b := \mathbf{B}_r^* \mathbf{H} \mathbf{B}_t, \quad (35)$$

where \mathbf{B}_t and \mathbf{B}_r are the unitary matrices whose columns are the basis vector in four directions for transmitter and receiver and \mathbf{H} is channel matrix of size $N_r \times N_t$ to get conventional MIMO. Thus, the capacity of MIMO systems when applying Butler matrix is given by

$$C = \log_2 \det \left(\mathbf{I}_{N_r} + \frac{P_t}{P_N N_t} \mathbf{H}^b \mathbf{H}^{b*} \right). \quad (36)$$

TABLE 3: The parameters used for measurements.

Parameters	Value
Antenna type	Monopole
Number of transmitted antennas (N_t)	4
Number of received antennas (N_r)	4
Center frequency (λ_c)	2.4 GHz
The normalized separation between the transmit antennas (Δ_t)	0.5
The normalized separation between receive antennas (Δ_r)	0.5
Distance between Tx and Rx at location 1	2.3 m
Distance between Tx and Rx at location 2	6.6 m
Distance between Tx and Rx at location 3	6.8 m
Distance between Tx and Rx at location 4	6.1 m
Distance between Tx and Rx at location 5	13.3 m

5. Measurement

Figure 6 shows a block diagram of measurement setup for 4×4 MIMO system. The network analyzer is used for measurement channel coefficients in magnitude and phase. The power amplifier (PA) is used at transmitter to provide more transmitted power. Low-noise amplifier (LNA) is used at the receiver to increase the received signal level [28]. The channel measurements are undertaken five times at each location. In each location, two modes of MIMO operation (conventional MIMO and open loop beamforming) are measured. The Butler matrices are inserted at both transmitter and receiver when measuring MIMO channels with open loop beamforming.

Figure 7 shows measurement scenarios. We choose a large room to provide various test conditions. The location of the transmitter is fixed as shown in Figure 7 with rectangular symbol. There are five measured locations for the receiver represented by circular symbol in Figure 7. It is easy to measure both conventional MIMO and open loop beamforming by using switches presented in Figure 6. The measured results achieved by network analyzer are used as a channel response in MIMO systems. Also seen in Figure 6, apart from Butler matrix, all components of conventional MIMO and open loop beamforming are the same. Therefore, the measured channels can be directly compared to each other as presented in the next section.

6. Results and Discussion

6.1. Simulation Results. The simulations are undertaken by MATLAB programming, and the capacity results are evaluated by using (8), (11), and (36). For conventional MIMO approach, the channel matrix \mathbf{H} is found by assumptions in (5), (6), and (7). For simulations, the channel matrix is generated by randomizing the attenuation a_i (range from 0 to 1) for each path. The authors use 100 scattering paths for summation in (4). For angle of arrival/departure (ϕ_r/ϕ_i), firstly the authors fix the angle spreads at transmitter and receiver. Then the angles are randomly generated within

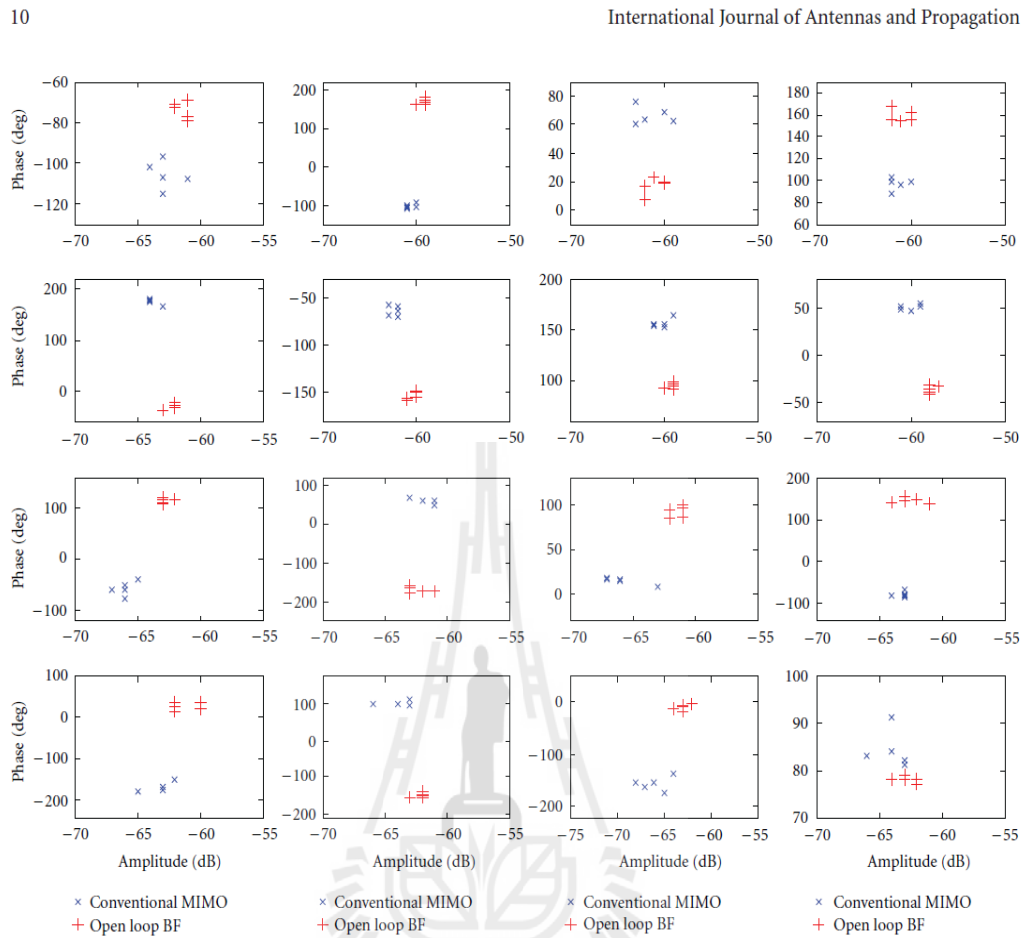


FIGURE 9: Measured 4×4 MIMO channels of conventional MIMO system and open loop beamforming (Butler matrix), at location 5.

TABLE 4: Average capacity (bps/Hz) of all locations when rotating the direction of array antennas for SNR = 10 dB.

Location	Direction					
	0°		45°		90°	
	Conv. MIMO	Open loop BF	Conv. MIMO	Open loop BF	Conv. MIMO	Open loop BF
1	8.72	10.12	9.99	11.68	11.01	11.59
2	8.43	8.52	10.54	10.98	9.61	10.84
3	6.46	6.65	6.88	9.69	9.67	10.00
4	6.88	7.37	6.66	10.69	6.67	10.69
5	10.57	11.03	11.11	11.52	11.31	11.59

these spreads. In this paper, four cases are considered as (i) 60° spread at transmitter and 360° spread at receiver, denoted as 60-360, (ii) 360° spread at transmitter and 60° spread at receiver, denoted as 360-60, (iii) 60° spread at transmitter and 60° spread at receiver, denoted as 60-60, and (iv) 360° spread at transmitter and 360° spread at receiver, denoted as 360-360. Note that case (iii) is equivalent to line-of-sight scenario while case (iv) is equivalent to Rayleigh fading channel.

In Figure 8, the average capacity comparison between 4×4 MIMO systems with conventional MIMO, open loop beamforming, close loop beamforming, and SISO system is presented. It is clearly seen that all MIMO systems offer better performance than SISO system. The results also indicate that using the open loop beamforming realized by Butler matrix offers better performance than conventional MIMO system for all cases of angle spreads. The range of capacity enhancement is from 2 to 5 dB depending on characteristic

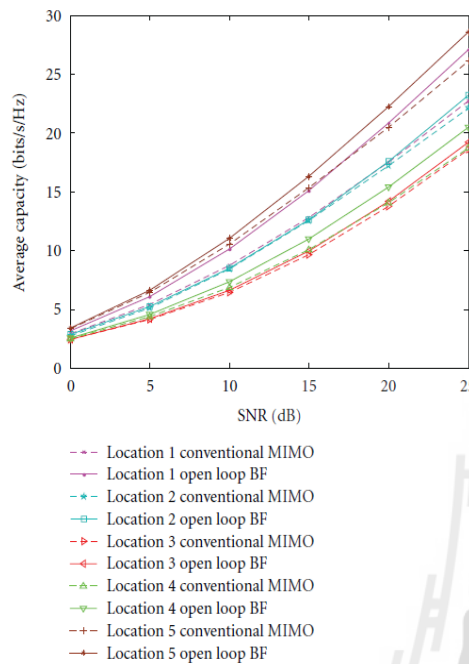


FIGURE 10: Average capacity (bits/s/Hz) versus SNR (dB) at each location.

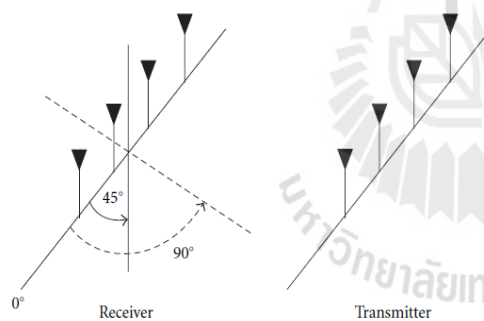


FIGURE 11: The rotating directions of array antennas for measurement scenarios.

of fading. Although the best performance is achieved by the optimum close loop beamforming technique but it requires the full knowledge of wireless channel at the receiver. Instead of additional complexity to implement close loop beamforming, the open loop beamforming can provide the significant improvement of MIMO capacity by just inserting Butler matrices and no extra complexity is required.

6.2. Measurement Results. The channel matrices H and H^b are found by measured data from network analyzer. The channel fading environments are measured by changing the locations of the receiver. Five locations are considered in

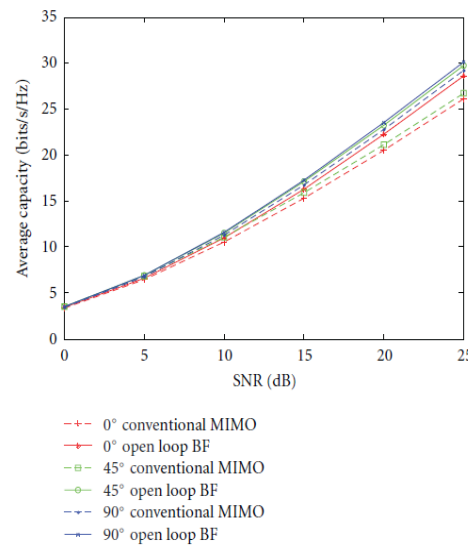


FIGURE 12: Average capacity (bits/s/Hz) versus SNR (dB) for various array directions at location 5.

Figure 7. We also believe that the mismatches among RF circuits in transmitting/receiving components and mutual coupling effects are included in the measured channel. The simulations are undertaken by utilizing measured data into MATLAB programming and the capacity results are evaluated by using (8) and (36).

Figure 9 shows comparison of conventional and open loop beamforming channels of 4×4 MIMO systems at location 5, where H_{ij} is referred to the channel coefficient at i th receive antenna and j th transmit antenna. It can be observed that channels of conventional MIMO and open loop beamforming are relatively different. The amplitude deviation is about ± 5 dB and the phase deviation is about $\pm 100^\circ$. These deviations are dominant to the capacity performance of MIMO systems. For other locations, the deviations of amplitude and phase are similar to location 5.

In Figure 10, the average capacity versus signal-to-noise ratio (SNR) at each location is presented. The results indicate that using the open loop beamforming realized by Butler matrix offers better performance than using conventional MIMO system. To compare between the simulation results presented in Figure 8 and the measurement results presented in Figure 10, the gaps between conventional MIMO and open loop beamforming in Figure 10 are different from the results in Figure 8. This is because the real propagation channel does not behave exactly as the channel modeled in simulations. However, both results provide the same agreement on improving MIMO capacity when using open loop beamforming technique.

For the measurements resulting in Figure 10, the set of transmitting and receiving antenna direction is based on face-to-face installation or 0° direction depicted in Figure 11. However, the proposed open loop beamforming

may be very sensitive to the antenna directions because both the transmitter and receiver have the fixed directivities. Accordingly, it is necessary to investigate on other array directions. The additional measurements have been done by rotating the array direction for 0° , 45° , and 90° degrees as depicted in Figure 11. The additional experiments are undertaken in all locations. Figure 12 shows the average capacity (bits/s/Hz) versus signal-to-noise ratio (SNR) in various directions at location 5. The results still indicate the significant improvement of using open loop beamforming in comparison with conventional MIMO system at each array direction. In order to justify the results of other locations, the numeric values of average capacity at SNR = 10 dB are given in Table 4. It is obviously noticed that the benefit of open loop beamforming is pronounced for all locations and all directions. Please remember that the improvement of MIMO capacity costs the little expense of inserting Butler matrices at both transmitter and receiver without any extra complexity.

7. Conclusion

This paper presented the performance of MIMO systems using open loop beamforming realized by Butler matrix. The simulation results reveal that the proposed system outperforms the conventional MIMO system for every fading case. Then, this paper verified the benefit of using open loop beamforming technique for 4×4 MIMO systems by measured results. The open loop beamforming realized by Butler matrix has been implemented and compared with conventional MIMO system. The results revealed that the open loop beamforming outperforms the conventional MIMO system for all fading locations. Hence, the proposed systems are very attractive to practically implement on MIMO systems due to low cost and complexity.

Acknowledgments

This paper is financially supported by Suranaree University of Technology, Thailand and the Royal Golden Jubilee Program of Thailand Research Fund, Thailand.

References

- [1] M. Bishwarup and W. H. Robert, "Performance analysis of quantized beamforming MIMO systems," *IEEE Transactions on Signal Processing*, vol. 54, no. 12, pp. 4753–4766, 2006.
- [2] A. Sirikiat Lek, J. Zheng, O. Eric, and J. Kim, "Subspace beamforming for near-capacity MIMO performance," *IEEE Transactions on Signal Processing*, vol. 56, no. 11, pp. 5729–5733, 2008.
- [3] X. Zheng, Y. Xie, J. Li, and P. Stoica, "MIMO transmit beamforming under uniform elemental power constraint," *IEEE Transactions on Signal Processing*, vol. 55, no. 11, pp. 5395–5406, 2007.
- [4] L. Sun, M. R. McKay, and S. Jin, "Analytical performance of MIMO multichannel beamforming in the presence of unequal power Cochannel Interference and Noise," *IEEE Transactions on Signal Processing*, vol. 57, no. 7, pp. 2721–2735, 2009.
- [5] S. L. Ariyavisitakul, E. Ojard, K. Joonsuk, Z. Jun, and N. Seshadri, "Subspace beamforming for near-capacity MIMO performance," in *Proceedings of Information Theory and Applications Workshop (ITA '08)*, pp. 333–338, San Diego, Calif, USA, January-February 2008.
- [6] R. D. Vieira, J. C. B. Brandao, and G. L. Siqueira, "MIMO measured channels: capacity results and analysis of channel parameters," in *Proceedings of the International Telecommunications Symposium (ITS '06)*, pp. 152–157, September 2006.
- [7] G. J. Foschini and M. J. Gans, "On Limits of Wireless Communications in a Fading Environment when Using Multiple Antennas," *Wireless Personal Communications*, vol. 6, no. 3, pp. 311–335, 1998.
- [8] I. E. Telatar, *Capacity of Multi-Antenna Gaussian Channels*, AT&T Bell Laboratories, Technical Memorandum, 1995.
- [9] G. J. Foschini, "Layered space-time architecture for wireless communication in a fading environment when using multi-element antennas," *Bell Labs Technical Journal*, vol. 1, no. 2, pp. 41–59, 1996.
- [10] J. P. Kermaol, P. E. Mogensen, S. H. Jensen et al., "Experimental investigation of multipath richness for multi-element transmit and receive antenna arrays," in *Proceedings of the 51st IEEE Vehicular Technology Conference*, vol. 3, pp. 2004–2008, Spring, Tokyo, Japan, May 2000.
- [11] R. Stridh, B. Ottersten, and P. Karlsson, "MIMO channel capacity on a measured indoor radio channel at 5.8 GHz," in *Proceedings of the 34th Asilomar Conference on Signals, Systems and Computers*, vol. 1, pp. 733–737, October 2000.
- [12] A. F. Molisch, M. Steinbauer, M. Toeltsch, E. Bonek, and R. S. Thomä, "Capacity of MIMO systems based on measured wireless channels," *IEEE Journal on Selected Areas in Communications*, vol. 20, no. 3, pp. 561–569, 2002.
- [13] L. Huang, J. W. M. Bergmans, and F. M. J. Willems, "Low-complexity LMMSE-based MIMO-OFDM channel estimation via angle-domain processing," *IEEE Transactions on Signal Processing*, vol. 55, no. 12, pp. 5668–5680, 2007.
- [14] L. Huang, C. K. Ho, J. W. M. Bergmans, and F. M. J. Willems, "Pilot-aided angle-domain channel estimation techniques for MIMO-OFDM systems," *IEEE Transactions on Vehicular Technology*, vol. 57, no. 2, pp. 906–920, 2008.
- [15] A. F. Molisch, X. Zhang, S. Y. Kung, and J. Zhang, "DFT-based hybrid antenna selection schemes for spatially correlated MIMO channels," in *Proceedings of the 14th International Symposium on Personal Indoor and Mobile Radio Communication*, September 2003.
- [16] A. Grau, J. Romeu, S. Blanch, L. Jofre, and F. De Flaviis, "Optimization of linear multielement antennas for selection combining by means of a Butler matrix in different MIMO environments," *IEEE Transactions on Antennas and Propagation*, no. 11, pp. 3251–3264, 2006.
- [17] A. Innok, P. Uthansakul, and M. Uthansakul, *Performance of MIMO Capacity Using Angle Domain Processing Realized by Butler Matrix*, ECTI-CON, KhonKhen, Thailand, 2009.
- [18] J. C. Liberti and J. T. S. Rappaport, *Smart Antennas for Wireless Communications*, IS-95 and Third Generation CDMA Applications, chapter 3, 1999.
- [19] G. Bakhshi, R. Saadat, and K. Shahtalebi, "A modified two-ring reference model for MIMO mobile-to-mobile communication channels," in *Proceedings of the International Symposium on Telecommunications (IST '08)*, pp. 409–413, August 2008.
- [20] D. Tse and P. Viswanath, *Fundamentals of Wireless Communication*, chapter 7, Cambridge, UK, 2005.

- [21] R. G. Tsoulos, *MIMO Systems Technology for Wireless Communications*, Electrical Engineering & Applied Signal Processing Series, chapter 4, 2006.
- [22] Z. Xiaolin, L. Zhaowei, W. Zongxin, H. A. Suraweera, and J. Armstrong, "Capacity analysis for a distributed MIMO-OFDM system in composite spatially correlated channels," in *Proceedings of the 2nd International Conference on Communications and Networking in China*, pp. 1116–1120, Shanghai, China, August 2007.
- [23] G. Levin and S. Loyka, "On the outage capacity distribution of correlated keyhole MIMO channels," *IEEE Transactions on Information Theory*, vol. 54, no. 7, pp. 3232–3245, 2008.
- [24] S. Jin, X. Gao, and X. You, "On the ergodic capacity of rank-1 Ricean-fading MIMO channels," *IEEE Transactions on Information Theory*, vol. 53, no. 2, pp. 502–517, 2007.
- [25] T. Ratnarajah, "Spatially correlated multiple-antenna channel capacity distributions," *IEE Proceedings: Communications*, vol. 153, no. 2, pp. 263–271, 2006.
- [26] M. Kang and M. S. Alouini, "Impact of correlation on the capacity of MIMO channels," in *Proceedings of the International Conference on Communications (ICC '03)*, vol. 4, pp. 2623–2627, May 2003.
- [27] S. Hyundong, Z. W. Moe, H. L. Jae, and C. Marco, "On the capacity of doubly correlated MIMO channels," *IEEE Transactions on Wireless Communications*, vol. 5, no. 8, pp. 2253–2264, 2006.
- [28] N. Promsuvana and P. Uthansakul, "Feasibility of adaptive 4×4 MIMO system using channel reciprocity in FDD mode," in *Proceedings of the 14th Asia-Pacific Conference on Communications (APCC '08)*, pp. 1–5, October 2008.

Research Article

Angular Beamforming Technique for MIMO Beamforming System

Apinya Innok, Peerapong Uthansakul, and Monthippa Uthansakul

School of Telecommunication Engineering, Suranaree University of Technology, Muang, Nakhon Ratchasima 30000, Thailand

Correspondence should be addressed to Apinya Innok, apinya_in@hotmail.com

Received 3 August 2012; Revised 2 October 2012; Accepted 6 November 2012

Academic Editor: Ananda Sanagavarapu Mohan

Copyright © 2012 Apinya Innok et al. This is an open access article distributed under the Creative Commons Attribution License, which permits unrestricted use, distribution, and reproduction in any medium, provided the original work is properly cited.

The method of MIMO beamforming has gained a lot of attention. The eigen beamforming (EB) technique provides the best performance but requiring full channel information. However, it is impossible to fully acquire the channel in a real fading environment. To overcome the limitations of the EB technique, the quantized beamforming (QB) technique was proposed by using only some feedback bits instead of full channel information to calculate the suitable beamforming vectors. Unfortunately, the complexity of finding the beamforming vectors is the limitation of the QB technique. In this paper, we propose a new technique named as angular beamforming (AB) to overcome drawbacks of QB technique. The proposed technique offers low computational complexity for finding the suitable beamforming vectors. In this paper, we also present the feasibility implementation of the proposed AB method. The experiments are undertaken mainly to verify the concept of the AB technique by utilizing the Butler matrix as a two-bit AB processor. The experimental implementation and the results demonstrate that the proposed technique is attractive from the point of view of easy implementation without much computational complexity and low cost.

1. Introduction

The multiple input multiple output (MIMO) systems provide a good quality of service such as channel capacity. In general, for MIMO systems, the consideration of channel capacity is based on the use of array antennas at both the transmitter and the receiver. Many works have proposed the eigen beamforming (EB) technique in the literature [1–5]. This technique utilizes the properties of estimated channels by performing singular value decomposition on channel matrix. Then the eigenvectors of the channel matrix are considered as pre- and postcoding schemes for MIMO systems. This technique can improve the capacity performance, but both transmitter and receiver have to have perfect knowledge of the channel information. However, there are many issues that make use of EB technique in practice such as a requirement of high system complexity and many procedures employed for channel feedback transmission. In this paper, we propose a new technique known as angular beamforming (AB) technique; the received channels are used to estimate the suitable pre- and postcoding schemes at the receiver side.

Then, a little number of bits are fed back to transmitter in order to form beam to the suitable direction according to the channel. The pre- and postcoding schemes are low complexity and offer high channel capacity. Therefore, the study of using AB technique is the focus of this paper.

Many works on MIMO system [6–9] have been proposed to enhance the channel capacity in order to satisfy the user demand for high data rate applications. Some of the studies were focused on theoretical works, and others performed measurements. Nevertheless, most of the paper developed techniques to enhance the channel capacity through channel behaviour [10–12] such as adjusting transmitted powers according to eigenvalue of channels which is known as water filling method. In general, it can be noticed that the theoretical consideration of channel capacity is based on the assumption that array antennas are employed at both the transmitter and the receiver. However, the channel characteristic is dependent on many angle-based parameters of multipath such as angle of arrival, angle of departure, and angle of spread. Therefore, it would be interesting to investigate the performance of MIMO system using

the angular beamforming (AB) instead of the conventional methods.

Recently, the authors in [13, 14] developed a channel estimation of MIMO-OFDM system based on angular beamforming (AB) consideration. The applicability of AB technique depends on the channel stochastic information available at the receiver. The design of suitable pilots is proposed by facilitating the direct implementation of analyzing the performances of different channel estimation techniques. Although the significant improvement on MIMO capacity can be expected by using AB method, so far in the literature, there is no work available that illustrates the capacity benefit of using AB method. The reason is the lack of pre- and post-coding schemes for angle transformations that can decrease the complexity on both transmitter and receiver. Hence, it is challenging to find a technique that can obtain lower cost and lower complexity that matches with the concept of AB method. In [15], a scheme was proposed that uses a discrete fourier transformation (DFT) to receive a signal vector in RF domain. This can be realized by placing a Butler matrix between the antenna elements and the receiver switch. However, [15] presented only the simulations results, and no measurement result was provided. With only simulation results, one cannot claim the practical advantages of the system. A low profile concept of angle domain processing has been conveniently implemented in [16] by only inserting Butler matrices before antenna array at transmitter and receiver. The authors of [17] investigated the correlation coefficients (line of sight and nonline of sight) via both simulation and measurement results. However, they did not discuss any analysis of correlation coefficients which was later presented by us in [18]. But, in our previous work, we did not consider the process of feedback bits for increasing channel capacity. In this paper, the complexity analysis of how Angular beamforming (AB) and quantized beamforming (QB) impact on the channel matrix is provided. We also provide reasons as to why the use of AB method for MIMO system offers a better performance over a QB method. Further, in this paper, we perform experimental campaigns by fabricating a Butler matrix so as to further demonstrate the usefulness of our system for practical application. The Butler matrix was chosen because it is just a low-complexity hardware that can offer the Angular beamforming (AB). In general, there are infinite choices to choose for the set of orthogonal steering vectors to form an AB. Therefore, it is hard to justify whether Butler matrix provides the best performance among others. To focus on hardware complexity, the other methods to form AB might need 16 phase shifters to simultaneously form 4 beams whereas the Butler matrix approach uses only one low-cost printed circuit board. This motivated the authors to construct the 4×4 MIMO system featuring AB by employing a Butler matrix which has a low profile concept and is convenient for implementation. This Butler matrix simultaneously forms multiple beams for providing departure or arrival angles into four directions. By only inserting Butler matrix into the antenna arrays, the conventional MIMO systems can be transformed into the MIMO systems with Angular beamforming (AB) without

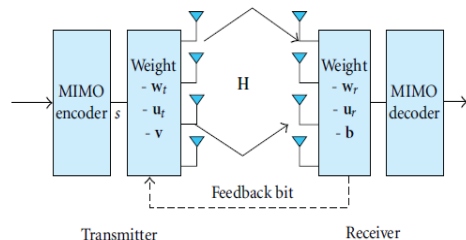


FIGURE 1: 4×4 MIMO system with beamforming.

the need for additional burden on processing units at both transmitter and receiver.

In summary, the contribution of this paper falls into three main categories. The first contribution is related to the comparisons in terms of channel capacity. Secondly, we demonstrate as to how the simulation complexity of AB method and QB method impacts on the channel matrix which is not available elsewhere. The main aim here is to help the reader to understand the key benefits offered by AB. The third contribution is to the implementation feasibility of AB method for 4×4 MIMO systems which has been demonstrated using a Butler matrix. All the three contributions either propose a new concept or confirm the actual benefit of employing MIMO with AB. The paper is organized as follows. In Section 2, the details of MIMO beamforming, AB, QB, and EB techniques are described. Then in Section 3, the simulation results and complexity analysis of using AB and QB are explained. The implementation and feasibility of using a Butler matrix to apply for AB are given in Section 4. Section 5 describes the details of channel measurements. Section 5 provides the measurement results of AB realized by Butler matrix in comparing with CM system. Finally in Section 6, the conclusion of this paper is given.

2. MIMO Beamforming

2.1. Angular Beamforming (AB). Referring to Figure 1, the transmitter, the data symbol s is modulated by the beamformer \mathbf{u}_t , and then the signals are transmitted into a MIMO channel. At the receiver, the signals are processed with the beamforming vector \mathbf{u}_r . Then the relation between transmitted and received signal is given by

$$\mathbf{y} = \mathbf{u}_r^* [\mathbf{H}\mathbf{u}_t s + \mathbf{n}]. \quad (1)$$

The transmit beamforming vector \mathbf{u}_t and the receive beamforming vector \mathbf{u}_r in (1) are usually chosen to maximize the receive SNR. Without loss of generality, we assume that $\|\mathbf{U}_t\|^2 = 1$, $E\{\|s\|^2\} = 1$. Then the received SNR is expressed as

$$\rho = \frac{E\{\|\mathbf{u}_r^* \mathbf{H} \mathbf{u}_t s\|^2\}}{E\{\|\mathbf{u}_r^* \mathbf{n}\|^2\}} = \frac{\|\mathbf{u}_r^* \mathbf{H} \mathbf{u}_t\|^2}{\sigma_n^2}. \quad (2)$$

To maximize the received SNR, the optimal transmit beamformer is chosen as the eigenvector corresponding to the

largest eigen-value of $\mathbf{H}\mathbf{H}^*$. The singular values can be obtained from SVD technique by using MATLAB. Thus the maximized received SNR is $\rho = (\lambda_{\max}(\mathbf{H}\mathbf{H}^*)) / (\sigma_n^2)$. The λ_{\max} is the maximum eigen-value of a matrix that is formed by identically distributed (i.i.d.) complex Gaussian random variables with zero-mean and variance σ_n^2 in [3].

There is an arbitrary number of physical paths between the transmitter and receiver [19]; the i th path having attenuation of a_i makes an angle of ϕ_{ti} ($\Omega_{ti} := \cos \phi_{ti}$) with the transmit antenna array and angle of ϕ_{ri} ($\Omega_{ri} := \cos \phi_{ri}$) with the receive antenna array. The channel matrix \mathbf{H} can be written using the following expressions:

$$\mathbf{H} = \sum_i a_i^b \mathbf{e}_r(\Omega_{ri}) \mathbf{e}_t(\Omega_{ti})^*, \quad (3)$$

where

$$a_i^b := a_i \sqrt{N_t N_r} \exp\left(-\frac{j2\pi d_i}{\lambda_c}\right),$$

$$\mathbf{e}_t(\Omega) := \frac{1}{\sqrt{N_t}} \begin{bmatrix} 1 \\ \exp[-j(2\pi\Delta_t\Omega)] \\ \vdots \\ \exp[-j(N_t - 1)(2\pi\Delta_t\Omega)] \end{bmatrix},$$

$$\mathbf{e}_r(\Omega) := \frac{1}{\sqrt{N_r}} \begin{bmatrix} 1 \\ \exp[-j(2\pi\Delta_r\Omega)] \\ \vdots \\ \exp[-j(N_r - 1)(2\pi\Delta_r\Omega)] \end{bmatrix}. \quad (4)$$

Also, d_i is the distance between transmit and receive antennas along i th path. Note that $(\cdot)^*$ is the conjugate and transpose operation. The vectors $\mathbf{e}_t(\Omega)$ and $\mathbf{e}_r(\Omega)$ are, respectively, transmitted and received unit spatial signatures along the direction Ω , and λ_c is the wavelength of the center frequency in a whole signal bandwidth. Assuming uniform linear array, the normalized separation between the transmit antennas is Δ_t (antenna separation/ λ_c), and the normalized separation between receive antennas is Δ_r (antenna separation/ λ_c). Note that the reason of normalization is because this proposed system can work in any frequency band. Hence, the normalization is made to neglect the unused parameter. Channel state information (CSI) is not available at the transmitter. The concept of Angular beamforming (AB) can be represented by the transmitted and received signals. It is convenient for implementation by just inserting \mathbf{u}_t and \mathbf{u}_r at both transmitter and receiver because the beamforming vectors depend on angle of arrival or departure. The numbers of feedback bits are defined by the angle (θ) , $\theta \in [0, \pi)$. The angles are divided equally. The angle can be expressed as $N_i = 2^{B_i}$, N_i denoting the number of angle levels. B_i is the number of feedback bits. When comparing with Quantized Beamforming (QB), the procedure to find beamforming vectors in QB is more

complex than that of AB. The detail of QB is shown in the next section. In general, \mathbf{u}_t and \mathbf{u}_r can be written as

$$\mathbf{u}_t = \frac{1}{\sqrt{N_t}} \exp(jlk\Delta_t \cos \theta); \quad l = 1, 2, \dots, N_t, \quad (5)$$

$$\mathbf{u}_r = \frac{1}{\sqrt{N_r}} \exp(jmk\Delta_r \cos \theta); \quad m = 1, 2, \dots, N_r,$$

where $k = 2\pi/\lambda_c$. We can use $\max \|\mathbf{u}_t^* \mathbf{H} \mathbf{u}_r\|^2$ that will be maximum for \mathbf{u}_t and \mathbf{u}_r . So the channel matrix of AB can be written as

$$\mathbf{H}_{\max}^a = \mathbf{u}_{r\max}^* \mathbf{H} \mathbf{u}_{t\max}. \quad (6)$$

Thus, the capacity [20] of MIMO systems using AB is given by

$$C = \log_2 \det \left(\mathbf{I}_{N_r} + \frac{P_t}{P_N N_t} \mathbf{H}_{\max}^a \mathbf{H}_{\max}^{a*} \right), \quad (7)$$

where P_t is the transmitted power and P_N is the noise power in each branch of antennas at the receiver. Note that the signal-to-noise power ratio (SNR) is defined as P_t/P_N . \mathbf{I}_{N_r} is the identity matrix having $N_r \times N_r$ dimension, and \mathbf{H} is the channel matrix having $N_r \times N_t$ dimension with \mathbf{H}^* being its transpose conjugate. In this paper, the channel matrix \mathbf{H} is normalized by $\|\mathbf{H}\|_F^2 = N_r N_t$. \mathbf{H}_{\max}^a is the channel matrix of size $N_r \times N_t$ streams.

2.2. Quantized Beamforming (QB). In eigen beamforming (EB) designs, we have assumed that the transmitter has perfect knowledge of CSI. However, in many real systems, having the CSI known exactly at the transmitter is hardly possible. The channel information is usually provided by the receiver through a bandwidth-limited finite-rate feedback channel, and quantization method, which has been widely studied for source coding [3], can be used to provide the feedback information. We assume herein that the receiver has perfect CSI. The transmit beamforming vector \mathbf{w}_t for QB is used under the uniform elemental power constraint. The expression for transmit beamformer $\mathbf{w}_t(\theta_0, \theta_1, \dots, \theta_{N_t-1})$ which is a function of N_t parameters $\{\theta_i, \theta_i \in [0, 2\pi)\}_{i=0}^{N_t-1}$ is obtained using simple manipulations as

$$\mathbf{w}_t(\theta_0, \theta_1, \dots, \theta_{N_t-1}) = \frac{1}{\sqrt{N_t}} e^{j\theta_0} \begin{bmatrix} 1 \\ e^{j\theta_1} \\ \vdots \\ e^{j\theta_{N_t-1}} \end{bmatrix}, \quad (8)$$

where $\|\mathbf{H}\mathbf{w}_t(\theta_0, \theta_1, \dots, \theta_{N_t-1})\|^2 = \|\mathbf{H}\mathbf{w}_t(\tilde{\theta}_1, \tilde{\theta}_2, \dots, \tilde{\theta}_{N_t-1})\|^2$. Since $\|\mathbf{H}\mathbf{w}_t(\theta_0, \theta_1, \dots, \theta_{N_t-1})\|^2 = \|\mathbf{H}\mathbf{w}_t(\tilde{\theta}_1, \tilde{\theta}_2, \dots, \tilde{\theta}_{N_t-1})\|^2$. We can reduce one parameter and quantize $\mathbf{w}_t(\tilde{\theta}_1, \tilde{\theta}_2, \dots, \tilde{\theta}_{N_t-1})$ instead of $\mathbf{w}_t(\theta_0, \theta_1, \dots, \theta_{N_t-1})$. Consider

$$\mathbf{w}_t(\tilde{\theta}_1^m, \dots, \tilde{\theta}_{N_t-1}^m) = \frac{1}{\sqrt{N_t}} \begin{bmatrix} 1 \\ e^{j\tilde{\theta}_1^m} \\ \vdots \\ e^{j\tilde{\theta}_{N_t-1}^m} \end{bmatrix}, \quad (9)$$

TABLE 1: Average capacity (bps/Hz) 4×4 MIMO beamforming for SNR = 10 dB.

Methods	Number of feedback bits							
	1	2	3	4	5	6	7	8
EB	5.113	5.113	5.113	5.113	5.113	5.113	5.113	5.113
AB	2.391	4.538	5.076	5.088	5.091	5.093	5.093	5.093
QB	3.711	3.711	5.09	5.09	5.09	5.09	5.09	5.09

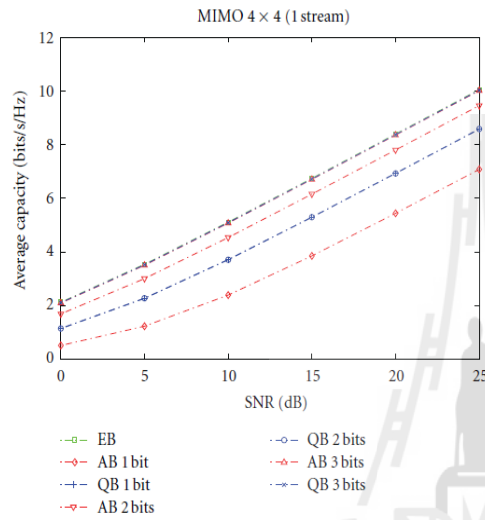


FIGURE 2: Capacity versus SNR.

where $\tilde{\theta}_i^{n_i} = (2\pi n_i)/(N_i)$, $0 \leq n_i \leq N_i - 1$, $i = 1, 2, \dots, N_t - 1$, with $N_i = 2^{B_i}$ and N_i denoting the number of quantization levels and feedback index of $\tilde{\theta}_i$, respectively, and where B_i is the number of feedback bits for $\tilde{\theta}_i$.

We quantize the parameters $\tilde{\theta}_i$ to the round-off grid point $\tilde{\theta}_i^{n_i}$, $i = 1, 2, \dots, N_t - 1$. Hence for this quantization scheme, we need to send the index set n_i from the receiver to the transmitter. Let \mathbf{w}_t and \mathbf{w}_r be the beamforming vectors. This requires $B = \sum_{i=1}^{N_t-1} B_i$ bits. The receive beamformer \mathbf{w}_r can be written as

$$\mathbf{w}_r = \frac{\mathbf{H}\mathbf{w}_t(\tilde{\theta}_1^{n_1}, \tilde{\theta}_2^{n_2}, \dots, \tilde{\theta}_{N_t-1}^{n_{N_t-1}})}{\|\mathbf{H}\mathbf{w}_t(\tilde{\theta}_1^{n_1}, \tilde{\theta}_2^{n_2}, \dots, \tilde{\theta}_{N_t-1}^{n_{N_t-1}})\|}. \quad (10)$$

We can use $\max \|\mathbf{w}_r^* \mathbf{H}\mathbf{w}_t\|^2$ that will provide maximum \mathbf{w}_t and \mathbf{w}_r . Then, the channel matrix \mathbf{H} when applying the maximum transmits beamforming ($\mathbf{w}_{t\max}$) and the maximum receive combining vector ($\mathbf{w}_{r\max}$) can be written as

$$\mathbf{H}_{\max}^q = \mathbf{w}_{r\max}^* \mathbf{H}\mathbf{w}_{t\max}. \quad (11)$$

Thus, the capacity [20] of MIMO system using QB is given by

$$C = \log_2 \det \left(\mathbf{I}_{N_r} + \frac{P_t}{P_N N_t} \mathbf{H}_{\max}^q \mathbf{H}_{\max}^{q*} \right), \quad (12)$$

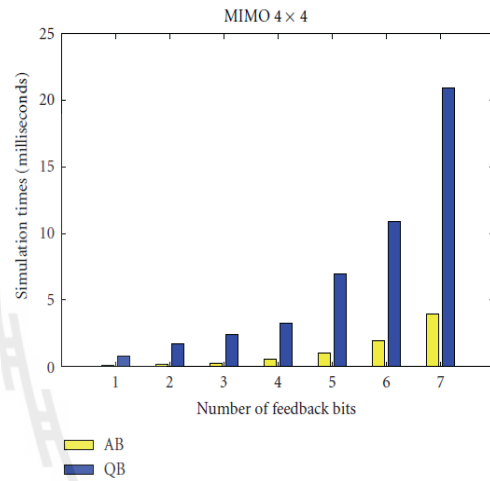


FIGURE 3: Simulation times versus number of feedback bits.

where \mathbf{I}_{N_r} is the identity matrix of size $N_r \times N_r$ and \mathbf{H}_{\max}^q is the channel matrix of size $N_r \times N_t$.

2.3. Eigen Beamforming (EB). Considering a MIMO channel with $N_r \times N_t$ channel matrix \mathbf{H} to be known at both the transmitter and the receiver, the eigenvectors can be found by applying SVD technique to the channel matrix as shown in the following:

$$\mathbf{H} = \mathbf{B}\mathbf{S}\mathbf{V}^*, \quad (13)$$

where $N_r \times N_r$ matrix \mathbf{B} and the $N_t \times N_t$ matrix \mathbf{V} are unitary matrices and \mathbf{S} is an $N_r \times N_t$ diagonal matrix. The beamforming vectors \mathbf{b} and \mathbf{v} can be found from unitary matrices \mathbf{B} and \mathbf{V} , respectively. The beamforming vectors are given by the first column of the unitary matrices. These two vectors are used as pre- and postcoding matrices at transmitter and receiver, respectively. So the channel matrix of EB can be written as

$$\mathbf{H}^e = \mathbf{b}^* \mathbf{H} \mathbf{v}. \quad (14)$$

Thus, the capacity of MIMO system using EB is given by

$$C = \log_2 \det \left(\mathbf{I}_{N_r} + \frac{P_t}{P_N N_t} \mathbf{H}^e \mathbf{H}^{e*} \right). \quad (15)$$

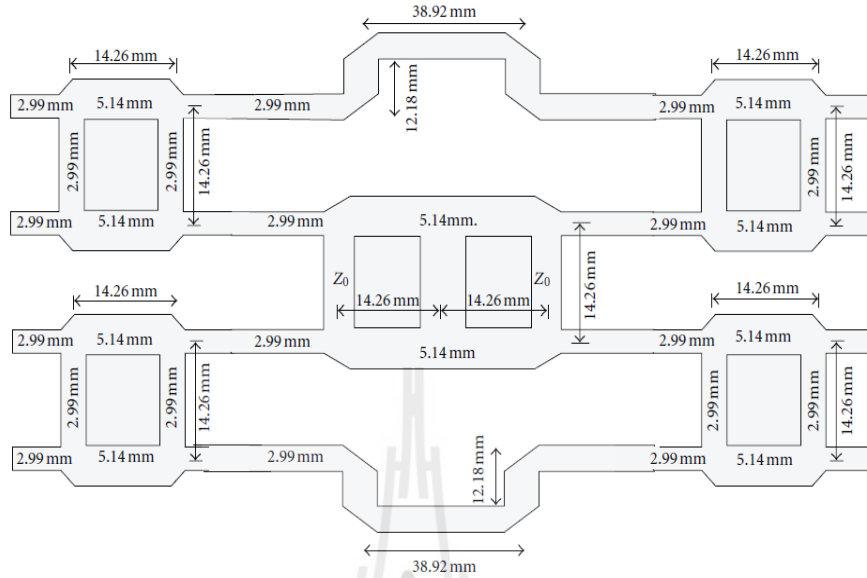


FIGURE 4: The dimensions of Butler matrix.

TABLE 2: The process of formation of FLOP with the QB.

QB	FLOP
$N_i = 2^{B_i}$	$B - 1$
$B_{a1} = \lfloor B/(N_i - 1) \rfloor$	2
$B_{a2} = B_{a1} + 1$	1
$N_s = B - B_{a1}(N_i - 1)$	3
$\hat{\theta}_i = \frac{2\pi n_i}{N_i}; 0 \leq n_i \leq N_i - 1$	2
Return loop $\theta_i^{n_i}$ can find from N_i	$B - 1$
$\mathbf{w}_t(\hat{\theta}_1^{n_1}, \dots, \hat{\theta}_{N_i-1}^{n_{N_i-1}}) = \frac{1}{\sqrt{N_i}} \begin{bmatrix} 1 \\ e^{j\hat{\theta}_1^{n_1}} \\ \vdots \\ e^{j\hat{\theta}_{N_i-1}^{n_{N_i-1}}} \end{bmatrix}$	$N_i - 1$
$\mathbf{w}_r = \frac{\mathbf{H}\mathbf{w}_t(\hat{\theta}_1^{n_1}, \hat{\theta}_2^{n_2}, \dots, \hat{\theta}_{N_i-1}^{n_{N_i-1}})}{\ \mathbf{H}\mathbf{w}_t(\hat{\theta}_1^{n_1}, \hat{\theta}_2^{n_2}, \dots, \hat{\theta}_{N_i-1}^{n_{N_i-1}})\ }$	$3(N_i - 1)$
$h_s = \frac{1}{\sqrt{N_i}} \ \mathbf{w}_r^* \mathbf{H}\mathbf{w}_t\ ^2$	5
Return loop and find maximum channel from $N_i = 2^{B_i}$	$B - 1$
Total	$2B^2 + 5B + 4BN_i - 4N_i - 7$

3. Simulation Results and Discussion

The simulations are performed using MATLAB, and the capacity results are evaluated by using (7), (12), and (15).

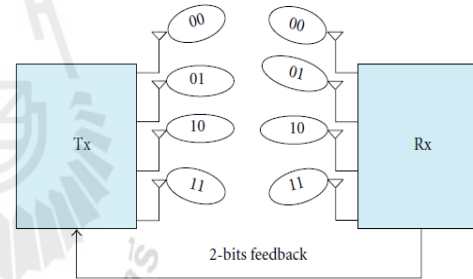


FIGURE 5: Illustration of applying two-bit feedback (Butler matrix) for 4×4 MIMO systems.

Figure 2 shows the average capacity versus SNR. We increase the number of feedback bits, since the range of capacity enhancement depends on the number of feedback bits. Also, the number of feedback bits can improve the channel capacity. The numerical values of average capacity at SNR = 10 dB for other bits are given in Table 1. It can be obviously noticed that the benefit of AB is pronounced for all the bits. It must be kept in mind that the improvement of MIMO capacity comes with a cost of inserting \mathbf{u}_t and \mathbf{u}_r at both transmitter and receiver and corresponding extra implementation complexity. The optimum EB offers better performance than both QB and AB. However, the implementation of AB is so easy that provides a very good tradeoff with EB.

The method of calculating feedback bits in AB is simpler than QB so that the operating time of AB is much shorter

TABLE 3: The process of formation of FLOP with the AB.

AB	FLOP
$N_i = 2^{B_i}$	$B - 1$
$\pi/2^B$	1
Return loop find θ from N_i	$B - 1$
$u_l = (1/\sqrt{N_l}) \exp(jlk\Delta_l \cos \theta)$; $l = 1, 2, \dots, N_l$	N_l
$u_r = (1/\sqrt{N_r}) \exp(jlk\Delta_r \cos \theta)$; $l = 1, 2, \dots, N_r$	N_r
$h_a = (1/N_i) \ u_a^* \mathbf{H} u_a\ ^2$	5
Return loop and find maximum channel from $N_i = 2^{B_i}$	$B - 1$
Total	$2B^2 + 2B + BN_l + BN_r - N_l - N_r - 4$

TABLE 4: Element phasing, beam direction, and interelement phasing for the Butler matrix shown in Figure 3 (conceptual).

b_l, b_r	E1 ($l = 1$)	E2 ($l = 2$)	E3 ($l = 3$)	E4 ($l = 4$)	Beam direction	Interelement phasing
Port 1 ($m = 1$)	$\frac{1}{\sqrt{4}} e^{-j45^\circ}$	$\frac{1}{\sqrt{4}} e^{-j180^\circ}$	$\frac{1}{\sqrt{4}} e^{j45^\circ}$	$\frac{1}{\sqrt{4}} e^{-j90^\circ}$	138.6°	-135°
Port 2 ($m = 2$)	$\frac{1}{\sqrt{4}} e^{j0^\circ}$	$\frac{1}{\sqrt{4}} e^{-j45^\circ}$	$\frac{1}{\sqrt{4}} e^{-j90^\circ}$	$\frac{1}{\sqrt{4}} e^{-j135^\circ}$	104.5°	-45°
Port 3 ($m = 3$)	$\frac{1}{\sqrt{4}} e^{-j135^\circ}$	$\frac{1}{\sqrt{4}} e^{-j90^\circ}$	$\frac{1}{\sqrt{4}} e^{-j45^\circ}$	$\frac{1}{\sqrt{4}} e^{-j0^\circ}$	75.5°	45°
Port 4 ($m = 4$)	$\frac{1}{\sqrt{4}} e^{-j90^\circ}$	$\frac{1}{\sqrt{4}} e^{j45^\circ}$	$\frac{1}{\sqrt{4}} e^{-j180^\circ}$	$\frac{1}{\sqrt{4}} e^{-j45^\circ}$	41.4°	135°

TABLE 5: Element phasing, beam direction, and interelement phasing for the Butler matrix shown in Figure 4 (manufactured).

b_l, b_r	E1 ($l = 1$)	E2 ($l = 2$)	E3 ($l = 3$)	E4 ($l = 4$)	Beam direction	Interelement phasing (average)
Port 1 ($m = 1$)	$\frac{1}{\sqrt{4}} e^{j158^\circ}$	$\frac{1}{\sqrt{4}} e^{j25^\circ}$	$\frac{1}{\sqrt{4}} e^{-j112^\circ}$	$\frac{1}{\sqrt{4}} e^{j118^\circ}$	138°	-130°
Port 2 ($m = 2$)	$\frac{1}{\sqrt{4}} e^{-j87^\circ}$	$\frac{1}{\sqrt{4}} e^{-j137^\circ}$	$\frac{1}{\sqrt{4}} e^{j176^\circ}$	$\frac{1}{\sqrt{4}} e^{j137^\circ}$	105°	-42°
Port 3 ($m = 3$)	$\frac{1}{\sqrt{4}} e^{j132^\circ}$	$\frac{1}{\sqrt{4}} e^{j178^\circ}$	$\frac{1}{\sqrt{4}} e^{-j139^\circ}$	$\frac{1}{\sqrt{4}} e^{-j98^\circ}$	76°	50°
Port 4 ($m = 4$)	$\frac{1}{\sqrt{4}} e^{j136^\circ}$	$\frac{1}{\sqrt{4}} e^{-j90^\circ}$	$\frac{1}{\sqrt{4}} e^{j40^\circ}$	$\frac{1}{\sqrt{4}} e^{j176^\circ}$	42°	138°

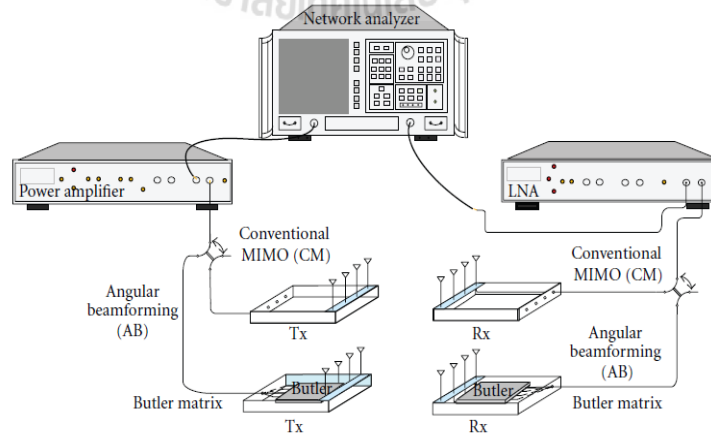


FIGURE 6: Block diagram of measurement setup.

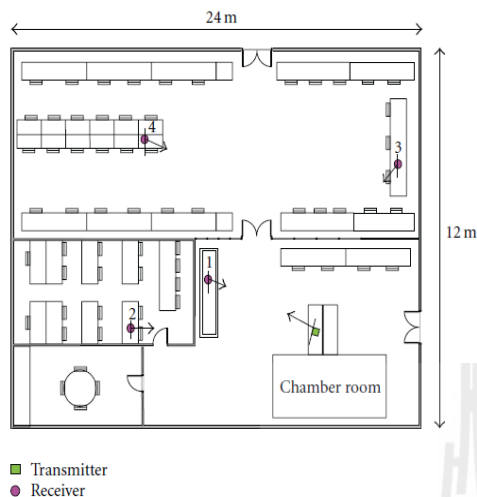


FIGURE 7: Measurement scenarios.

than QB. The complexity of QB and AB can be expressed in Tables 2 and 3, respectively. We evaluate the complexity [21] of AB and QB in terms of FLOPs. It is clearly seen that the Flop in Table 3 of AB is less than Flop of QB presented in Table 2. This implies that the lower processing time for AB can be obtained, which is shown in Figure 3. Figure 3 also shows the time spent computation with feedback information for 4×4 MIMO beamforming. The simulation times versus number of feedback bits using AB and QB technique are presented. It is demonstrated that AB requires less processing time than QB.

4. Feasibility of Practical Implementation

The feasibility of implementing AB processing for 4×4 MIMO systems is explored here by using Butler matrix [22]. Butler matrix constitutes four 90° hybrid couplers and two phase shifters with 45° phase and a crossover. Figure 4 shows the dimensions of Butler matrix which has been calculated by using transmission line theory. The fixed beamforming matrix is a bidirectional transmission. Hence, it can be used for either receiver or transmitter.

It can be easily shown that the weight vectors corresponding to each port presented in Table 4 are mutually orthogonal. Therefore, instead of using (5), the vector beamforming of applying Butler matrix can be written by the following expressions:

$$\begin{aligned} \mathbf{b}_t &= \frac{1}{\sqrt{N_t}} \exp(jlk\Delta_t \cos \phi); \quad l = 1, 2, \dots, N_t, \\ \mathbf{b}_r &= \frac{1}{\sqrt{N_r}} \exp(jmk\Delta_t \cos \phi); \quad m = 1, 2, \dots, N_r, \end{aligned} \quad (16)$$

where ϕ is the beam direction in Table 5. The characteristic of fabricated prototype is also confirmed by measuring interelement phasing and beam direction which are shown

in Table 5. In this table, the distributions of all interelement phasing are similar to conceptual Butler matrix but they are slightly deviated by ± 10 degree. However, the beam direction is deviated only by just 0.6 degree.

Figure 5 illustrates the beam direction of applying 2-bit feedback (Butler matrix) to both transmitter and receiver. It is interesting to see that the concept of AB is successfully achieved by simply adding Butler matrices next to antenna elements. We use the beamforming vector \mathbf{b}_t , representing beam direction 0° ; \mathbf{b}_{t_2} , \mathbf{b}_{t_3} , and \mathbf{b}_{t_4} represent beam direction 0° , 10° , and 11° degrees, respectively. Then, the channel matrix realized by Butler matrix can be written as

$$\mathbf{H}^b = \mathbf{b}_r^* \mathbf{H} \mathbf{b}_t, \quad (17)$$

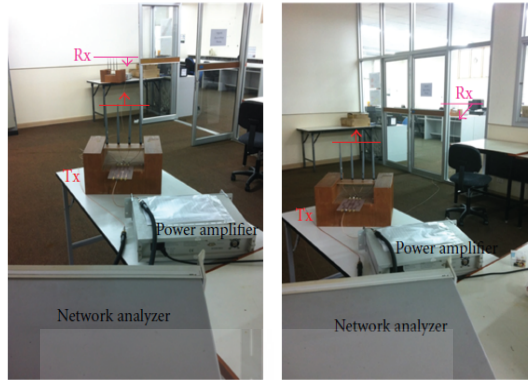
where \mathbf{b}_t and \mathbf{b}_r are the beamforming vectors whose rows are the vectors in four directions for transmitter and receiver and \mathbf{H} is channel matrix of size $N_r \times N_t$ to get conventional MIMO. Thus, the capacity of MIMO systems when applying Butler matrix is given by

$$C = \log_2 \det \left(\mathbf{I}_{N_r} + \frac{P_t}{P_N N_t} \mathbf{H}^b \mathbf{H}^{b*} \right). \quad (18)$$

5. Measurement Results and Discussion

Figure 6 shows a block diagram of measurement setup for 4×4 MIMO system. The network analyzer is used for measuring channel coefficients in magnitude and phase. The power amplifier (PA) is used at transmitter to provide more transmitted power. Low noise amplifier (LNA) is used at the receiver to increase the appropriate by the received signal level [23]. Four measurements on the channel are undertaken at each location. In each location, two modes of MIMO operation (conventional MIMO and AB) are measured. The Butler matrices are inserted at both transmitter and receiver when measuring MIMO channels with AB. Figure 7 shows measurement scenarios. We chose measurements in a large room to provide various test conditions. The location of the transmitter is fixed as shown in Figure 7 with rectangular symbol. There are four measured locations for the receiver represented by circular symbol in Figure 7. The antenna is a monopole. The numbers of transmitted and received antennas are 4×4 . The center frequency (λ_c) is 2.4 GHz. The normalized separation between transmit and receive antennas (Δ_t, Δ_r) is 0.5. Distance between Tx and Rx locations 1, 2, 3, and 4 is 2.3, 6.1, 6.8, and 13.3 meters, respectively. It is easy to measure both conventional MIMO and AB by using switches presented in Figure 6. The measured results obtained by network analyzer are used as a channel response in MIMO systems. As seen in Figure 6, apart from Butler matrix, all the other components are the same for both conventional MIMO and AB. Therefore, the measured channels can be directly compared to each other as presented in the following. Figure 8 shows the photo of measurement areas for LOS (location 1) and NLOS (location 4).

The channel matrices \mathbf{H} and \mathbf{H}^b can be realized from the measured data from vector network analyzer. The channel fading environments are measured by changing the locations of the receiver. We also believe that the mismatches



(a) LOS

(b) NLOS

FIGURE 8: The photo of measurement areas for LOS and NLOS.

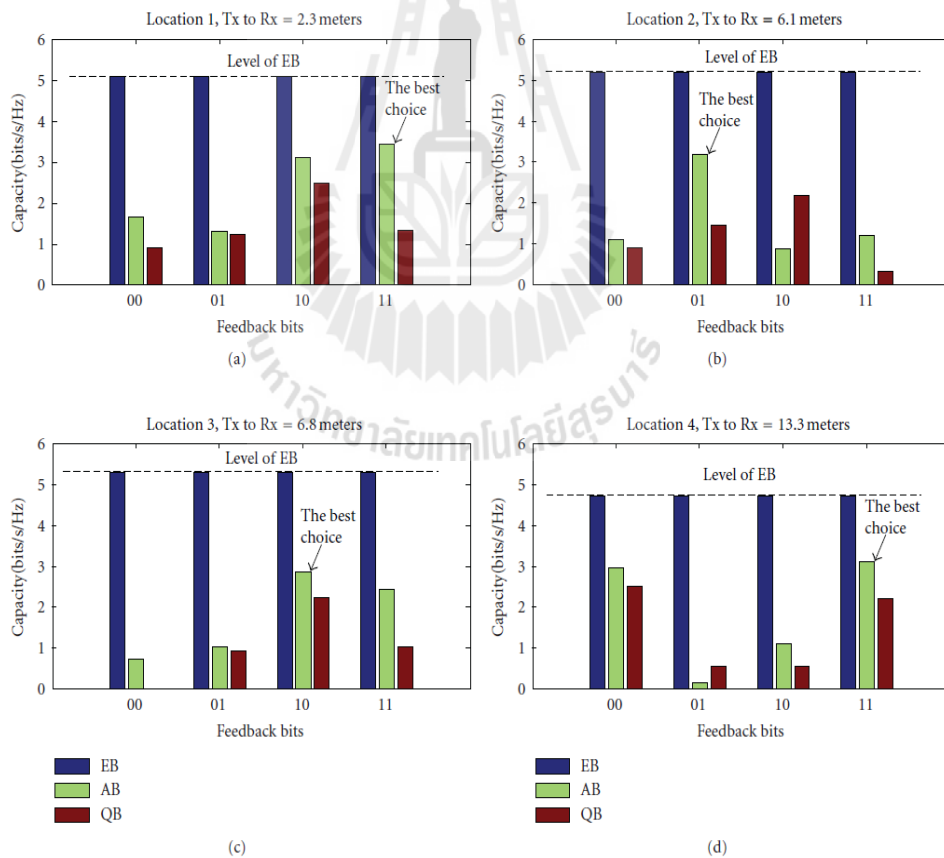


FIGURE 9: Average capacity versus beam direction for two-bit feedback, locations 1, 2, 3, and 4.

among RF circuits in transmitting/receiving components and mutual coupling effects are included in the measured channel. We use 2 bits of feedback for QB. The simulations are undertaken by utilizing measured data into MATLAB programming. We have made comparisons between EB, QB, and AB. The capacity results are evaluated by using (12), (15), and (18).

In Figure 9, the average capacity versus beam direction for feedback of two bits is presented, in order to justify the results of all locations at SNR = 10 dB. The results indicate that AB offers a better performance than QB. It is obviously noticed that the benefit of using AB is pronounced at all locations. The gap deviation is about 1.83 bits/s/Hz. Please be reminded that the improvement of MIMO capacity comes at a little expense of inserting Butler matrices at both transmitter and receiver but without any extra complexity when compared with EB.

6. Conclusion

This paper presents the performance of MIMO beamforming systems using EB, QB, and AB techniques. The result reveals that the proposed system, AB technique, is attractive to be practically implemented because it offers a low complexity while offering the similar performance as that of QB. We have also presented the performance of MIMO systems using AB realized by using Butler matrix. Further, the benefit of using AB technique for 4×4 MIMO systems is verified by measured results. The AB method as realized by Butler matrix has been implemented and compared with EB and QB. The results have revealed that the EB outperforms the AB and QB at all locations. The reason for this is that the EB uses the maximum eigenvalue for finding channel capacity. It is concluded that the proposed system is very attractive to practically implement on MIMO systems due to its low cost and complexity.

Acknowledgments

This work is financially supported by Suranaree University of Technology, Thailand, and the Royal Golden Jubilee Program of Thailand Research Fund, Thailand.

References

- [1] B. Mondal and R. W. Heath, "Performance analysis of quantized beamforming MIMO systems," *IEEE Transactions on Signal Processing*, vol. 54, no. 12, pp. 4753–4766, 2006.
- [2] A. S. Lek, J. Zheng, O. Eric, and J. Kim, "Subspace beamforming for near-capacity performance," *IEEE Transactions on Signal Processing*, vol. 56, no. 11, pp. 5729–5733, 2006.
- [3] X. Zheng, Y. Xie, J. Li, and P. Stoica, "MIMO transmit beamforming under uniform elemental power constraint," *IEEE Transactions on Signal Processing*, vol. 55, no. 11, pp. 5395–5406, 2007.
- [4] L. Sun, M. R. McKay, and S. Jin, "Analytical performance of MIMO multichannel beamforming in the presence of unequal power Cochannel Interference and Noise," *IEEE Transactions on Signal Processing*, vol. 57, no. 7, pp. 2721–2735, 2009.
- [5] S. L. Ariyavitakul, J. Zheng, E. Ojard, and J. Kim, "Subspace beamforming for near-capacity MIMO performance," *IEEE Transactions on Signal Processing*, vol. 56, no. 11, pp. 5729–5733, 2008.
- [6] R. D. Vieira, J. C. B. Brandão, and G. L. Siqueira, "MIMO measured channels: capacity results and analysis of channel parameters," in *Proceedings of the International Telecommunications Symposium (ITS '06)*, pp. 152–157, Fortaleza, Brazil, September 2006.
- [7] G. J. Foschini and M. J. Gans, "On limits of wireless communications in a fading environment when using multiple antennas," *Wireless Personal Communications*, vol. 6, no. 3, pp. 311–335, 1998.
- [8] I. E. Telatar, "Capacity of multi-antenna Gaussian channels," AT&T Bell Laboratories, Technical Memorandum, 1995.
- [9] G. J. Foschini, "Layered space-time architecture for wireless communication in a fading environment when using multiple-element antennas," *Bell Labs Technical Journal*, vol. 1, no. 2, pp. 41–59, 1996.
- [10] J. P. Kermaol, P. E. Mogensen, S. H. Jensen et al., "Experimental investigation of multipath richness for multi-element transmit and receive antenna arrays," in *Proceedings of the 51st Vehicular Technology Conference 'Shaping History Through Mobile Technologies' (VTC '00)*, pp. 2004–2008, May 2000.
- [11] R. Stridh, B. Ottersten, and P. Karlsson, "MIMO channel capacity on a measured indoor radio channel at 5.8 GHz," in *Proceedings of the 34th Asilomar Conference*, pp. 733–737, November 2000.
- [12] A. F. Molisch, M. Steinbauer, M. Toeltsch, E. Bonek, and R. S. Thomä, "Capacity of MIMO systems based on measured wireless channels," *IEEE Journal on Selected Areas in Communications*, vol. 20, no. 3, pp. 561–569, 2002.
- [13] L. Huang, J. W. M. Bergmans, and F. M. J. Willems, "Low-complexity LMMSE-based MIMO-OFDM channel estimation via angle-domain processing," *IEEE Transactions on Signal Processing*, vol. 55, no. 12, pp. 5668–5680, 2007.
- [14] L. Huang, C. K. Ho, J. W. M. Bergmans, and F. M. J. Willems, "Pilot-aided angle-domain channel estimation techniques for MIMO-OFDM systems," *IEEE Transactions on Vehicular Technology*, vol. 57, no. 2, pp. 906–920, 2008.
- [15] A. F. Molisch, X. Zhang, S. Y. Kung, and J. Zhang, "DFT-based hybrid antenna selection schemes for spatially correlated MIMO channels," in *Proceedings of the 14th IEEE International Symposium on Personal, Indoor and Mobile Radio Communications (PIMRC '03)*, pp. 1119–1123, September 2003.
- [16] A. Innok, M. Uthansakul, and P. Uthansakul, "The enhancement of MIMO capacity using angle domain processing based on measured channels," in *Proceedings of the Asia Pacific Microwave Conference (APMC '09)*, pp. 2172–2175, Singapore, December 2009.
- [17] A. Grau, J. Romeu, S. Blanch, L. Jofre, and F. De Flaviis, "Optimization of linear multielement antennas for selection combining by means of a butler matrix in different MIMO environment," *IEEE Transactions on Antennas and Propagation*, no. 11, pp. 3251–3264, 2006.
- [18] P. Uthansakul, A. Innok, and M. Uthansakul, "Open-loop beamforming technique for MIMO system and its practical realization," *International Journal of Antennas and Propagation*, vol. 1, 13 pages, 2011.
- [19] D. Tse and P. Viswanath, *Fundamentals of Wireless Communication*, chapter 7, Cambridge, UK, 2005.
- [20] R. G. Tsoulos, *MIMO Systems Technology for Wireless Communications*, The Electrical Engineering and Applied Signal Processing Series, chapter 4, 2006.

- [21] P. Uthansakul, *Adaptive MIMO Systems Explorations For Indoor Wireless Communications, Appendix D*, 2009.
- [22] J. C. Liberti and J. T. S. Rappaport, *Smart Antennas for Wireless Communications, IS-95 and Third Generation CDMA Applications*, chapter 3.
- [23] N. Promsuvana and P. Uthansakul, "Feasibility of adaptive 4×4 MIMO system using channel reciprocity in FDD mode," in *Proceedings of the 14th Asia-Pacific Conference on Communications (APCC '08)*, pp. 1–5, October 2008.



BIOGRAPHY

Miss Apinya Innok was born in Nakhonratcahsima, Thailand, in 1985. She graduated with the Bachelor and Master Degree of Engineering in Telecommunication Engineering in 2007 and 2010, respectively from Suranaree University of Technology, Nakorn Ratchasima, Thailand. Then, she is currently pursuing her Ph.D program in Telecommunication Engineering, School of Telecommunication Engineering, Suranaree University of Technology. Her research interests are MIMO on wireless communication and its application.

